CHARACTERIZATION AND SOURCE IDENTIFICATION OF AMBIENT PARTICULATE MATTER ($PM_{2.5}$) IN THE GREATER ACCRA METROPOLITAN AREA, GHANA

This thesis is submitted to the University of Ghana, Legon, in partial fulfillment of the requirement for the award of

Doctor of Philosophy, Chemistry Degree

By

KOJO AYITTEY

(10807409)

Department of Chemistry

March 2024

DECLARATION

I, Kojo Ayittey, declare that except for the references to other people's work, which have been duly cited, this thesis is the result of my own research and that it has neither in part nor whole been presented for the award of any degree elsewhere.

……

CANDIDATE: KOJO AYITTEY

DATE: April 03, 2024

SUPERVISORS:

……

Dr. ENOCK DANKYI

Date: April 03, 2024

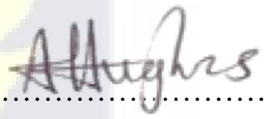

……

Dr. ALLISON FELIX HUGHES

Date: April 03, 2024

……

Dr. OWIREDU GYAMPO

Date: April 03, 2024

DEDICATION

This thesis is dedicated to my wife-Her Ladyship Justice Ama Sefenya Ayittey (Mrs.) and my children- Delali Yao Ayittey, Sedem Kobla Tetteh Ayittey, Akorfa Afi Dede Ayittey and Nuna Ama Korkor Ayittey.

ACKNOWLEDGEMENTS

I am primarily thankful to the Almighty God for guiding my steps and providing me with ample grace over the years in order to bring me this far. May His name be glorified forever.

My special thanks go out to all of my supervisors: Dr. Enock Dankyi of the Department of Chemistry, University of Ghana, Dr. Allison Felix Hughes of the Department of Physics, University of Ghana, and Dr. Owiredu Gyampo, the head of Nuclear Applications Center, National Nuclear Research Institute of the Ghana Atomic Energy Commission. I appreciate all your supports, advice, and belief in me. May God richly reward you.

My sincere gratitude to Accra Technical University's management for funding this doctoral study. Additionally, I appreciate the support and encouragement I received from the following: Prof. Felix Kutsenadze, Dean of School of Engineering, Professor Edmund Ameko, former Pro-Vice Chancellor, Dr. Henry Kwadwo Hackman, Director of Quality Assurance, Reverend Abraham Quarcoo and Professor Alice Abakah Mensah, Dean of School of Applied Sciences, all of Accra Technical University. I am grateful to Dr. Andrew N. Boa of the Department of Chemistry, University of Hull, UK for all your support.

I am appreciative of the management of the Environmental Protection Agency (EPA) in Accra, Ghana, particularly Mr. Emmanuel Appoh, Mrs. Esi Neequaye-Tetteh, Jeremiah Asumbere, Mathias Borketey and the Air Monitoring team of the Environmental Quality Laboratory. My profound gratitude goes to the current and former Heads of Department, all senior members and staff of the Department of Chemistry, University of Ghana and the late Professor Augustine Donkor for their love and encouragement. I sincerely thank Professor Johannes Awudza of the Department of Chemistry, KNUST for your inspirations. I express my gratitude to Mr. Karikari

Williams of Mountains Research Institute (MRI) as well as the management and staff of Pure Earth, Labone- Ghana. I want to express my gratitude for the invaluable assistance that Dr. Owiredu Gyampo and Mr. Mathias Borketey provided throughout the entire analysis and writing process.

I would like to thank my family, especially my wife, Her Ladyship Justice Mrs. Ama Sefenya Ayittey for their support and prayers. I am also thankful to my brothers and sisters for their support and encouragement. There are many who behind the scenes have encouraged and supported my work, but whose names have not been mentioned. I find it appropriate to acknowledge all of you who made my life easier every day. I pray God bless you all abundantly. Finally, I would like to extend my gratitude to the Ghana Meteorological Agency (GMA), and the Driver's and Vehicle Licensing Authority (DVLA), Cantonments, Accra-Ghana, for the provision of data on meteorology and automobiles in Accra.

ABSTRACT

A 2-year research was conducted to investigate mass concentration, weather impacts, chemical composition and sources of ambient particulate matter ($PM_{2.5}$) and their fingerprints in the Greater Accra Metropolitan Area, Ghana. Sampling of the $PM_{2.5}$ fraction of airborne particulate matter was done 24-hourly every six days on a polytetrafluoroethylene (PTFE) filter of pore size 0.2 µm using an ARA N-FRM sampler. The investigation was carried out at three separate sites within the Greater Accra Metropolitan area: Adabraka (AD), Dansoman (DA) and the University of Ghana (UG) spanning January 2021 to December 2022.

Gravimetric analysis and energy-dispersive X-ray fluorescence (EDXRF) spectroscopy were employed to determine the mass concentration and characterization of the airborne particulate matter. The samples were positioned in the XRF equipment and subjected to high-energy X-rays. The X-rays excite the atoms in the sample, which makes them give off secondary (fluorescent) X-rays that showed what elements are in the sample. X-rays released were detected and analyzed to ascertain the presence of components in the $PM_{2.5}$ samples. Every element possesses a distinct X-ray energy or wavelength, facilitating accurate quantification. The intensity of the fluorescent X-rays correlates with the concentration of each element in the sample. Calibration with standards Iron (Fe) and Molybdenum (Mo) were employed to translate observed intensities into quantitative concentrations.

The minimum, maximum, and annual mean mass concentration values for $PM_{2.5}$ obtained at the three locations during the research periods were AD 60.76 µgm^{-3} (20.70 µg m^{-3} - 133.07 µg m^{-3}), DA 49.90 µgm^{-3} (8.32 µg m^{-3} - 120.59 µg m^{-3}) and UG 42.49 µgm^{-3} (8.32 µg m^{-3} - 120.59 µg m^{-3}) respectively, for the 2021 study period. For the 2022 study period, the minimum,

maximum, and annual mean mass concentration values were AD (20.79 μg m^{-3}, 162.18 μg m^{-3}, 60.54 μg m^{-3}), DA (16.63 μg m^{-3}, 138.86 μg m^{-3}, 49.28 μg m^{-3}), and UG (12.48 μg m^{-3}, 153.86 μg m^{-3}, 46.37 μg m^{-3}) respectively. These annual mean mass concentration values exceeded the air quality standards of Ghana, as well as those set by the World Health Organization (WHO), the United States Environmental Protection Agency (USEPA), and the European Union (EU). Analysis of meteorological parameters and their possible impacts on particulate matter levels revealed a positive correlation between temperature and $PM_{2.5}$ mass concentrations (r = 0.23), and negative correlations with relative humidity (r = -0.22), rainfall (r = -0.18), and wind speed (r = -0.31) during the entire study period. These findings underscore the influence of meteorological conditions on $PM_{2.5}$ concentrations.

Notably, the presence of crustal components was highest during the seasonal Harmattan period, from late December to early February, characterized by the transportation of Saharan dust over West Africa. Using the Enrichment Factor (EF) modeling tool, the extent of anthropogenic influence on species present in the observed elemental composition of $PM_{2.5}$ sampled was assessed. Source apportionment analysis using the U.S. EPA's positive matrix factorization (PMF) 5.0 model identified and differentiated six anthropogenic sources. The contributions from various sources to pollution levels are as follows: Biomass burning contributes 20% in AD, 20% and 21% in DA, and 17% and 19% in UG. Solid waste burning accounts for 17% and 14% in AD, 7% and 6% in DA, and 19% in UG. Sea salt spray contributes 9% and 7% in AD, 10% and 8% in DA, and 7% and 6% in UG. Vehicular and industrial emissions are significant, with 25% and 28% in AD, 29% and 35% in DA, and 24% and 22% in UG. Soil dust has contributions of 13% in AD, 16% and 11% in DA, and 14% in UG. Lastly, re-suspended dust accounts for 16% and 18% in AD,

18% and 19% in DA, and 19% and 20% in UG. This emphasizes their substantial impacts on $PM_{2.5}$ levels at the studied sites in Greater Accra Metropolitan Area. This study provides valuable insights into the dynamics of ambient $PM_{2.5}$ in Greater Accra Metropolitan Area, contributing to a better understanding of air quality management and mitigation strategies in urban environments in sub-Saharan Africa.

Table of Contents

List of Tables

List of Figures

ABBREVIATIONS

AD	Adabraka
ADT640	Adabraka Teledyne 640
AMA	Accra Metropolitan Area
APM	Atmospheric Particulate Matter
AXIL	Analysis of X-ray Spectra by Iterative Least-squares
BAM1020	Beta Attenuation Monitor1020
CA	Cluster Analysis
CBD	Central Business District
CMB	Chemical Mass Balance
DA	Dansoman
DPP	Digital Pulse Processor
DPPMCA	Digital Pulse Processor Multi Channel Analyzer
DMS	Dimethyl sulphide
DVLA	Driver's Vehicle Licensing Authority
EDXRF	Energy Dispersive X-ray Fluorescence
EF	Enrichment Factor
EC	Elemental Carbon

EPA-Ghana	Environmental Protection Agency of Ghana
ET	Emission Transmission
EQL	Environmental Quality Laboratory
EU	European Union
FET	Field Effect Transistor
FRM	Federal Reference and Equivalent Method
FFP	Full Fundamental Parameters
GAEC	Ghana Atomic Energy Commission
GMA	Ghana Meteorological Agency
GS	Ghana standards
IAEA	International Atomic Energy Agency
IMPROVE	Interagency Monitoring of Protected Visual Environments
INAA	Instrumental Neutron Activation Analysis
ITCZ	Inter-Tropical Convergence Zone
MC	Mass Concentration
MC	Microscopic Analysis
MCA	Multichannel analyzer
NNRI	National Nuclear Research Institute

N-FRM	Near- Federal Reference and Equivalent Monitor
NO_2	Nitrogen dioxide
NO_3^-	Nitrate ion
OECD	Organization for Economic- Co-operation and Development
OC	Organic Carbon
O_3	Ozone
PCA	Principal Component Analysis
PIGE	Particle Induced Gamma-ray Emission
PIXE	Particle Induced X-ray Emission
PM	Particulate Matter
$PM_{2.5}$	Particulate Matter with aerodynamic diameter of less than 2.5 µm
PM_{10}	Particulate Matter with aerodynamic diameter of less than 10 µm
PMF	Positive Matrix Factorization
PTFE	Polytetrafluoroethylene
PVC	Polyvinyl chloride
QXAS	Quantitative X-ray Analysis system
RH	Relative Humidity
SQ	Simple Quantitative

SD	Standard deviation
SDD	Silicon Drift Detector
SES	Socio economic status
SO_2	Sulphur dioxide
SSA	Sub-Saharan Africa
SSI	Size selective unit
VOC	Volatile Organic Compound
UG	University of Ghana
UGT640	University of Ghana Teledyne 640
UN	United Nation
UNEP	United Nations Environment Programme
USAID	United States Agency for International Development
U.S EPA	United States Environmental Protection Agency
WHO	World Health Organization
XRF	X-ray Fluorescence

CHAPTER 1
INTRODUCTION

1.1 BACKGROUND

Air pollution is a significant issue in today's global discussions and is generally seen as a threat to both public health and economic development, especially in developing nations (1,2). Pollution of air is the emission of toxic solids, liquids, and gaseous substances into the atmosphere (1). Emissions can emanate from a wide variety of sources and may undergo chemical or physical changes before returning to surfaces such as soil, plants, trees, monuments and structures (3,4). The emission sources can be categorized into two: particulate matter (PM) and gaseous emissions. Gaseous emissions include toxic gases such as nitrogen gases (NO_x), Sulphur gases (SO_x), ozone (O_3), methane (CH_4) and other greenhouse gases. Particulate matter refers to a suspension of a mixture of compact particles and liquid droplets that are shaped in the atmosphere, with varying sizes and chemical compositions, particulate matter ≤ 1 micron in aerodynamic diameter (PM_1), particulate matter ≤ 2.5 microns in aerodynamic diameter ($PM_{2.5}$), and particulate matter ≤ 10 microns in aerodynamic diameter (PM_{10}) (5,6). Particulate matter can also be referred to as aerosol particles. Aerosol particles exhibit a wide range of sizes, ranging from tiny molecule clusters measuring 0.001 µm to larger fog and sand particles that may reach a few hundred micrometers in size.

The World Health Organization (WHO) in 2021 estimated that air pollution is responsible for around 7 million deaths worldwide (7). Despite efforts to alleviate it, citizens in many countries in central and southern Asia and sub-Saharan Africa (SSA) consistently endure high levels of air pollution (8). According to the United Nations (UN), over half of the global population, which amounts to over 7 billion people, lives in urban areas that cover only 3% of the Earth's land.

Additionally, it is estimated that 87 % of the world's population is exposed to air pollution levels that exceeds the annual guidelines set by the World Health Organization (WHO) (7). By 2030, it is estimated that more than 65% of the world's population will be living in urban areas. A significant proportion of these new urban inhabitants will live in slums and informal residents in low-income countries, where air quality is often poor. Africa is one of the most economically deprived continents on the planet. The fastest urbanization rate in the world occurs in SSA, where the urban population is growing at a pace of more than 1.7% annually (9). The population of Africa, now about 1.1 billion, is projected to double by 2050. Over 80% of this growth is expected to occur in slum areas (10).

In the last ten years, several large cities in sub-Saharan Africa (SSA) have seen significant growth in urbanization, industry, and motorization. Decisions made in anticipation of this growth will have a significant impact on the urban design of cities in developing nations such as SSA and their effects on the health of future city residents and the global environment. These cities in the SSA region suffer from severe pollution because of their low-income levels and limited financial means to tackle these problems (11).

Local urban air pollution has negative health consequences for the exposed population. The disease burden from exposure to air pollution is disproportionately borne by expanding urban populations in the developing world, where pollution levels are significantly higher than in high-income nations (12). According to the WHO, urban air pollution causes approximately 4.2 million premature deaths each year. These fatalities are attributed to lung cancer, cardiovascular diseases, and respiratory disorders caused by exposure to fine particulate matter in both indoor and outdoor air pollution (13). A recent study conducted by the Organization for Economic Co-operation and Development (OECD) reveals that if no measures are implemented to improve air quality, outdoor

air pollution resulting from particulate matter could exceed all other environmental factors and become the leading cause of premature deaths. According to the OECD, global PM is expected to cause about 9 million premature deaths annually by 2060, with the bulk of these fatalities occurring in developing economies (14). The main sources of urban air pollution in sub-Saharan Africa (SSA) include the burning of biomass for cooking and heating, as well as the use of fossil fuels in transportation, electricity generation, industry, and residential areas. Additional sources include trash incineration, re-suspended dusts, building debris, and naturally occurring wind-blown particles (12,15–18).

Bauer et al. (2019) (19) reported that urban air pollution in Africa causes about 1.1 million premature deaths each year, with the use of solid fuels for indoor cooking being responsible for a much higher number, about eight times more. The effect is more severe in sub-Saharan African nations (19), with asthma, stroke, bronchitis, and other respiratory and cardiovascular diseases, and associated with air pollution-related fatalities (20–22).

There are many and diverse causes of air pollution. The origins of urban air pollution in Africa exhibit notable disparities compared to many other regions (23–25). Nevertheless, there are substantial gaps in understanding the sources of particulate matter (PM) and their respective contributions in cities throughout sub-Saharan Africa (SSA). Agyei-Mensah et al (2018) (26) reported that among countries within the sub-Saharan region, only a few, including South Africa, Ghana, Kenya, Uganda, Ethiopia, Nigeria, have air quality monitoring programs. The monitoring of aerosols has become a priority, particularly in urban areas of sub-Saharan Africa. Although there have been notable improvements in understanding aerosols and their impact on environment, there is still a paucity of comprehensive data on particulate matter in cities in sub-Saharan Africa. This lack of data on air pollution has greatly impeded efforts to analyze and comprehend the levels

of particulate matter concentrations and to develop program measures to improve air quality. Understanding the makeup of aerosol particles in the atmosphere is crucial for determining their origins and forecasting their influence on different atmospheric developments and health consequences. Several countries in the SSA have begun monitoring particular size fractions of particulate matter, namely PM_{10} and $PM_{2.5}$, along with their chemical characteristics (27–30). Identification and apportionment of particulate matter to its sources is a crucial step in managing air quality. These will also provide valuable information for governmental agencies and those responsible for generating the emissions. By using advanced data analysis techniques known as receptor models, it is possible to identify and apportion the sources responsible for PM pollution within Greater Accra. In order to achieve this, an effective multivariate receptor model such as positive matrix factorization (PMF) is employed.

1.2 STATEMENT OF THE PROBLEM

Urban air pollution in sub-Saharan Africa is on the rise due to increasing particulate matter. Air quality in metropolitan areas of emerging countries like Ghana has worsened significantly due to rapid population growth, urbanization, industry and increased vehicle use, open burning and high use of biomass for cooking and heating. The adverse health effects of ambient particulate matter pollution have been established by accumulating epidemiological evidence (31–33). The paucity of data on the amounts and composition of particulate matter in Ghana poses challenges in assessing the magnitude and attributes of air pollution and its impact on the population. In order to effectively manage particle levels in the urban atmosphere, it is necessary to have a comprehensive understanding of the size distribution, chemical composition, and origins of aerosol particles. This information is crucial for evaluating and addressing the impacts of particulate matter pollution.

1.3 AIM OF STUDY

This research aims to assess the ambient particulate matter ($PM_{2.5}$), determine the influence of meteorological factors on particulate matter < 2.5 microns in diameter ($PM_{2.5}$), characterize and identify potential sources of particulate matter in the Accra metropolitan area of Ghana.

1.4 SPECIFIC OBJECTIVES

The specific objectives are as follows.

1. Measure the mass concentration of $PM_{2.5}$ in selected locations in the Greater Accra Metropolitan Areas i.e., Adabraka (AD), Dansoman (DA), and the University of Ghana, campus, Legon (UG).

2. Investigate the influence of meteorological factors in Greater Accra on the emission of particulate matter.

3. Characterize the chemical composition and concentrations of the sampled $PM_{2.5}$ using energy dispersive X-ray fluorescence (EDXRF) technique.

4. Determine natural and anthropogenic contributions to air pollution at different receptor sites using enrichment factor (EF) modelling.

5. Use the U.S. EPA's Positive Matrix Factorization (PMF) 5.0 modeling tool to identify natural and anthropogenic sources and apportion their contributions to $PM_{2.5}$ in the Greater Accra Metropolitan Area.

1.5 JUSTIFICATION FOR STUDY

Accra, the capital of Ghana, is undergoing rapid urbanization and industrialization, resulting in a rise in air pollutants emissions. The growing population of Greater Accra is vulnerable to the risks

of air pollution, which poses serious threat to both environmental pollution and human health. Research in this field is vital for understanding the health hazards and repercussions of air pollution on the population of Accra. Exposure to air pollution is associated with respiratory illnesses, cardiovascular disorders, and other health problems. The use of local air quality data can aid in the development of focused intervention plans to reduce these risks. The justification for conducting research on air pollution in Greater Accra, Ghana, is due to its significant influence on public health, urban growth, climate change, economic expenses, and the well-being of vulnerable communities. In addition, the study involves the monitoring and evaluation of the effects of these advancements and offer valuable insights on how to regulate industrial operations and urban planning in order to mitigate pollution levels. Furthermore, it will enhance the sustainable growth of the city while actively fostering the development of a cleaner, healthier environment.

CHAPTER 2
LITERATURE REVIEW

2.1 ATMOSPHERIC PARTICULATE MATTER

Particulate matter (PM) refers to the presence of liquid and solid particles suspended in a gaseous phase in the atmosphere. Aerosol refers to the particles as well as the surrounding environment in which they are suspended. However, in the literature, it is conventional to use only the word "aerosol" to designate atmospheric particles or the particulate component (3,34–37). The primary focus of this study is on the particle component due to its significant effects on both human health and the environment. The behaviour of particulate matter in the urban environment and its possible impacts on human health and atmospheric visibility depend on the following properties:

- Physical (size and shape).
- Chemical (composition and concentration).
- Geographic location, season, day, and time of day of emissions.

Furthermore, the physical and chemical properties of particles depend on the specific source and processes by which they are formed, whether in the atmosphere or at the source of emission (38). Particulate matter is an intricate blend of many chemical components. Particulate matter can originate from stationary or mobile sources, either naturally or directly or indirectly, as a result of human activities and it consists of a vast array of particles of various origins, sizes, and constituents. They may be categorized as primary or secondary based on their creation method. Primary particles are discharged directly into the atmosphere by origins, whereas secondary particles are generated by atmospheric processes such as photochemistry or undergo changes in chemical composition after being emitted (39). Primary particles may be classified as either

anthropogenic or natural, depending on their origin. Due to the intricate composition of particulate matter, which consists of several chemical components, it becomes challenging to ascertain the source of secondary particles.

Nevertheless, secondary particles may arise from the chemical conversion of primary emissions, including nitrogen oxides (NO_X), Sulphur dioxide (SO_2), ozone (O_3), and organic gases originating from both natural and human activities. Furthermore, primary or secondary mechanisms may produce particles in both natural and human activities (40). The abundance of primary particles in the atmosphere is dependent upon their emission rate, rates of transit and dispersion, as well as rates of removal. Primary particles are mostly found in the larger particles, whereas secondary particles are mainly found in the smaller particles (41). The coarse fraction comprises particles with a diameter bigger than 2.5 µm and smaller than 10 µm, which are often discharged into the atmosphere by anthropogenic or natural means. The fine fraction comprises particles with a diameter smaller than 2.5 µm, most of which are formed through gas-to-particle conversion. This process involves the oxidation and condensation of gases like Sulphur dioxide (SO_2), nitric oxide, nitrogen oxides (NO_X), and volatile organic compounds (VOCs) (42).

2.2 STUDIES ON AIRBORNE PARTICULATE MATTER IN AFRICA

Findings from African Development Bank outlook report in 2023 revealed that Africa's economic growth rate comes second only to that of Asia (43). This is relevant to air pollution, as rapid economic development can often be associated with increased industrialization and urbanization, leading to higher levels of air pollution. As Africa experiences notable economic growth, there is the potential for increased industrial activities, transportation, and energy consumption, all of which can contribute to high levels of air pollution.

Air pollution has long-range transportability and may have far-reaching effects beyond its source. Due to the rapid increase in vehicle traffic, open burning of waste, and the presence of sizable industries close to residential areas, many major cities in sub-Saharan Africa (SSA) are currently dealing with similar air pollution problems. These issues can be specifically attributed to particulate matter generated by human activities.

Studies on air pollution in African countries are still in the early stages of development. Unlike other regions such as North America and Europe, there is a scarcity of data on air pollution resulting from particulate matter in many SSA countries, including Ghana. This lack of information on air pollution is troubling considering the adverse effects it has on human health, visibility, and climate. In many SSA countries, data on airborne particulate matter is limited due to the lack of routine monitoring. This has greatly impeded further assessment of the source allocation of particulate matter. In Greater Accra, studies conducted during the past few years have identified three to six potential sources of the composition of particles, including vehicular emissions, biomass burning, re-suspended dusts, solid waste burning, soil dusts and sea salt spray (27,28,44).

Hence, it is crucial to conduct air pollution assessments in African urban areas. Furthermore, it is crucial to understand the origins and impacts of particulate matter in Accra, Ghana, in order to formulate improved regulations and guidelines for the management of emissions.

2.3 CURRENT SITUATION OF AIR POLLUTION IN GHANA

Ghana has a high population density compared to other nations in the sub-region, with an estimated population of more than 32 million and a growth rate of 2.03%, a birth rate of 27.5 births per 1,000 inhabitants, and a mortality rate of 7.6 deaths per 1,000 inhabitants annually (45). The country's urban cities are home to over 58% of the population (46).

In Ghana and most of the SSA nations, air quality monitoring for air quality assessment has been infrequent or non-existent. Therefore, there are data gaps regarding the concentrations and properties of atmospheric particulate matter and other major pollutants. Due to the paucity of logistics and resources, only the Environmental Protection Authority of Ghana (EPA-Ghana) has conducted routine monitoring programs to measure PM_{10} and $PM_{2.5}$ in Accra. A study by Hughes (28) revealed that air quality evaluated at monitoring stations is primarily influenced by tail-pipe vehicular emissions, open burning of garbage and other materials, emissions from industries, domestic heating and cooking, business activity, and resuspended dust (Figure 1.1).

Figure 1.1 (a) Cooking using solid fuel (b) Automobile exhaust emission (c) Traffic congestion (d) Accra's Harmattan/wind-blown dust

Elevated levels of particulate matter in close proximity to highways and in busy urban areas have the potential to adversely affect public health (47). In a growing number of major urban centers in sub-Saharan Africa, traffic congestion is the leading source of pollution. The level of motorization in the Greater Accra Metropolitan Area (AMA) is significant compared to other African regions, with a ratio of 148 automobiles per 1,000 residents. In contrast, Nigeria has a lower ratio of 34.9 vehicles per 1,000 inhabitants (48,49). This is due in part to the abundance of taxis, commercial buses, “okada”, and “pragia”, (okada and pragia refers to motorbikes that are used for business purposes). This trend is on the rise, as 90% of imported automobiles continue to be located in metropolitan areas. Hughes (24) conducted a study that presented a comprehensive overview of

vehicle registration data collected by the Driver and Vehicle Licensing Authority (DVLA) in Accra over a 10-year period (2010 - 2019). The findings from this study indicate that traffic congestion in Accra is a prevalent issue, particularly during peak periods. In addition, the study emphasizes the high usage of vehicles, a notable dependence on unofficial private bus services, and the ineffective execution of traffic control strategies. Furthermore, it identifies insufficient infrastructure for pedestrians and cyclists, inadequate road safety measures, and a high incidence of accidents.

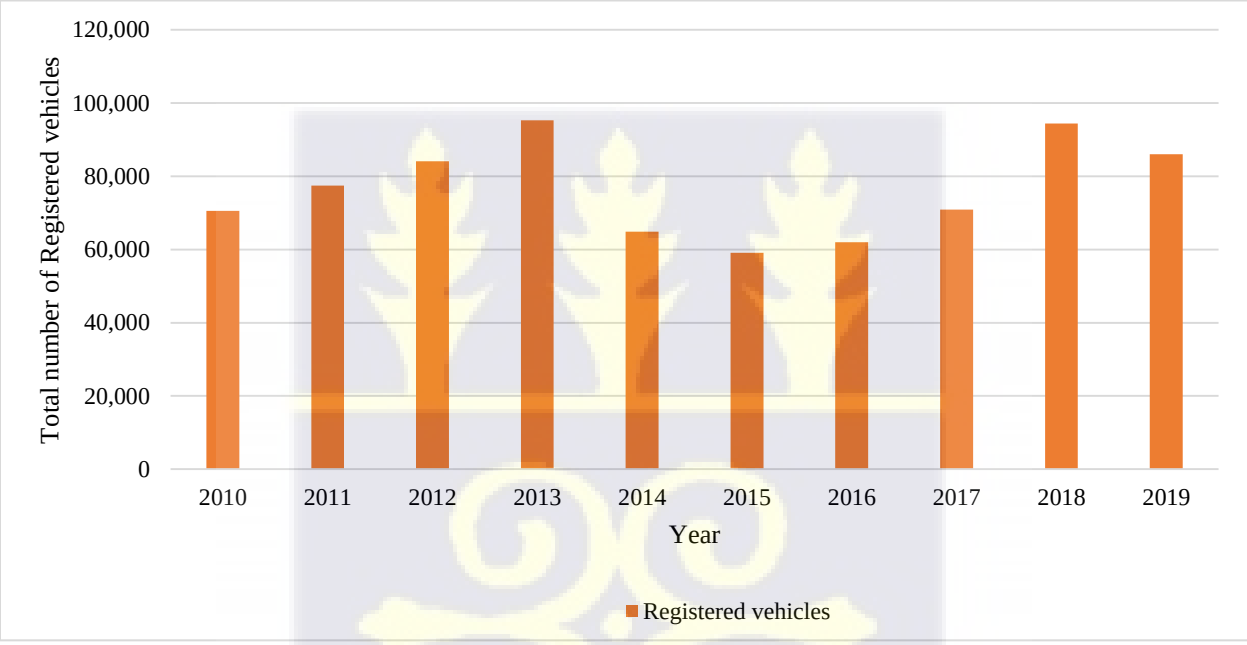

Figure 2.1 Plot of annual summary of registered vehicles from 2010-2019 in Accra (50).

Biomass burning is another significant origin of atmospheric particulate matter pollution in Ghana. Ghana's most prevalent solid fuels are wood and charcoal (51). Over 60% of Accra's inhabitants use biomass fuels (charcoal or firewood) as their main cooking fuel, according to research conducted in 2011 by Zhou (52). Mudu (47) identified the following as the country's top air quality concerns in his work on Ghana's environmental pollution - open waste burning, poorly maintained

automobiles, inefficient fuel utilization, unplanned modes of transportation, widespread bushfires, industrial estates and inefficient cook stoves.

2.4 AN OVERVIEW OF GHANA'S CLIMATE

Ghana is located on the western coast of Africa, along the Gulf of Guinea, as seen in Figure 2.2. The location is situated within the latitudes of 4.5°N and 11.5°N and the longitudes of 3.5°W and 1.3°E. The country has a land area of 238,533 km^2 and a water area of 110,000 km^2 (53). Ghana is bordered by the Republic of Togo to the east, Côte d'Ivoire to the west, Burkina Faso to the north, and the Gulf of Guinea or the Atlantic Ocean to the south. The country has 16 administrative regions.

Ghana has a tropical and humid environment. Three distinct air masses: the Tropical Maritime Air Mass (mT), also known as the South-West Monsoon; the Tropical Continental Air Mass (cT), also known as the North-East Trade Wind; and the Equatorial Eastern (E) air mass, all have an impact on Ghana's climate. The South-West Monsoon, which originates from the Atlantic Ocean, and the Tropical Continental Air Mass known as Harmattan, which comes from the Sahara Desert, intersect at the Inter-Tropical Convergence Zone (ITCZ). The ITCZ is a region of low atmospheric pressure where these two air masses come together (54,55). Most parts of the country have two seasons of heavy rainfall. Normally, the northern regions of the nation have a single rainy season spanning from May to September. In southern Ghana, there are two distinct periods of rainfall. The primary rainy season occurs from April to July, while the secondary rainy season occurs from September to November. The Inter-Tropical Convergence Zone (ITCZ) is the region where the arid and dusty air mass originating from the Sahara Desert in the northern hemisphere intersects with the cool and humid air mass from the South Atlantic monsoon in the southern hemisphere.

Figure 2.2 Map of Ghana illustrating its 16 administrative regions and their respective boundaries (56).

Typically, wooded areas receive higher amounts of rain and have lower temperatures compared to coastal areas. In contrast, the northern Savannah region has harsh and dry weather, with daily

temperatures consistently exceeding 41 °C during much of the year. The annual movement of the Inter-Tropical Convergence Zone (ITCZ) from north to south is what causes the nation's fluctuation in precipitation patterns throughout the year. As indicated earlier, the Inter-Tropical Convergence Zone (ITCZ) is the region where the arid and dusty air mass originating from the Sahara Desert in the northern hemisphere intersects with the cool and humid air mass originating from the South Atlantic monsoon in the southern hemisphere (57–59). Figure 2.3 illustrates the movement of the northern and southern Inter-Tropical Convergence Zones (ITCZs). The northeasterly Harmattan winds, originating from the Sahara Desert, blow in a south-west direction from October to April. These winds bring chilly and dusty conditions, resulting in reduced visibility to less than 1 km and somewhat lower nighttime temperatures. Addaney (60) has shown that the Harmattan phenomenon is prevalent in the northern regions from November to March. Additionally, it temporarily affects the southern coastal districts for a period of a few weeks to a month in December and January.

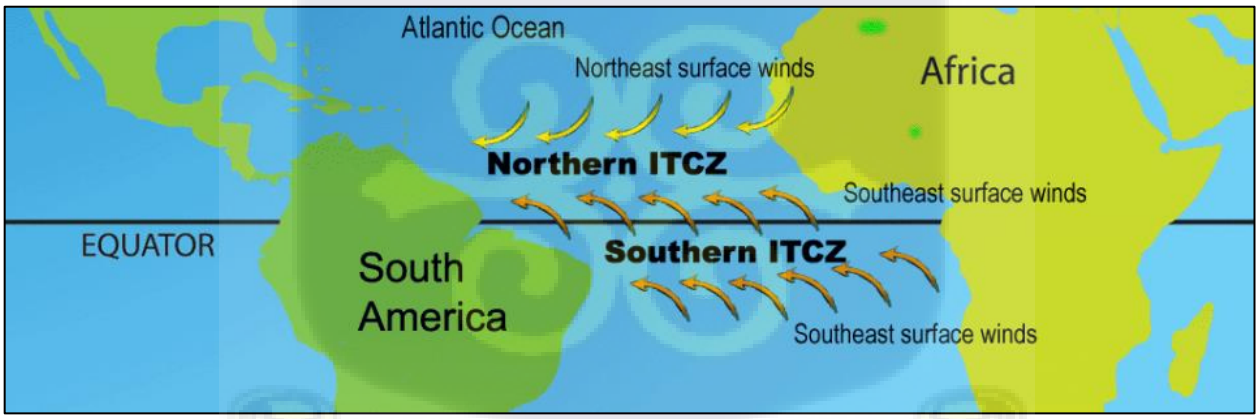

Figure 2.3 Inter-Tropical Convergence Zones' Movements (61).

The average annual rainfall in the north is between 750 and 1050 mm, while the upper East receives an average of 2,000 mm annually. The annual average precipitation in the southern and

southwestern regions of the nation varies between 1,250 and 2,050 mm. Large bodies of water, such as the ocean, rivers, lagoons, and streams, have an effect on the relative humidity. The relative humidity in the northern and southern sectors of the country varies between 70% and 80% respectively (62,63). Moreover, the country's temperatures vary with the seasons and altitude. March and August have the highest and lowest temperatures, respectively, in the majority of the country. The typical temperature ranges between 25 ℃ and 30 ℃ (57,64).

2.4.1 LOCAL CLIMATE

Ghana has six distinct agro-ecological zones, namely the Sudan Savannah, Guinea Savannah, Coastal Savannah, Forest/Savannah Transition Zone, Deciduous Forest Zone, and Rain Forest Zone (as shown in Figure 2.4). Accra is situated in the coastal-savannah region, characterized by a moderately humid climate and a low annual precipitation of 600 mm to 900 mm. On average, Accra receives approximately 800 mm of rainfall, which is spread over fewer than 80 days per year. Typically, the relative humidity is considerable, fluctuating between 65% during the day and 95% throughout the night (58,65,66).

The main rainy season in Accra occurs from April to July, whereas the secondary rainy season is from September to October (Table 2.2). The main season of aridity takes place from November to mid-March or early April (67). The current period of less rainfall coincides with the Harmattan period, which usually takes place between November and March. The Harmattan is a parched and dusty wind originating from the northeast, blowing from the Sahara Desert. The mean temperature range in the city is 21℃ to 44 ℃ (68). The city's closeness to the equator results in a consistent and equal length of daylight throughout the year. The dominant wind direction in Accra is mostly from the west-southwest to the north-northeast sectors, with average wind speeds ranging from 8

km/h to 16 km/h. In May 2021, the wind speed in Accra reached a maximum of 61.1 km/h, while in December 2022, it peaked at 75.63 km/h.

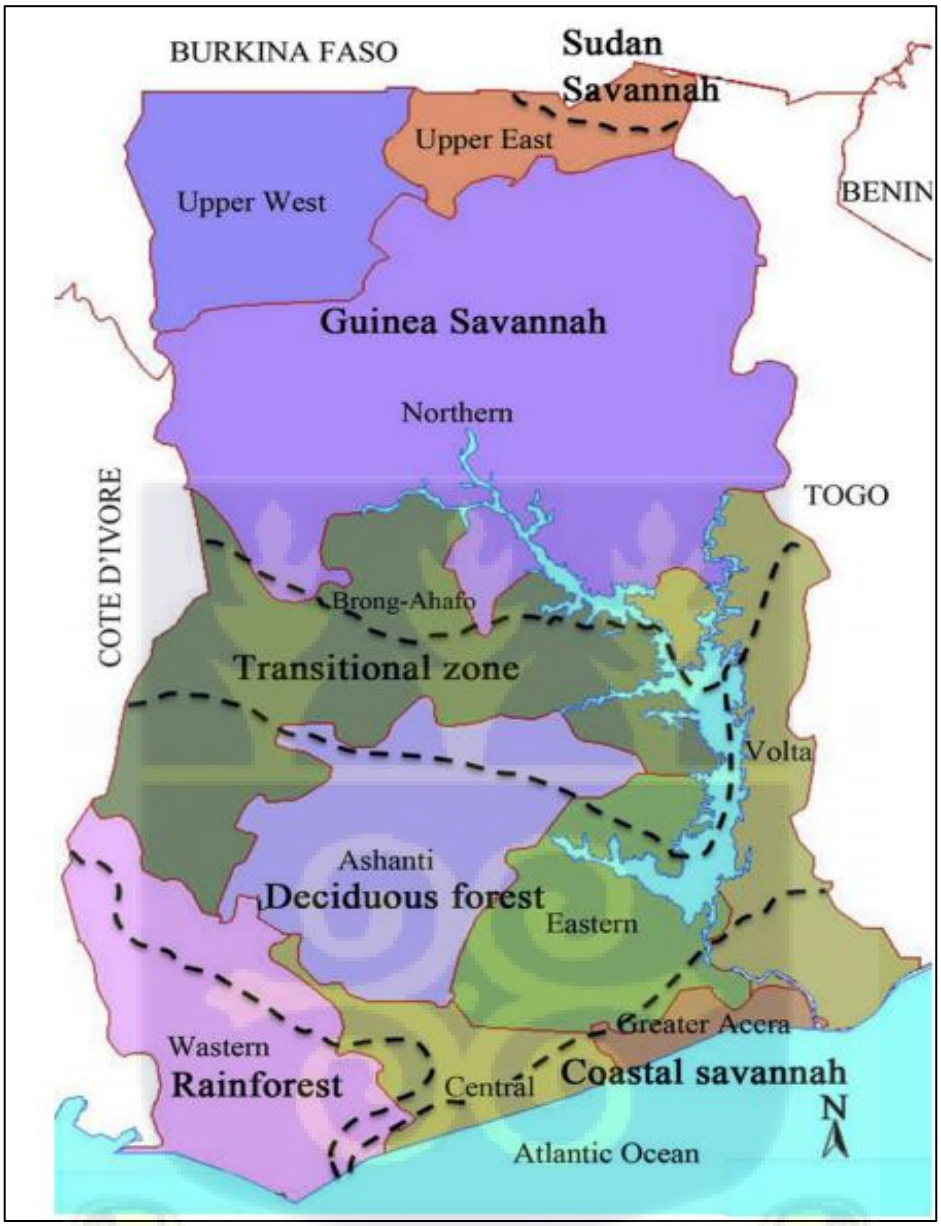

Figure 2.4 Map of Ghana illustrating the six agro-ecological zones (65).

Table 2.2 Typical rainfall patterns in Ghana's agro-ecological zones.

Agro-ecological zone	Area (km^2)	Mean annual rainfall (mm)	Range (mm)	Major rainy season	Minor rainy season
Sudan Savannah	2200	850	800-900	May – Sept	-
Guinea Savannah	147900	1000	800-1300	May- Sept	-
Transitional zone	8400	1300	1100-1500	Mar-July	Sept – Oct
Deciduous forest	66000	1500	1200-1700	Mar-July	Sept-Nov
Rain forest	9500	2000	800-2900	Mar-July	Sept-Nov
Coastal Savannah	4500	800	600-1200	Mar-July	Sept- Oct

(-) = Region experiences single maxima rainfall (69).

2.5 PARTICULATE MATTER AND WEATHER PARAMETERS

When studying ambient particulate matter, it is crucial to take into account meteorological parameters. This is because these parameters can impact the chemical transformations that happen in the air, the movement and scattering of pollutants in the atmosphere, and the rates and mechanisms by which pollutants are removed from the atmosphere. Research has shown that several meteorological elements, such as temperature, relative humidity (RH), wind speed, wind direction, and precipitation, influence the levels of $PM_{2.5}$ in the surrounding air (70–74).

2.6 ORIGINS OF PARTICULATE MATTER (PM) IN URBAN ATMOSPHERE

Urban settings are characterized by a diverse range of sources that contribute to the presence of particulate matter. These sources are natural (produced without human intervention) or anthropogenic (caused by human activity) (44,75,76). The sources of natural aerosols are

uncontrollable, whereas the sources of anthropogenic aerosols are controllable, albeit challenging. Natural and anthropogenic emissions are both impacted by industrial development and human activity. Industrial development and human activities substantially affect both natural and manmade pollution emissions. Anthropogenic emissions, including those from fossil fuel combustion, industrial activities, and transportation, rise directly with industrial expansion. These operations emit significant quantities of pollutants such as Sulphur dioxide (SO_2), nitrogen oxides (NO_x), and particulate matter (PM), which deteriorate air quality and exacerbate climate change. Natural emissions are indirectly influenced by industrial and anthropogenic activities. Deforestation, agriculture, and urbanization modify ecosystems, resulting in heightened emissions from soil and vegetation. Wetland drainage and livestock agriculture exacerbate natural methane (CH_4) emissions, whereas fertilizer use increases ammonia () emissions. Industrial activities similarly exacerbate global warming, amplifying natural phenomena such as wildfires, which emit substantial quantities of carbon dioxide (CO_2) and particulate matter (PM). Moreover, anthropogenic alterations to atmospheric chemistry affect natural emissions. Elevated concentrations of anthropogenic pollutants can influence the atmospheric oxidation capacity, hence influencing the generation of secondary pollutants such as ozone and Sulphate aerosols from natural precursors.

Consequently, industrial expansion and human activity not only exacerbate anthropogenic emissions but also interfere with natural processes, establishing a complicated feedback loop that accelerates environmental and atmospheric alterations.

When examining the impact of air pollutants on health, especially in densely populated metropolitan areas, it is essential to recognize the role of human activities as the primary causes of

pollution. Consequently, efforts to mitigate air pollution primarily target these anthropogenic sources. Table 2.3 provides a concise summary of the primary causes of air pollution.

Table 2.3 Major air pollutant sources

Source type	Source	Causal action
Natural	Volcano eruption.	Release of solid particle, gases and heat waves.
	Sand storm	Dust particles spread through wind circulation around the earth.
	Vegetation fire	Smoke from wildfire or forest management.
	Plant Pollen	Spread of plant pollen through wind motion.
	Sea spray	Liquid droplets spread through wings near coastlines.
Anthropogenic (man-made)	Transport	The process of burning petrol or diesel fuel results in the production of particles and gases.
	Power generation	Emission of particles and gases.
	Industry	The activities include the production and fabrication of steel, non-ferrous metals, textiles, petroleum refining, and material handling.
	Construction	Particle pollution caused by the processing of materials and other related operations.
	Agriculture	Emissions resulting from the act of ploughing and the application of fertilizers, herbicides, and insecticides.
	Domestic	Indoor combustion of solid organic substances, including charcoal, firewood, dung, and agricultural leftovers.

Source (47).

2.6.1 NATURAL SOURCES

Natural sources of particulate matter include wind-borne dust, Harmattan dust, natural vegetation (such as plant fragments, microorganisms, pollen, etc.), wildfires, and sea spray. Most natural aerosols consist mostly of crustal debris, biogenic matter, and sea salt. The dust that the wind picks up from construction sites, roads, and other natural surfaces is the primary origin of crustal elements, including Si, Ca, Fe, Al, Mg, K, Na, Ti, and O. Pollen, spores, and microorganisms, including viruses, bacteria, fungi, protozoa, algae, and insect fragments, are types of particles that constitute the main biogenic aerosol particles. In urban and suburban settings, viruses and bacteria are larger in size compared to plant residues and fungal spores, which fall under the coarse-mode category in terms of particle size (28,77).

2.6.2 ANTHROPOGENIC SOURCES

Urban and industrial regions are the primary producers of anthropogenic particulate matter. In some regions, human-caused emissions may reach levels of several undesirable chemical substances (pollutants) that greatly diminish the quality of the air and visibility (78–80) and can pose human health risks (1,81,82). Human-generated aerosols consist of primary pollutants such as carbon components, heavy metals, secondary carbonaceous material (organic carbon), and inorganic compounds including nitrates, sulphates, ammonium, and water.

Human activities are responsible for the emission of particulate matter and the gases that lead to its formation. These activities include the release of pollutants from many sources, such as automobiles, factories, cooking and heating practices, agricultural operations, wood burning, electricity production from plants, heavy-duty diesel engines, construction and demolition activities, and the disruption of land leading to the development of dust (83–85). They are mostly generated by the processes of fossil fuel burning, the wearing out of tyres and brake pads, and the

re-suspension of dust particles (86–90). Industrial processes, such as incineration, manufacturing, and smelting, produce a variety of heavy metals, including lead (Pb), cadmium (Cd), copper (Cu), zinc (Zn), vanadium (V), chromium (Cr), manganese (Mn), cobalt (Co), nickel (Ni), arsenic (As), and barium (Ba).

2.6.2.1 PARTICULATE MATTER EMISSION BY VEHICLES

The transportation sector is the primary source of urban air pollution (91). The World Health Organization (WHO) estimates that vehicle emissions account for approximately 98% of urban air pollution in low- and middle-income countries (92). The swiftly increasing number of motor vehicles in the urban areas of developing nations poses a grave threat to the population's health.

Most of the particles released by automobiles in traffic fall into the submicron or fine-mode range. These particles have the ability to profoundly infiltrate the respiratory system, namely the alveolar areas of the lungs. The major elements responsible for vehicle emissions problems in urban areas in sub-Saharan Africa are the widespread presence of obsolete and poorly maintained cars without catalytic converters, together with the utilization of low-grade fuel (93). In addition, the increasing number of used vehicles and inadequate road networks have caused traffic congestion in the majority of African cities. Nearly 70% of imported vehicles into Ghana are used vehicles (94). Congestion can significantly increase vehicle emissions, leading to elevated human exposure to traffic-related pollutants (95). Urban traffic congestion impedes economic growth, endangers public health, and reduces the overall quality of life.

Tailpipe emissions from diesel and gasoline-powered automobiles in urban settings are recognized as a major contributor to primary and secondary man-made aerosols. Urban road traffic emissions come from several sources, including vehicle exhaust or tailpipe emissions resulting from the

combustion of gasoline and lubricating oil, as well as particle emissions from cars that are not emitted via their tailpipes (96). Early studies indicate that in developed nations, exhaust emissions are primarily responsible for fine particulate matter (PM), and non-exhaust emissions are primarily responsible for coarse PM. Particles produced by incomplete combustion in internal combustion engines constitute vehicle discharge emissions.

Elemental carbon (EC) and organic carbon (OC) are the predominant components of the particulate matter released by vehicle exhaust. The emissions released from the exhaust pipe are influenced by factors such as the engine's type and age, the kind of gasoline and lubricant used, and the design of the vehicle (97–99). Cu, Zn, Pb, Br, Fe, Ca, Cr, and Ba are among the heavy metals frequently associated with automobile emissions (100–102). Non-exhaust emissions are the particles that on-road cars produce. These particulates come from the wear of tyres and brakes, the abrasion of the road surface, and the stirring up of road dust due to turbulence induced by vehicles (101,102).

Brake linings and tyres undergo abrasion, which, together with windblown dust, causes the discharge of particles into the environment. These particles include small amounts of metals such as strontium (Sr), copper (Cu), molybdenum (Mo), barium (Ba), cadmium (Cd), chromium (Cr), manganese (Mn), and iron (Fe). The windblown dust depends on several parameters, such as the condition of the road surface, the level of humidity, the intensity of traffic, and the speed of the wind (103). The road or tyre source is the main contributor to Al, Si, K, Ca, Ti, Mn, Fe, Zn, and Sr, primarily in the larger particle size range. The total amount of particulate emissions from the transportation sector may include particles that are not the result of exhaust. Nevertheless, the absence of data about non-exhaust emissions in poor countries poses a challenge to accurately measuring their impact on overall ambient concentrations.

2.7 PROPERTIES OF AEROSOLS

2.7.1 SIZE DISTRIBUTION

The size of particles is the primary determinant of their attributes, affecting their production, physical and chemical characteristics, transformation, movement, and elimination from the atmosphere (104–106). The fundamental determinant of deposition in the human respiratory system is particle size. Arquero and Anglada (107,108) have shown that several processes, such as vapour species condensation, evaporation, wet and dry deposition, and coagulation, alter both the size and chemical content of particles. The impacts of particulate matter on people, plants, and materials vary based on the chemical compositions of these particles.

The dimensions of a particle have a significant impact on its volume, mass, settling velocity, transportation, deposition, and movement within the environment (3,44). Previous research conducted by Fakinle and Falaiye in 2020 has classified particles based on their physical dimensions, which span from a few nanometers (nm) to tens of micrometers (µm) in diameter (109,110). The magnitude of particles plays a pivotal role in determining their impact on human health and the environment (111). Particulate matter ranging from 0.1 to 10 µm in diameter is recognized to have significant impacts on human health, climate, and the environment (108,112). The term "diameter" is often used to describe the size of particles. Particle size is measured using an "equivalent" diameter, which is determined by a physical attribute rather than a geometric one, considering differences in shape and density. The aerodynamic diameter is a commonly utilized metric to represent a particle's comparable size (113,114). The term refers to the diameter of a sphere with a density of 1 g cm^{-3} that experiences the same rate of descent in air as the particle being studied (112,113). Equation 2.1 gives the particle aerodynamic diameter, as D_p.

$$D_p = D_g k \sqrt{\frac{P_p}{P_o}} \qquad \textbf{2.1}$$

where D_g is the particle geometric diameter, ρ_ρ is the density of the particle, ρ_o is the reference density (1 g cm^{-3}), and k is a shape factor, which is 1.0 in the case of a sphere (112). Unless otherwise specified, particle diameter in this work refers to the aerodynamic diameter.

Atmospheric particulate matter is often categorized into ultrafine particles for the purpose of regulatory control and assessing its impact on human health ($PM_{0.1}$: $D_p < 0.1$ µm), fine or respirable ($PM_{2.5}$: $D_p < 2.5$ µm), and coarse or inhalable (PM_{10}: $D_p < 10$ µm) particle size fractions. The majority of inhalable particles are deposited in the upper respiratory tract or nose system. Smaller particles, also known as thoracic particles, are deposited in the pulmonary or lung system and remain in the body. The distinction between PM_{10} µm and $PM_{2.5}$ µm particles is essential because of their varied sources, creation techniques, compositions, atmospheric durations, geographical distributions, and temporal fluctuations, all of which have detrimental impacts on human health (115). The main objective of regulating particulate matter is to decrease the mass concentrations of both PM_{10} µm and $PM_{2.5}$ µm rather than emphasize number of concentrations.

2.7.2 MODES OF FORMATION

Particle size distributions in the atmosphere exhibit non-uniformity. Instead, when mass or volume is plotted against aerodynamic diameter (Figure 2.5), particles tend to show a trimodal size log-normal distribution. These modes are a reflection of the various source categories and atmospheric transformation processes (116,117). Usually, the three distinct modes or fractions are classified as follows:

(a) Nucleation mode: $D_p < 0.1$ µm

(b) Accumulation mode: 0.1 µm < D_p< 2.5 µm and

(c) Coarse or sedimentation mode: $D_p > 2.5$ µm

2.7.2.1 NUCLEATION MODE

Nucleation mode particles, often referred to as "nuclei mode" or "Aitken mode" particles, are produced through the condensation of heated vapours in combustion processes and the transformation of gas into particles in the atmosphere. Nuclei-mode particles are recently generated particles with a diameter below 10 nm that are produced as a consequence of active nucleation processes. Due to higher precursor concentrations, smaller particles that are developing experience coagulation or nucleation, which results in the formation of these particles (90,113,117).

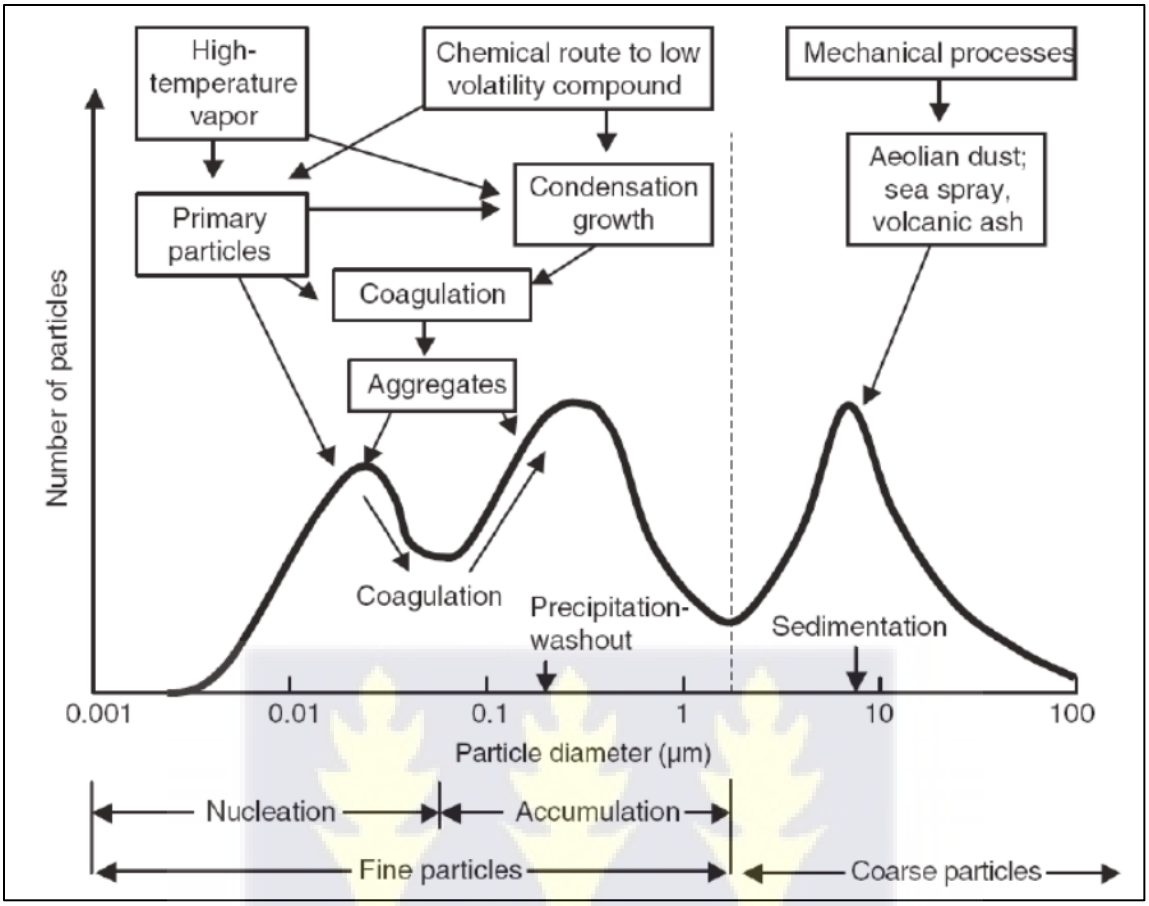

Figure 2.5 Pattern of particle distribution, deposition, and combination in the air (118).

The nucleation, or Aitken mode, contains the largest quantity of particles. Yet, their small diameters have a minimal impact on the total mass. Nucleation-mode particles in the atmosphere have a brief lifespan, often ranging from a limited minutes to some hours, as they quickly combine with larger particles through coagulation or grow in size through condensation. Their elimination occurs via the process of raindrop diffusion. Ultrafine particles include the nucleation mode as well as a substantial proportion of the Aitken mode.

2.7.2.2 ACCUMULATION MODE

Accumulation mode particles are a diverse group of particles that are often formed by the merging of smaller nuclei mode particles and the conversion of gas-phase vapours into solid or liquid

particles that attach to existing particles (116). Particles in the accumulation-size range can be emitted into the atmosphere due to the incomplete combustion of wood, oil, coal, petrol, and other fuels. Typically, these particles include substantial amounts of organic and soluble inorganic compounds, including ammonium, nitrate, and Sulphate (119).

Due to their expansive surface area, they make up a substantial proportion of the overall particle mass. The nomenclature of the mode indicates that particle removal techniques are ineffective within this size range. As a result, they may be carried across long distances and remain in the atmosphere for many days or weeks. Furthermore, they are responsible for the bulk of the reduction in vision in arid atmospheres. Surface water drainage or precipitation can remove particles from the atmosphere when it is in accumulation mode (120). The process of particles coming together and forming in the accumulation and nucleation phases is commonly known as fine particles.

2.7.2.3 **COARSE MODE**

Mechanical processes like grinding, wind, or erosion are primarily responsible for producing coarse or sedimentation-mode particles. Coarse particles consist mostly of human-made and natural dust particles that disappear from the atmosphere quickly via sedimentation and collision (116). Raindrops can also eliminate them. Additionally, inorganic substances like sand or sizable salt particles from sea spray typically dominate the chemical composition of coarse particulates. Due to the limited coagulation strength of particles in the accumulation mode, only a small proportion of their mass is transferred to the coarse mode. Together with the accumulation mode, they constitute the majority of the mass of suspended particles. Their residence period in the atmosphere is limited to a few hours or days, depending on factors such as their size, prevailing meteorological conditions, and altitude (121).

2.8 CHEMICAL COMPOSITION

Fine and coarse particulate matter have significantly distinct chemical compositions, indicating that they originate from different sources (44). Various factors such as the pollution source's location, atmospheric chemical processes, time of day, and meteorological conditions greatly influence the composition of these particles (122). Additionally, human-caused elements, such as the level of urban development, industrial and agricultural operations, and the kind and amount of vehicle movement, impact the makeup of particulate matter.

Typically, particles have a chemical makeup that consists of a mixture of species originating from several sources. Particles usually contain a chemical composition that includes a blend of species from many origins. The particles may contain varying levels of Sulphate, ammonium, nitrate, sea salt (sodium and chloride), trace metals, crustal components, and carbonaceous substances (123–125). A precise understanding of the chemical makeup of aerosol particles is essential for assessing their impact on human health and the environment. To comprehend the physical and chemical processes of aerosols and determine the origins and impacts of ambient particles, it is essential to analyze the chemical composition of particulate matter.

Anthropogenic and natural Sulphur-containing substances, such as Sulphur dioxide (SO_2) and dimethyl Sulphide (DMS), undergo oxidation and serve as the primary origin of atmospheric Sulphates (119). The predominant Sulphate included in the fine portion of PM is ammonium Sulphate, with a smaller amount of marine-derived sodium Sulphate being detected. Sulphur dioxide emissions originate from both natural and anthropogenic sources.

Anthropogenic SO_2 emissions are generated by burning fossil fuels, biomass, agricultural waste, metal smelting, and other industrial operations (126,127). Among the natural sources of SO_2 emissions are the oxidation of dimethyl sulphide (DMS), primarily in the form of sea salt, and

wildfires (128). In 2021, the World Health Organization (WHO) determined that the average yearly levels of sulphur dioxide in metropolitan regions of underdeveloped nations varied between 60 and 130 μgm^{-3}. In North America and Europe, the concentrations ranged from 15–35 μgm^{-3}, while in European Union (EU) cities, the concentrations ranged from 8–25 μgm^{-3} (129).

Nitrate (NO_3^-) is a major component of atmospheric aerosols, which are predominantly oxidized nitrogen oxides (NO_X). Nitrate is present in both coarse and fine particulate matter. The main origin of nitrate in fine particles is the chemical interaction between gaseous nitric acid and gaseous ammonia, resulting in the formation of ammonium nitrate. The main origin of nitrate in large particles is the interaction between gaseous nitric acid and pre-existing large particles. Additionally, temperature and relative humidity have a significant impact on the amount of nitrate in the atmosphere (130). Chloride is mostly emitted in the form of sodium chloride (NaCl), mainly from sea salt particles. Chlorides enter aerosol particles as a result of hydrochloric acid (HCl) vapour neutralizing with ammonia. Particulate matter includes carbonaceous substances, comprising elemental carbon and organic carbon. Elemental carbon (EC) is sometimes referred to as black carbon (BC) or smog. It primarily enters the atmosphere from the combustion of biomass and fossil fuels and has a chemical makeup similar to that of impure graphite. Ethyl carbamate (EC) is often used as a marker to track the release of pollutants from vehicles driven by diesel fuel. The carbonaceous aerosol portion is mostly composed of organic carbon (OC). The emissions originate from the combustion of fossil fuels, the burning of biomass in residential areas, the cooking of meat, and biogenic sources (131,132).

Coarse particles mostly include crustal minerals such as aluminium (Al), silicon (Si), calcium (Ca), titanium (Ti), magnesium (Mg), and iron (Fe). The proportion of these components changes depending on the geological characteristics of the area and the prevailing surface conditions. Both

tiny and coarse particles may contain potassium (K). The source of potassium in coarse PM is the soil, while the source of potassium in fine PM is the burning of biomass. Both fine and coarse particles include trace elements including sodium (Na), potassium (K), iron (Fe), chromium (Cr), cobalt (Co), nickel (Ni), manganese (Mn), copper (Cu), selenium (Se), barium (Ba), chlorine (Cl), gallium (Ga), cesium (Cs), europium (Eu), tungsten (W), and gold (Au). Residential wood combustion and forest fires release trace elements into the atmosphere via the burning of biomass. The main source of trace metals found in fine particulate matter is human activity, including the burning of fossil fuels, the incineration of garbage, and the refining of metals. Many of these components may function as indicators of certain origins. Sodium (Na) is a tracer mostly found in sea salt. Similarly, silicon and aluminium serve as indicators for mineral dust, whereas elemental carbon particles are mostly produced as byproducts of combustion. Ultimately, the vaporous substances that give rise to the secondary constituents (sulphate, nitrate, and ammonium) may be seen.

2.9 ANALYTICAL METHODS

Concentration of elements in airborne particulate matter tells their process of generation. Thus, to detect the sources of particulate matter, it is essential to determine their elemental and/or chemical composition. The primary goal of measuring and analyzing particulate matter is to identify the origin of the particles and, where relevant, investigate the physical and chemical processes that take place inside the particles as they are transported through the atmosphere.

Various pieces of equipment are available for measuring different features of ambient particulate matter. The primary metrics for assessing aerosols are the concentration of particles and the size of particles that are deposited on a filter substrate. Filter sampling is cost-effective in comparison to online measurements, but it requires manual procedures and the analysis of a substantial number

of filters before any significant deductions can be drawn. Analyzing the chemical makeup of particulate matter in the air is essential for assessing emissions from different sources that emit these particles. To achieve accurate gravimetric analysis, it is necessary to use filters that have low dielectric constants, good filter integrity, and are inert towards water vapour and other gases. By using a low temperature and relative humidity equilibrium, it is possible to remove water-filled particle deposits effectively. Nevertheless, some particles have the potential to vaporize if they are exposed to the surrounding atmosphere for a period exceeding one or two days (133,134).

Depending on the amount of air drawn through a filter, with sometimes-high ambient particle levels, only a small amount of sample is available for chemical analysis. Typically, the amount of particulate matter loading on a low-to medium volume sampler is less than 5 mg and usually, many of the chemical species of interest that need to be measured are less than 1µg in the deposit. The importance of any analytical technique in environmental science is to conduct measurements in order to achieve a targeted goal. Hence, it is essential that the sample and testing methods be appropriate. Therefore, in this study and any other analysis, it is necessary to determine the qualitative characteristics of the sample and the quantitative measurements or concentrations present in order to make well-informed conclusions. When analyzing particulate matter, it is crucial to consider three key aspects in all analytical procedures, especially when dealing with tiny deposits of collected mass. These factors depend on the specific analytes of interest including:

- Specificity: is the ability of an analytical technique to differentiate between a certain substance and other similar chemicals.

- Sensitivity: refers to the capacity of an analytical procedure to identify certain elements at low concentrations that are of interest. This ability may vary across different instruments

due to factors such as the frequency of the X-ray generator, the sensitivity of the multichannel analyzer, and interferences from the sample.

• Detection limit: refers to the minimum concentration or quantity that can be accurately determined (7, 17, 18).

Various analytical techniques are available to determine the elements present in a substance on a filter medium. These methods include gas chromatography-mass spectrometer (GC-MS), thermo-optical and light scattering techniques (for measuring total, organic, and black carbon (BC), proton (or particle) elastic scattering analysis (PESA), energy dispersive x-ray fluorescence (EDXRF), proton-induced x-ray emission (PIXE), total reflection x-ray fluorescence (TXRF), synchrotron-induced x-ray fluorescence (S-XRF), and scanning electron microscopy with x-ray fluorescence (SEM/XRF) (138–143).

In general, the equipment required for analysis of airborne particulate matter depends on their convenience, sensitivity, accuracy and precision. Several spectrometric techniques rely on the electromagnetic spectrum that the sample under study emits or absorbs. The elements or chemical substances in the sample are identifiable by their spectra. Analyses are performed by comparing sample results to calibration standard values acquired under identical conditions. Instruments often include devices that are designed to isolate certain discrete energy levels or ranges of energies (or wavelengths) for accurate measurement.

The spectrometric methods to be applied depends on the electromagnetic spectrum that the sample being studied emits or absorbs. The spectra provide an accurate representation of the chemical elements or compounds in the sample. Analysis is performed by contrasting sample results with calibration standard results acquired under identical circumstances. The crucial component of such

equipment is the inclusion of devices that can effectively isolate and measure a specific discrete energy or a range of energies (or wavelengths).

The energies (or wavelengths) that analytically relevant elements and chemical compounds emit or absorb span from the gamma- and x-ray (< 100 Å or 10^{-8}m) through the ultraviolet, visible, and infrared (7000 Å) spectrums. One spectrometer cannot cover the entire range, which is roughly 1–150,000 eV. Therefore, instruments with good performance in a variety of applications are versatile and valued. This category includes the widely used X-ray spectrometers, particularly X-ray Fluorescence (XRF) and electron probe analysis systems currently used worldwide.

2.10 SAMPLING OF ATMOSPHERIC PARTICULATE MATTER

There are several techniques available to determine the integrated mass concentration of particulate matter in the atmosphere. Gravimetric techniques based on filters are the most typical and conventional method. Almost exclusively, mass measurement of filters in a laboratory setup uses gravimetric analysis. Gravimetry calculates the filter's pre- and post-sampling weights using a microgram-sensitive balance in a temperature and relative-humidity controlled environment to determine the net mass (44). The gravimetric technique is used to quantitatively collect airborne particulate matter on a filter. This is achieved by pulling air into a particle-size classification intake via a pre-weighed Teflon filter. The process is driven by a high-flow electrical pump (7, 20). For collecting samples of particulate matter, the ARA N-FRM sampler uses a measuring method based on gravimetric analysis. This process spans a duration of 24 hours and utilizes 47-mm Teflon filters. At the conclusion of this time, the exposed filters were manually taken out of the ARA N-FRM samplers and put in Petri dishes. Manual samplers are required for sampling airborne particles for gravimetric mass determination. A sampler equipped with an internal filter is

primarily used to achieve comprehensive sample collection and get a concentration measurement that is averaged over time.

2.10.1 DESCRIPTION OF FILTER MEDIA AND AEROSOL SAMPLER USED

2.10.1.1 FILTERS

In finding the composition of atmospheric particles, one of the most common methods entails the analysis of deposits collected on filter substrate. Gravimetric analysis is mainly used to attain mass measurements of filters in a laboratory environment. Gravimetry determines the net mass by weighing the filter before and after sampling with a microgram-sensitive balance in a temperature- and relative humidity-controlled setting. Accurate gravimetric analysis requires the use of filters with low dielectric constants, high filter integrity, and inertness with respect to absorbing water vapour and other gases.

Filters are permeable media for collecting aerosol particles. Aerosol sampling filter comprise a plastic membrane with small pores or a tightly woven fiber mat. Fibrous filters and membrane filters are the two main categories of filters. Low-pressure drop and good collection efficiency for all particle sizes are two characteristics of fibrous filters. Quartz, cellulose, glass, and plastic fibers are a few of the primary fiber types used as filter. Particles larger than 0.3 microns have a strong tendency to be retained by glass and quartz fiber filters (144). Fibrous filters are categorized by two important qualities: they have a low-pressure drop and exhibit great collection efficiency for particles of all sizes. The filter utilizes many key fiber types, including quartz, cellulose, glass, and plastic fibers. Particles of a size above 0.3 microns have a pronounced inclination to be captured by filters made of glass and quartz fibers.

Membrane filters retain particles on the filter's surface, allowing for non-depth studies such as X-ray fluorescence (XRF). They exhibit characteristics of increased flow resistance and decreased loading capabilities in comparison to fiber filters, resulting in greater costs. Commonly used membrane filters include Teflon, polyvinyl chloride (PVC), cellulose ester, and polycarbonate. The filter media for event monitoring must possess suitable physical and chemical characteristics that align with the sampling strategy and laboratory analysis methods used.

2.10.1.2 FIBROUS FILTERS

Fibrous filters contain a non-uniform arrangement of fibers that have been compressed together, sometimes with a binding agent, with most of the fibers oriented perpendicular to the airflow direction. In contrast to liquid filtration, which uses microscopic sieves in which only particles smaller than the pore size can pass, these types of filters remove aerosol particles when they impact and attach to the surface of the fibers.

These filters come in sizes from sub-micron to 100 µm and range in porosity from 70 to more than 99%. The most prevalent varieties are glass fiber, quartz, and cellulose (paper). They are ideal for high volume sampling because they have reduced pressure drops across them. Air passes through high-efficiency filters at a slow rate. The filter materials are therefore pleated in order to get a broad filter area in an element of practical size. Particles larger than 0.3 µm are highly retained by glass and quartz fiber filters.

Glass fiber filters possess a significant capacity, although they have a notable downside in their capability to convert Sulphur dioxide into Sulphate, therefore growing the particulate matter burden in their original location. Quartz fiber filters are not affected by this problem. The glass fiber filters are unsuitable for trace element analysis, particularly when using nuclear analytical

methods, due to their very high blank values for many elements. Fibrous filters are inappropriate for EDXRF analysis because of the uneven penetration of particles into the filter matrix. While cellulose filters can be employed for ambient monitoring, sustaining uniform humidity levels for exposed and uncovered filters presents difficulties, leading to minimal utilization.

2.10.1.3 POROUS MEMBRANE FILTERS

Polyvinyl chloride, Teflon (polytetrafluoroethylene, PTFE), sintered metals, cellulose esters, and other plastics are used to create porous membrane filters. They differ structurally from fibrous filters and have porosity levels between 50 and 90 percent lower than the fibrous filters. Through the intricate pore structure, gas flows through the filter in an erratic fashion. As the aerosol is drawn through the filter, particles are deposited on the structural components that form the pores. Even for particles smaller than the manufacturer's specified pore diameters, which are based on liquid filtration, membrane filters have a high efficiency increased airflow obstruction and higher pressure loss compared to other filter types. Table 2.4 shows examples of some characteristics of filters.

Table 2.4 Example of filters and their characteristics (137).

Filter and Filter Composition	Density (mg/cm^2)	pH	Filter Efficiency (%)
Teflon® (Membrane) $(CF_2)n$ (2 µm Pore Size)	0.5	Neutral	99.95
Cellulose (Whatman 41) $(C_6H_{10}O_5)n$	8.5	Neutral (Reacts with HNO_3)	58 % at 0.3 µm
Glass Fiber (Whatman GF/C)	5.16	Basic pH 9	99.0
"Quartz" Gelman Microquartz	6.51	pH 7	98.5
Polycarbonate (Nuclepore) $C_{15}H_{14}+ CO_3^-$ (0.3 µm Pore Size)	0.8	Neutral	93.9
Cellulose Acetate/Nitrate Millipore $(C_9H_{13}O_7)n$ (1.21 µm Pore Size)	5.0	Neutral (Reacts with HNO_3)	99.6

Polytetrafluoroethylene (PTFE) Teflon filters with a ring (Pall Life Science, Teflon filters with a particle size of 0.2 µm and a diameter of 47 mm) were used to collect $PM_{2.5}$ samples for the study. The use of Teflon filters in low-volume sampling is favoured because of their inertness and ability to reduce particle bouncing. Additionally, they provide low background levels for many analytes and produce the clearest infrared (IR) absorbance spectrum (145).

The patented flow technology used in the ARA N-FRM sampler draws air through a particle size-classifying inlet. The sharp-cut ARA VIS-A Cyclone physically selects particles 2.5 µm size fraction and below. The N-FRM inertial separator ($PM_{2.5}$ Impactor) is designed to operate at a nominal sampling rate of 16.7 L/min where particles larger than the cut point (2.5 µm) are removed by impaction onto a slightly greased plate to reduce the risk of particle bounce. The ARA N-FRM

Sampler, shown below incorporates a microprocessor-based active flow control to maintain the sampling rate as ambient conditions and filter loading changes. The sampling rate is monitored and adjusted several times a second and logged at 5-min intervals along with all other important sampling parameters. For each sampling event, the N-FRM Sampler generated a summary of important sampling parameters such as start and stop times, total sampling volume, and average ambient temperature and pressure as well as 5-min averages of all ambient and sampler operational parameters. The filter holder assembly contains a filter cassette in which the 47mm diameter filter is supported by a filter support screen (146). The operational technique of the ARA N-FRM sampler used in this study was derived from the ARA N-FRM sampler operation manual (147).

Figure 2.6 ARA N-FRM Sampler (147).

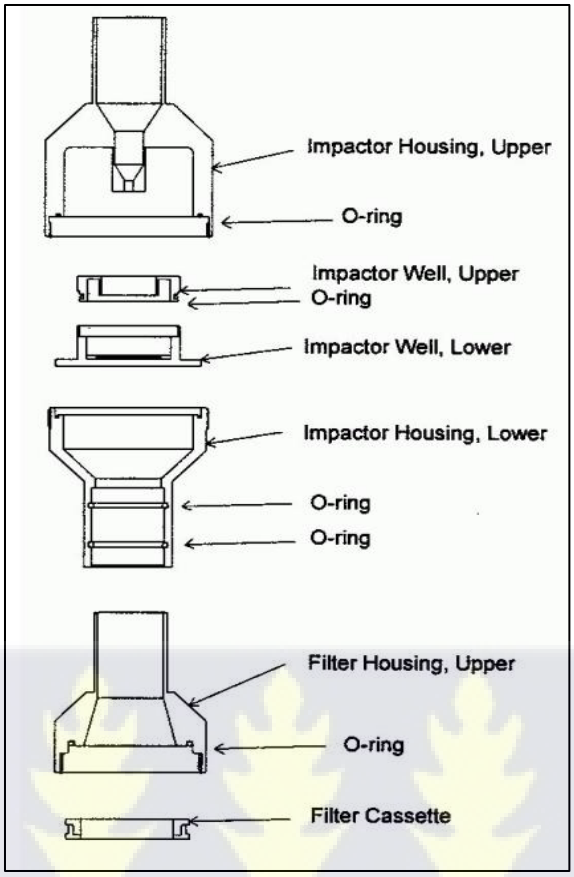

Figure 2.7 Schematic diagram of ARA N-FRM $PM_{2.5}$ impactor well and filter (147).

The choice of aerosol-sampling equipment is determined by the item under examination, its properties, and the specific information needed from the collected data. There are a wide range of methods available for monitoring airborne particulate matter (APM) in investigations on particulate matter (PM) (148). Commonly used particle samplers for $PM_{2.5}$ collection encompass the United States Environmental Protection Agency (U.S. EPA) Federal Reference and Equivalent Method (FRM) samplers, dichotomous samplers, Interagency Monitoring of Protected Visual Environments (IMPROVE) samplers, MiniVol Tactical Air samplers, and ARA N-FRM samplers.

2.11 CHARACTERIZATION OF ATMOSPHERIC PARTICULATE MATTER USING ENERGY DISPERSIVE X-RAY FLUORESCENCE ANALYSIS (EDXRF)

The term "X-ray florescence" refers to a spectrometric system that uses electromagnetic spectrum (X-rays) with wavelengths ranging from 10^{-5} to 100Å. This method entails examining the elemental composition of aerosols collected on a filter material (149). It can analyze the composition of various materials without causing damage, making it useful in a wide range of scientific and industrial applications. This method can provide both qualitative and quantitative data on the concentration of many elements in particulate matter. The application of receptor models for source apportionment as well as source identification work both require this data. Numerous investigations using the EDXRF spectrometry technique on the elemental content of particulate matter have been published (28,44,121,150–152).

In EDXRF technique, a high energetic beam of X-rays irradiation is incident on the sample on the filter. As a result, photoelectrons are ejected from the inner shells of the atoms in the sample. The kinetic energy of these photoelectrons (E-φ) is equal to the energy difference between the incoming particle (E) and the binding energy of the atomic electron (φ). Following a short duration, the atomic electrons undergo reorganization, whereby an electron from a shell with greater energy occupies the empty space created by the expelled electron in the atom's electronic configuration. Fluorescence is the process in which an atom emits an X-ray photon with an energy that matches the difference in energy between its beginning and final states. By detecting a photon and accurately measuring its energy, it is possible to identify the specific element and electronic transition from which it came (153).

Any electron in an atom's inner shells can be evicted, and different electrons can "drop" into the empty space from the outer shells. As a result, there are various permitted transitions that follow

the rules of quantum physics, each of which has a unique energy or line. The three primary kinds of transitions, or spectrum series, are identified by the letters K, L, or M, which represent the shells from which the electron was originally extracted. The K series, the L series, and finally the M series have the highest levels of intensity. Each transition in the series is shown by a subscript that starts with α, β, γ, etc., which tells you the upper energy shell that is relaxing, and then a number that tells you the quantum state inside that upper energy shell (154).

Nevertheless, fluorescence is not the only mechanism for an excited atom to return to its ground state. It rivals the Auger effect by inducing the emission of a second photoelectron to regain stability. Auger effect is, therefore, a radiation-less transition. The fluorescence yield, which increases with increasing atomic number for all three series, describes the relative numbers of excited atoms that fluoresce (154). The ejection of photoelectrons and consequent fluorescence emission of characteristic radiation is not limited to high-energy electrons. Comparable outcomes may be attained by using high-energy X-ray photons, which enable the stimulation of a sample using the emission of an X-ray tube or any other suitable source of photons. In addition, X-rays emitted from a tube are used to stimulate secondary fluorescence, resulting in the emission of photons. These photons are then used to stimulate the sample in different applications of X-ray fluorescence (XRF) spectroscopy (155).

X-rays primarily interact with samples when they strike them through absorption and scattering processes. Compton scattering is the phenomenon where an unpredictable quantity of energy is lost, whereas Rayleigh scattering is the dispersion of an X-ray without any alteration in energy. The phenomenon of X-ray scattering in Energy Dispersive X-ray Fluorescence (EDXRF) is a common problem that results in elevated amounts of background radiation (153). The origin of

this photon may be determined by detecting it and measuring its energy, which allows for identification of the precise element and electronic transition it originated from. This is the foundation for the X-ray fluorescence (XRF) technology, which allows compositions to be categorized quantitatively and qualitatively depending on their rate of emission (156).

EDXRF has many benefits compared to other analytical methods. Some of these benefits are:

- It is non-destructive, thus, samples are preserved after analysis so they can be used for additional analyses using different techniques as necessary.
- It entails little or no sample preparation or operator time after the samples are loaded into the analyzer.
- It is fast and can be used to measure the concentrations of many elements simultaneously with atomic numbers between 11 (Na) to 92 (U).

When a sample's X-ray strikes the detector, it interacts with the detector's material. The X-ray energy induces ionization inside the detector. Each energy photon that enters the detector causes complete ionization, which is then translated into voltage signals. The amplitude of these signals is directly proportional to the energy of the input photons. A pulse processor unit converts the voltage signal into digital pulses which are in turn converted into an energy dispersive x-ray spectrum through a multichannel analyzer. The sample's characteristic X-ray spectrum is used for both qualitative and quantitative analysis (157).

2.11.1 INSTRUMENTATION

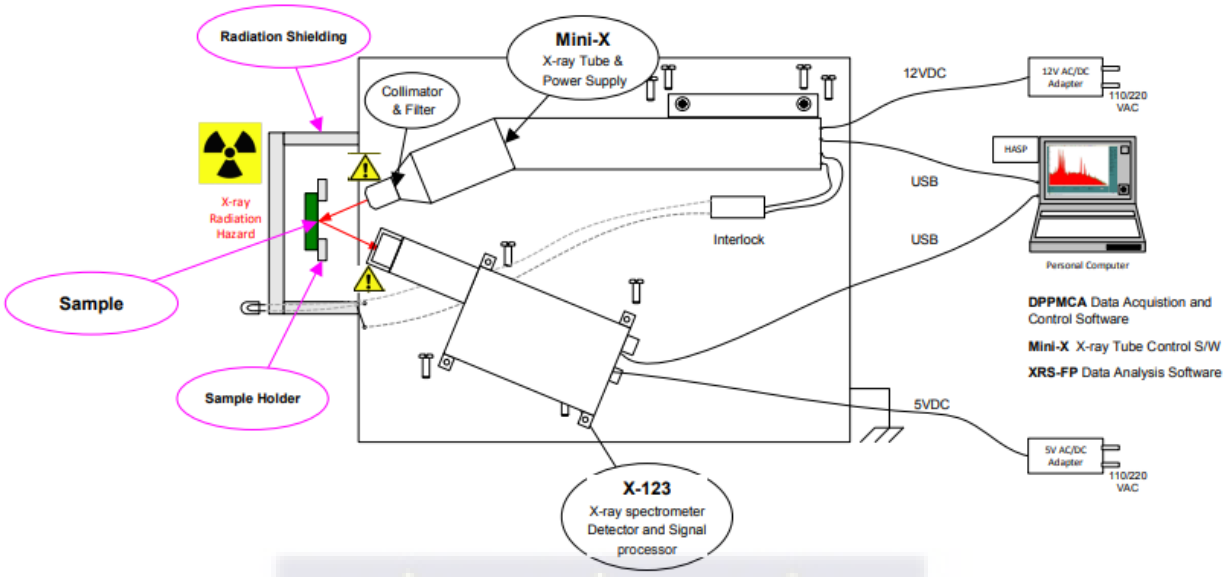

Figure 2.8 Schematic diagram of Amptek XRF spectrometer (158).

The diagram shown above (Figure 2.8) showcases the Amptek XRF kit, which primarily consists of a compact X-ray tube, a high-voltage power supply, a silicon drift detector (SDD), a sample chamber, a digital pulse processor (DPP), and a computer system. The tiny X-ray tube has a silver anode target and emits X-rays with an average energy of 22.1 kilo electron volts (keV). The X-ray tube functions within a voltage range of 5 kilovolts (kV) to 50 kilovolts (kV), and a current range of 5 microamperes (µA) to 200 microamperes (µA). The X-rays are used to irradiate filters containing sampled particulate matter placed on the shielded sample holder. Silicon Drift Detector (SDD) is a form of photodiode that functions similarly to planar photodiodes but has a different electrode structure. It has a substantially lower capacitance than a planar diode of the same area, and because electronic noise is proportional to capacitance at short shaping times, the SDD produces much lower noise at short shaping times. This results in higher count rates and improved energy resolution.

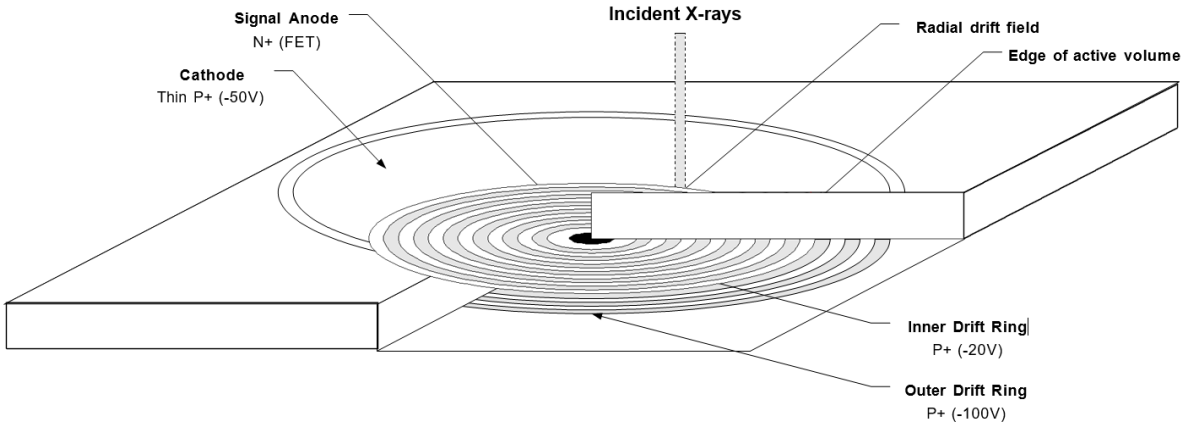

Figure 2.9 Amptek XRF spectrometer Silicon Drift Detector (158).

The electrode configuration of Amptek SDD is depicted in the diagram above (Figure 2.9). A series of drift rings that form a radial field, lead electrons to a very small, low capacitance anode (0.035 pF in an Amptek 25mm^2 SDD). X-rays pass through the planar front contact, which is an extremely thin p + junction with minimal dead layer. The signal anode is connected to a discrete JFET (field effect transistor) where the signal current is collected, and electrons produced throughout the active volume drift to it.

The X-123 Digital Pulse Processor (DPP) system (Figure 2.10) is a component of the Amptek Experimenter's Spectrometer complete signal processing electronics. The core technology that runs through this spectrometer is digital pulse processing. The X-123 DPP replace many different components in a traditional instrumentation system: the shaping amplifier, the multichannel analyzer, logic devices, and several auxiliary components.

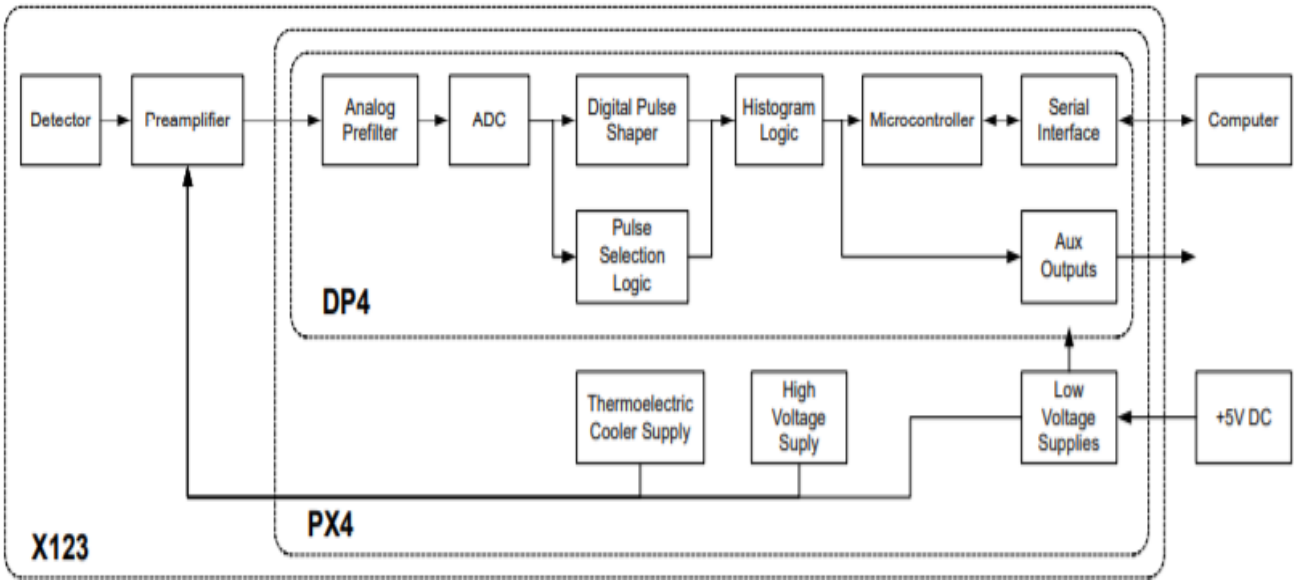

Figure 2.10 Amptek spectrometer Digital Pulse Processor

The output from the preamplifier (a charge sensitive preamplifier) is a small, fast voltage step. The gain of the Amptek XR100 is 1mV/keV, hence the preamp output signal for X-rays is in the tens of mV range. The goal is to achieve a resolution of a few hundred eV, or around 0.2mV. The signal has a rise time of about 100 nanoseconds and a decay time of several milliseconds or more. Due to thermal noise in the preamplifier, shot noise in the detector, and other factors, this signal is superimposed on a changing DC baseline and has a lot of white noise. The signals occur at unpredictable intervals, with tens of thousands of events per second. This preamplifier output is sent to a shaping amplifier and subsequently to a multichannel analyzer (MCA). The objective of the shaping amplifier is to allow for precise peak height determination. Pulse shaping removes the DC baseline, decreases overlapping pulse distortions, and filters out broadband noise. The pulse is also amplified by the shaping amplifier, allowing for precise measurements. The pulse amplitude is ultimately collected in a digital form, resulting in an energy spectrum in the MCA memory.

The sample chamber is the part of the spectrometer where samples are placed for irradiation. The sample chamber has a radiation shielding which protects the operator from radiations. Samples are however, placed in the sample chamber for the acquisition and display of spectra. These analytical methods helped identify sources and assign pollutant concentrations to those sources at specific locations in Accra: Adabraka, Dansoman Police Station, and the University of Ghana, Legon.

2.12 SOUCRE APPORTIONMENT OF PARTICULATE MATTER

Identifying the primary sources of particulate matter and accurately attributing the measured quantities of aerosol particles to these sources enables the development of more effective strategies to reduce air pollution levels. Source apportionment approaches facilitate the creation of efficient and successful strategies for controlling particulate matter, as well as the establishment of regulations to avoid human exposure. Pant and Harrison (2012) (159) defined source apportionment as a systematic method to quantify the contributions of various source categories to the observed levels of particulate matter in the atmosphere. APM emissions comprise several chemical species from multiple sources. Source apportionment methods analyze the mass and chemical compositions of particulate matter at a specific location to determine the principal sources and their contributions to the observed ambient particulate matter at that site (160,161). The emissions of particulate matter from various sources usually possess a distinct characteristics that may be used to determine their contribution to the overall aerosol particles at the receiving end (162).

2.12.1 RECEPTOR MODELLING METHODS

Receptor models are mathematical or statistical methods utilized to identify and quantify the origins of airborne pollutants at a particular site during sampling. Mass balancing analysis is a technique used to attribute ambient particulate matter concentrations to individual emission sources. This is done by using the core premise of receptor modelling, which is mass conservation (163). The premise behind many receptor models for source apportionment is that the pollution level at the receptor site is equivalent to the total pollution levels from all of the nearby emission sources (160,164). Therefore, the main purpose of receptor models is to find out where particulate pollutants might come from and how much they add to the total mass of bulk particles.

Receptor models are often classified into two main categories: mass balance and multivariate methods (165). The selection of the right approach is dependent on preexisting knowledge about the sources and their profiles. Chemical Mass Balance (CMB) models are applicable when the sources are identified and there is access to comprehensive source profile data. When the sources of pollution are unknown but the concentration of ambient pollution is known, it is preferable to use multivariate approaches like Positive Matrix Factorization (PMF). The Positive Matrix Factorization (PMF 5.0) program, developed by the U.S. Environmental Protection Agency (EPA), is widely used in the field of physical and chemical sciences for receptor modelling purposes (166–168). The association between the sources and the receptor was discovered by the use of enrichment factor analysis and multivariate approaches such as correlations and Positive Matrix Factorization (PMF).

2.12.2.1 POSITIVE MATRIX FACTORIZATION

The PMF offers many benefits compared to traditional component analysis methods like Cluster Analysis (CA) and Principal Component Analysis (PCA):

- Unreliable data in the PMF analysis, like observations below the detection limit or nonexistent values, can be accounted for by assigning them low weights to minimize their impact on the models (169).

- Down-weighting the model's influence on the extreme points can also help manage data with a strongly positive skewed distribution (170).

- The PMF model assumes the non-negativity of factors and does not rely on information from the correlation matrix, instead employing a point-by-point least squares minimization scheme that takes the uncertainty of each data point into consideration (171).

In PMF a matrix X (n x m), where n is the number of samples and m is the number of chemical species, is factored into two matrices, G (n x p) and F (p x m), where p is the number of independent source types or factors extracted, and a residual matrix E is used to account for the portion of X that remains unexplained. The factor analysis model can be expressed in matrix form as follows in equation 2.2:

$$X = G.F + E \qquad \textbf{2.2}$$

or as component parts

$$x_{ij} = \sum_{k=1}^{p} g_{ik} f_{kj} + eij \qquad \textbf{2.3}$$

where x_{ij} is the measured concentration of a receptor for the j^{th} species in the i^{th} air sample, g_{ik} is the particulate mass concentration from k^{th} source type contributing to the i^{th} air sample, f_{ik} is the

j^{th} species mass fraction from the k^{th} source, and e^{ij} is the residual measured and modelled concentration for the j^{th} species in the i^{th} sample.

The goal of multivariate receptor modelling is to identify the optimal number of sources (p), source contributions (g_{ik}), and chemical profiles (f_{ik}) of the identified sources. In order to get the best possible fit for the model, PMF aims to minimize the objective function, which is the chi-squared value, taking into account the uncertainty associated with each observation.

The following equation represents the object function:

$$Q = \sum_{i=1}^{m} \sum_{j=1}^{n} \left(\frac{eij}{sij}\right)^2 \quad \textbf{2.4}$$

$$Q = \sum_{i=1}^{m} \sum_{j=1}^{n} \frac{\left(x_{ij} - \sum_{k=1}^{p} g_{ik} f_{kj}\right)^2}{{s_{ij}}^2} \quad \textbf{2.5}$$

where s_{ij} is the uncertainty in the j^{th} species in the ith sample; gik ≥ 0; and fik ≥ 0; k = 1,…, p. PMF simultaneously adjust the elements G and F in each interactive step until a minimum vale of Q is obtained (169). The Q value may be used to determine the ideal number of parameters. The theoretical Q value may be approximated as the product of n and m, where n represents the number of entries in the data array and m represents the number of degrees of freedom for each data point in the data collection.

2.12.2.2 ENRICHMENT FACTOR (EF)

The enrichment factor model differentiates between components originating from human actions and those originating from natural sources. Its main purpose is to provide an early evaluation of the impact of human activities on the measured levels of elemental substances in the atmosphere.

Therefore, it is used to gauge the extent of pollution resulting from human activities. Enrichment factor (EF) analyses have been extensively used in research on particle source apportionment to identify the primary sources of air pollution and accurately assess the contributions from all sources of all measured pollutants (3,172).

$$EF = \frac{\left(\frac{C_x}{C_{Ref}}\right)_{Sample}}{\left(\frac{C_x}{C_{Ref}}\right)_{crust}} \qquad \textbf{2.6}$$

where C_x represents the concentration of the element of concern and C_{Ref} represents the concentration of the normalization reference element.

Particulate matter denotes an intricate mixture of solid and liquid particles that are suspended in the atmosphere. Particulate matter (PM) is a very dangerous kind of air pollution. According to the United States Environmental Protection Agency (USEPA), particulate matter (PM) is a mixture of solid particles and liquid droplets created in the atmosphere (113). PM is characterized by its variability in terms of size and chemical composition (173,174). The aforementioned entities are minuscule particles that possess the ability to stay suspended in the atmosphere for a lengthy duration, ranging from several hours to multiple days. Furthermore, these particles have the capacity to traverse significant distances from their respective origins.

In the context of research, particulate matter (PM) has been categorized into three primary size fractions: coarse (PM_{10}), fine ($PM_{2.5}$), and ultra-fine ($PM_{0.1}$). PM_{10} refers to particles with an aerodynamic diameter of less than 10µm, while fine $PM_{2.5}$ refers to particles with an aerodynamic diameter of less than 2.5 µm, and ultra-fine $PM_{0.1}$ refers to particles with an aerodynamic diameter of less than 0.1µm. This classification has been established (175–178). The dimensions of particles

significantly impact both their transportation characteristics and their potential health effects on human beings.

The majority of particles present in the atmosphere are of small size, namely those with a diameter less than 2.5 µm, and particularly those with a diameter less than 0.1 µm. They possess the capability to go to more profound regions inside the lungs. Both fine (< 2.5 µm) and ultrafine (<0.1 µm) particles are produced as a consequence of combustion sources, and they have a greater correlation with negative health impacts compared to coarse particles, according to Hinds (179), Basagaña et al. (175), Susanna (19), Mukesh (180) and Guangqin (181). Large particles are unable to penetrate beyond the nasal and throat regions. Zare et al., (182) reported that fine particles are present in abundance and possess a larger surface area compared to bigger particles of same mass. Consequently, fine particles are often regarded as being more harmful.

CHAPTER 3
METHODOLOGY

3.1 DESCRIPTION OF SAMPLING SITES

Accra, the capital of Ghana, serves as the administrative and economic hub of the country. Located at coordinates 5° 33' N, 0° 13' W, Accra is experiencing rapid growth and is among the fastest-growing cities in sub-Saharan Africa. The population of Accra is 4.9 million (53) and has a metropolitan area population of 2,557,000 representing an estimated growth rate of approximately 1.71%. The Greater Accra Region has a population density of 1,300 individuals per square kilometer, accounting for 47% of the total population of the Greater Accra Region. This places it as the 11th largest metropolitan area in Africa (45,183).

Ambient fine particulate matter samples were collected at three locations of varying socioeconomic areas (SEA) in the Greater Accra Metropolitan Area (GAMA) between January 2021 and February 2022 to cover the wet, dry and Harmattan periods. The exact locations of the air samplers were: Adabraka, St. Joseph Roman Catholic School (AD) (5° 33' 19.908" N, 0° 12' 50.184" W); Dansoman Police Station, (DA) (5° 32' 37.536" N, 0° 15' 54.684" W) and the Physics Department of the University of Ghana, Legon (UG) (5° 39' 5.04" N, 0° 11' 8.376" W). The sample sites were located along the coast of the Gulf of Guinea, reaching the northern boundaries of the Accra Metropolitan Area (AMA), as shown in Figure 3.1.

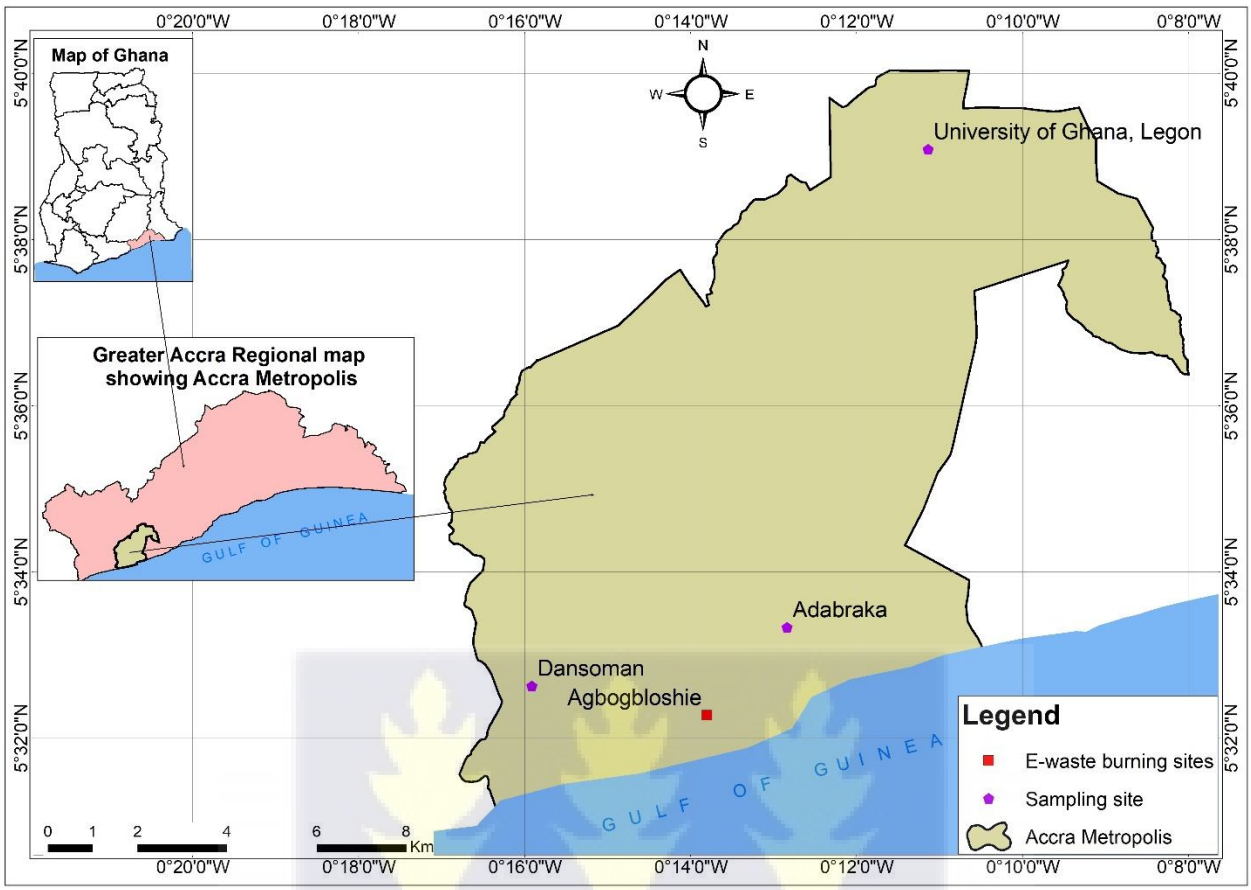

Figure 3.1 Map showing the various sampling sites within the Greater Accra Metropolitan Area (GAMA).

3.2 STUDY DESIGN

In this study, three selected locations in the Greater Accra Metropolitan Area with monitoring sites used were based on the following:

1. Two locations, namely Adabraka, St. Joseph Roman Catholic School and Dansoman Police Station, were about 5 meters from a road with consistently high traffic throughout the day. The air sampler was installed at a height of at least 3 meters above ground level.

2. One site among the three locations was selected due to academic environments and office setups. This was sited about 5 meters above ground level and 40 m from the road with less significant traffic than the other sites, even though within this site there are possibly other potential polluting sources such as open burning of refuse, biomass burning, or wind-blown dust.

3. Factors such as equipment security, power availability, absence of public disruption, and continuous access to equipment for operation and maintenance influenced the selection of the locations. In addition, the locations were chosen to provide adequate air circulation near the samplers' entrance, hence preventing the collection of still air or heavily shielded microenvironments.

3.1.1 DANSOMAN TOWN (DA)

Dansoman is a suburban town located in the Greater Accra Region of Ghana, situated near the Gulf of Guinea coast, 14 km southwest of Accra Central Business District (ACBD) of the Accra Metropolitan Area. The inhabitants of Dansoman are predominantly middle to high-income earners, and at approximate elevation of 127 m above sea level. DA with an approximate population of 153,490 people is known to be one of the largest estates in West Africa (183). Dansoman has large blocks of residential areas with major roads paved or tarred. The main local sources of air pollution in Dansoman are congestions emanating from medium to heavy vehicular emission, industrial processes, sea spray, road and wind-blown soil dust, open burning of refuse, used tyre, and less biomass burning for domestic and commercial cooking all day or during parts of the day.

3.1.2 ADABRAKA TOWN (AD)

Adabraka is situated approximately 1.8 km from central Accra, the heart of city commercial events, and is largely middle-income with a population of about 36,500 people with a terrain elevation of 97 km above sea level. The location of this area is in the northeastern part of the Accra city center. It is bordered by Asylum Down to the east, Kaneshie to the west, Kokomlemle to the north, and James Town to the south. The Adabraka suburb has a well-designed layout with a well-constructed and interconnected system of paved streets (184). AD was the first and most posh neighborhood in Ghana during the colonial era. Air pollution in the local area is primarily caused by the open burning of garbage and biomass by houses and street food sellers, traffic-related pollution, dust from roads and wind-blown soil dust, vehicular emissions, and industrial activities.

3.1.3 THE UNIVERSITY OF GHANA CAMPUS, LEGON (UG)

The main campus of the University of Ghana (UG) is situated at Legon, about 10 km inland from the coast. It is positioned to the north of Accra International Airport and 13 km northeast of the central business area of Accra city (185). The neighborhood of Legon is an affluent and tranquil suburb, characterized by a low population density and well-designed residential areas. It has excellent infrastructure and is home to an academic community. The campus is renowned for its lush, green, well-maintained gardens, sprawling lawns which cover the top soil with a variety of indigenous, exotic and matured trees (186). The road network inside the university community has much lower vehicle congestion during peak morning and evening commute hours compared to other areas. Notwithstanding the lower vehicular congestion, some possible polluting sources at this location include biomass burning, road dust as well as transport of regional emissions.

The mass concentration of air particulate matter was determined by analyzing the Teflon filters using gravimetric analysis. The mass concentration of particulate matter ($PM_{2.5}$) in the air was determined by dividing the mass of the particulate matter by the volume of the measured air and the sampling period. Additionally, the elemental composition of the particulate matter was characterized using non-destructive energy dispersive X-ray fluorescence (EDXRF) spectroscopy. The net mass of the measured airborne particulate matter was determined by subtracting the pre-weighed mass of the filter from the mass of the filter after sampling. The filters used in this investigation were conditioned at the Environmental Quality Laboratory (EQL) of Ghana's Environmental Protection Agency (EPA) and distributed to all sample locations. The loaded filters and field blanks were transported to the X-ray spectroscopy Laboratory of the National Nuclear Research Institute (NNRI) of Ghana Atomic Energy Commission (GAEC) for gravimetric and elemental analysis. The schematic design methodology used for the study is shown in Figure 3.2.

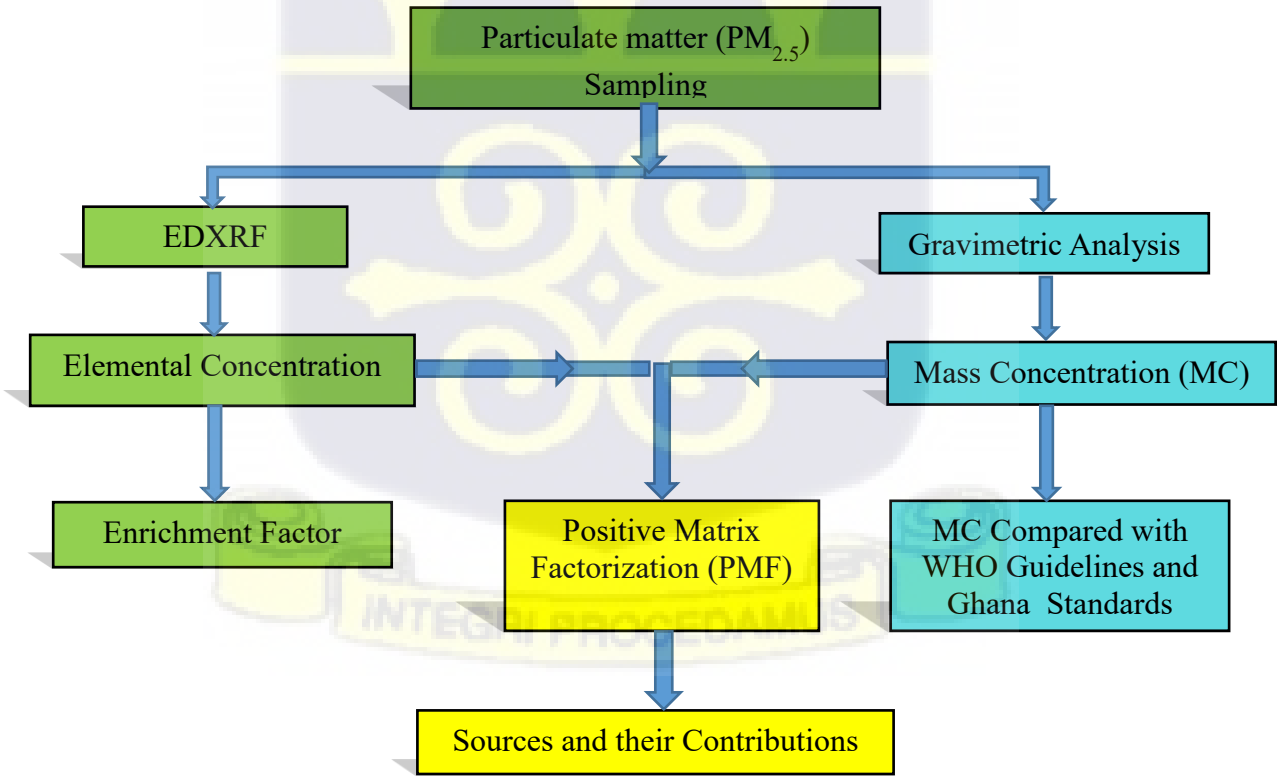

Figure 3.2 Organization and integration of research work.

3.2 SAMPLING PERIODS

The collection of ambient particulate matter occurred between January 2021 and December 2022 in the Greater Accra Metropolitan Area (GAMA) with sampling site designated at the 3 locations:

The sampling was over 24- hour period once every six days at the three different locations.

3.3 METEOROLOGICAL DATA

For the purpose of this study, meteorological data for Accra (January 2021 to December 2022) was obtained from the Ghana Meteorological Agency.

It is important to look into how meteorological factors and PM levels are related because the weather in a given area might change often throughout a single day. The Ghana Meteorology Agency in Accra provided data on temperature, rainfall, relative humidity, wind speed, and wind direction for three selected areas in the absence of site-specific meteorological information. The obtained meteorological measurements were considered to be typical of the monitoring sites.

The Harmattan season (November–March) and the non-Harmattan season (April–October) were analyzed individually for 2021 and 2022 since meteorological factors impact the levels of particulate matter in the air. Seasonal fluctuations in this study are separated into Harmattan and non-Harmattan seasons. The Harmattan era lasted from November 2021 to March 2022. Non-Harmattan periods are those beginning in September 2021, ending in October 2021, and beginning in April 2022 and ending in October 2022. Consequently, the full study's period was from January 2021 to December 2022.

3.4 AIRBORNE PARTICULATE MATTER SAMPLER

In this study, ARA N-FRM sampler was used for integrated aerosol particle mass quantification. The ARA N-FRM sampler was first set up for $PM_{2.5}$ particulate sampling by configuring the sampling inlet components prior to the filter medium.

ARA N-FRM impactor samplers were placed on roofs at different heights between 5m and 7m above ground level at each monitoring location. This ensured that the air was adequately mixed and less susceptible to significant influence from nearby sources (12). The inlet nozzles of the samplers were positioned around 1.2m above the rooftop level using an extended pole for easy installation and retrieval from brackets. The setting was selected to ensure that the sampler inlet can efficiently sample wind from all directions. Figure 3.3 displays a standard setup of the ambient monitoring system.

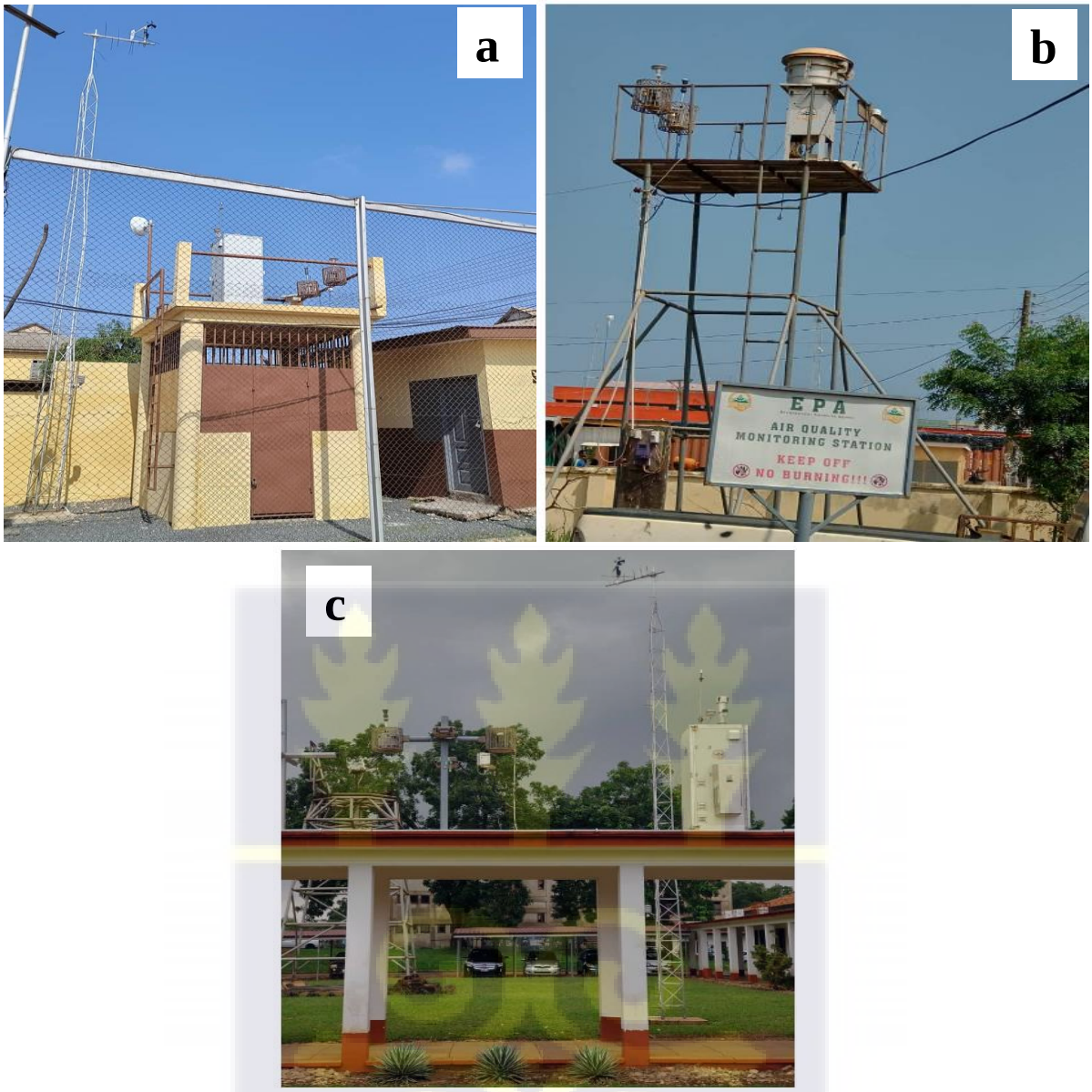

Figure 3.3 A standard configuration of the ambient monitoring system including ARA N-FRM samplers. Adabraka (a), Dansoman (b), and the University of Ghana (c).

The filters were weighed in a clean weighing room at the Environmental Quality Laboratory of the Environmental Protection Agency (EPA) in Ghana. A Secura26-1S microbalance was used to measure the initial and final weights of all the filters utilized for sampling purposes. The filters were conditioned before and after sampling. The filters were conditioned by placing them in a

desiccator in the weighing room at a controlled temperature (25 ± 0.2 °C) and relative humidity (39 ± 2 %) for a minimum of 24 hours before weighing (187–190). Filters were weighed three times during pre- and post-weighing and the average was taken. This method was used to enhance the gravimetric analysis' precision and get rid of outliers caused by significant analytical mistakes. A set of class "S" weights were used to check the microbalance's zero, span, and linearity after each batch of 10 filters. Equation 3.1 provides the precise calculation for determining the total mass of the particulate matter that had been accumulated on a Teflon filter, expressed in micrograms.

$$M = [(M_f - M_i)\ \text{mg} \times 10^3]\ \mu\text{g} \qquad \textbf{3.1}$$

where,

M = total mass of particulate matter collected during sampling period (µg)

M_f = final mass of conditioned filter after sample collection (mg)

M_i = initial mass of conditioned filter before sample collection (mg)

Equation 3.2 gives the total volume of ambient air passing through the sampler (V) in cubic meters.

$$V = [(Q_{avg})\ \text{L/min} \times t\ \text{min} \times 10^{-3}]\ \text{m}^3 \qquad \textbf{3.2}$$

where,

V = total volume of sample (m^3)

Q_{avg} = average flow rate over the entire duration of the sampling period (L/min)

t = duration of sampling period (min)

Thus, the PM concentration in µg/m^3 can be calculated using equation 3.3.

$$PM = \frac{M}{V} \qquad \textbf{3.3}$$

where,

PM = mass concentration of PM (µg/m^3)

M = total mass of PM collected during sampling period (µg)

V = total volume of air sampled (m^3)

3.5 DATA ANALYSIS

The $PM_{2.5}$ mass concentration data was analyzed with data analysis software packages. The Open Air package of R- software was used to analyze the mass concentration data in determining the influence of meteorological conditions on particulate matter as well as the trends of particulate matter over the study period. The U.S. EPA's Positive Matrix Factorization (PMF) 5.0 model tool was used to investigate the sources of pollution in the particulate matter monitored during the period of study.

3.6 X-RAY SPECTROMETRY ANALYSIS

The elemental analysis of particulate sampled was done using Energy Dispersive X-ray Fluorescence Spectrometry (EDXRF). Amptek Experimenter's Kit Spectrometer was used at the X-ray Spectrometry Laboratory, National Nuclear Research Institute, Ghana Atomic Energy Commission to analyze the elemental contents of $PM_{2.5}$ samples collected from all monitoring stations in the Greater Accra. The spectrometer is made up of a Mini-X X-ray tube with a Silver (Ag) target (X-ray source) equipped with a power supply, a X-123 Silicon Drift Detector (SDD) complete X-ray spectrometer (8 µm Be window thickness, Si drift 25mm^2 x 500 µm, 2 stage cooler, 1.5" detector extension, an internal multilayer collimator and a resolution of 125 eV full width at half maximum (FWHM) resolution at 5.9KeV (^{55}Fe) with a peaking time of 6.4 microseconds) and a sample chamber. The X-ray source operates with voltages ranging from 5 to 50 KeV and currents ranging from 5 to 200 µA (158).

The X-ray beams were directed towards the sample at an incident angle of 67.5^0 and characteristic X-ray fluorescence radiation from elements in the samples were directed to the detector at a takeoff angle of 67.5^0. The spectra were obtained using a Digital Pulse Processor Multi-Channel Analyzer (DPPMCA). The spectra data were stored and can be displayed as an X-ray spectrum on a computer monitor.

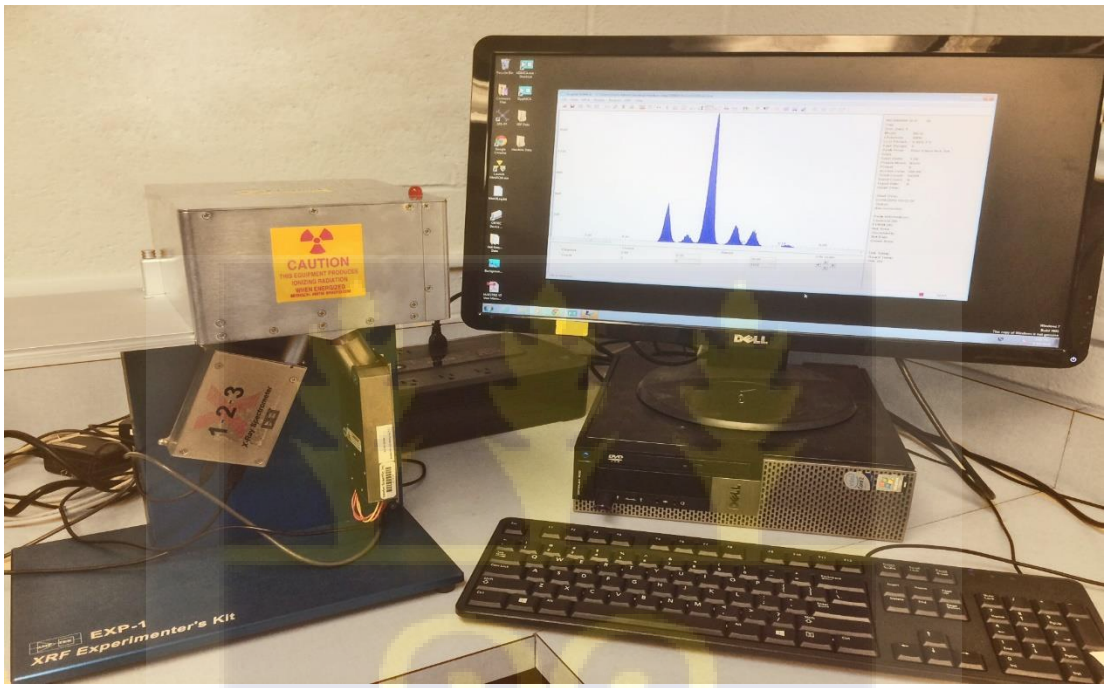

Figure 3.4 Amptek XRF Spectrometer at NNRI, GAEC-Ghana

3.6.1 Energy Calibration

The energy scale was calibrated using two peaks of known energy. For best results, the peaks used were widely separated in energy with good statistics and no overlapping peaks. Fe and Mo peaks were used. The regions of interest (ROIs) around these two peaks were marked. The calibration dialog box was open and the energies of Fe and Mo, 6.40keV and 17.44 keV respectively, of the centroids were defined. The software performed a linear regression and the calibration was

obtained in the DPPMCA. The calibration was verified by acquiring a spectrum of a known element, i.e. Cr and confirmed that the Cr peak was at the energy 5.4 keV. The energy resolution of the detector was checked by checking the FWHM of Fe Kα peak which was slightly higher than the FWHM listed on the data sheet supplied with the detector.

3.7 QUANTITATIVE ANALYSIS

3.7.1 Spectra Acquisition

Samples were irradiated and spectra acquired at a voltage of 45V and current of 5μA for a period of 180 seconds. The dead time was below 1% throughout the spectra acquisition. The spectrum was acquired using the Amptek DPPMCA software.

3.7.2 Sample Analysis

Spectra acquired from the samples were processed and quantitatively analyzed using the bAxil software (version 1.7.0 released on November 2017) a quantitative analysis software using "Fundamental Parameter". The bAxil FP (bAxil Fundamental Parameter) uses two methods for quantitative elemental calculations: standard-less Fundamental Parameter method and Standard-based Fundamental Parameter method. The latter was used in this work where measured spectra from standard or reference micro-matter samples were input in the software and from them the software established the calibration concentration parameters that are used to calculate the elemental concentrations on the "unknown" filter papers. The reference material used was a NIST Traceable Reference Material, MICROMATTER^{TM} – XRF Calibration Standards.

3.8 ENRICHMENT FACTOR (EF) ANALYSIS

Enrichment factor (EF) analysis can differentiate the elemental makeup of airborne particulate matter from either anthropogenic or natural origins. It may as well calculate the level of human

impact (172,191,192). The Enrichment Factor (EF) method checks the amounts of important parts found in measured amounts of particulate matter (PM) against the amounts of the same parts found in geological material. This is done to see if the contributions come from both natural and human-caused sources. The reference elements that are widely favoured are aluminium (Al), silicon (Si), titanium (Ti), and iron (Fe). These elements are naturally abundant in soil, exhibit strong chemical stability, and are relatively unaffected by human-induced pollution. However, there is no established criterion for selecting a reference element (193). The primary continental compositions of the earth's crust were obtained from Housh et al (1985), with Fe serving as the reference element in this investigation.

$$EF = \frac{(X/E)sample}{(X/E)crust} \qquad \textbf{3.4}$$

where *X* and *E* refer to concentration ($\mu g\, m^{-3}$) of the element of interest (*X)* and the reference element (*E)* respectively.

If the EF (enrichment factor) of an element is <10, it is generally presumed to originate from a crustal or natural source. However, if the EF value is > 10, it indicates that a significant proportion of the element originates from a source other than the Earth's crust or human activities (194–196). EF levels >100 are considered highly enriched, while values >1000 are considered very enriched by anthropogenic sources. Table 3.2 displays the mean values of the crustal components used in the investigation. The enrichment factor (EF) for each element in $PM_{2.5}$ at the three sample locations was calculated using Equation 3.4.

3.9 SOURCE IDENTIFICATION AND APPORTIONMENT USING POSITIVE MATRIX FACTORIZATION

The U. S. EPA's Positive Matrix Factorization (PMF) version 5.0 modeling software was used to identify and allocate the source of APM (197). Six sources were identified by PMF in the $PM_{2.5}$ fractions. The model may have different meanings depending on changes in the signal-to-noise ratio (S/N) of particular components. Paatero and Hopke state that S/N provides some indication that when determining whether the recorded concentrations are within the measurement noise level or the real concentrations. Any computed S/N falling between $0.2 < S/N < 2.0$ is considered "weak" and can be down-weighted (i.e., have its uncertainty raised). $S/N > 2.0$ indicates "strong" species and was taken into consideration in the analysis. Species with S/N ratio < 0.2 should be labelled as "bad" species and must not be included in the study (198). Tables 4.10 and 4.11 for $PM_{2.5}$ show the S/N ratios for the species that were measured at all the three locations in 2021-2022, respectively.

When the concentration of a species was less than the minimum detection limit (MDL), it was changed to half of the MDL. This made the level of uncertainty 5/6 of the MDL. The missing concentration was substituted with the geometric mean of the recorded concentration, and the uncertainty was adjusted to four times this geometric mean. The PMF model study used the observed $PM_{2.5}$ mass concentrations as an independent variable to directly determine the mass apportionment, eliminating the need for the traditional multilinear regression. In the model study, the PM mass values were adjusted by reducing the weights of the uncertainty to four times the mass concentrations.

Table 3.1 The enrichment factors of particulate matter ($PM_{2.5}$) for all samples at different locations in Accra are calculated using the averages of crustal components.

Atomic Number	Element	Crustal Average (ppm)
13	Al	82300
14	Si	281500
15	P	1050
16	S	260
17	Cl	130
19	K	20900
20	Ca	41500
21	Sc	22
22	Ti	5700
23	V	135
24	Cr	100
25	Mn	950
26	Fe	56300
27	Co	30
28	Ni	100
29	Cu	55
30	Zn	70
35	Br	2.5
37	Rb	90
38	Sr	375
40	Zr	165
58	Ce	66
82	Pb	12.5

Source (28,199).

CHAPTER 4

RESULTS AND DISCUSSIONS

4.1 PARTICULATE MATTER ($PM_{2.5}$) MASS CONCENTRATION

The variation of particulate matter across different sites is usually influenced by various factors, including diurnal changes in emission rates through anthropogenic activities, wind direction shifts, and atmospheric dispersion and advection (81,105). Table 4.1 summarizes the inhalable particulate matter ($PM_{2.5}$) concentrations monitored at the various sampling sites during the study period. The table shows a summary of the number of samples taken (n) over the entire study period and the mean, standard deviation, minimum, maximum, and median mass concentrations of $PM_{2.5}$ at Adabraka (AD), Dansoman (DA), and the University of Ghana (UG) from January 2021 to December 2022. The standard deviation of the concentration values indicates the extent of variation in the data during the duration of the research in relation to the mean value (i.e., the degree of data fluctuation over the study period). For the gravimetric method, the number of samples for each site ranged between 51 and 58 in 2021 and 49 and 56 in the 2022 sampling period.

Table 4.1 Descriptive summary of $PM_{2.5}$ mass concentrations ($\mu g\ m^{-3}$) during the entire study period in 2021 and 2022.

Year	Site	n	Mean(μ)	SD	Min	Q1	Median	Q3	Max
2021	**AD**	54	60.76	25.06	20.79	41.58	58.22	70.69	133.07
	DA	51	49.90	19.96	8.32	37.43	45.74	60.30	120.59
	UG	58	42.49	23.10	8.32	25.99	37.43	49.90	120.59
2022	**AD**	56	60.54	29.14	20.79	41.58	57.14	66.53	162.18
	DA	49	49.28	20.84	16.63	33.27	49.90	58.22	138.86
	UG	55	46.37	28.60	12.48	29.11	45.74	54.06	153.86

n = number of samples collected, μ= mean, SD = standard deviation, min= minimum, max= maximum

For the study period, the means of $PM_{2.5}$ levels for 2021 and 2022 ranged from $42.49\ \mu g\ m^{-3}$ to $60.76\ \mu g\ m^{-3}$. The AD site recorded the highest mean $PM_{2.5}$ concentration of $60.76\ \mu g\ m^{-3}$, while DA and UG recorded $49.90\ \mu g\ m^{-3}$ and $42.49\ \mu g\ m^{-3}$ respectively in 2021. Similarly, in 2022, the AD site recorded the highest mean $PM_{2.5}$ of $60.54\ \mu g\ m^{-3}$, followed by the DA site with $49.28\ \mu g\ m^{-3}$, and the UG site with the least of $46.37\ \mu g\ m^{-3}$. The mean $PM_{2.5}$ at all the three sampling sites were all above the recommended limits of $35\ \mu g\ m^{-3}$ and $15\ \mu g\ m^{-3}$ as prescribed in the Ghana standard for ambient air quality (GS1236:2019) and the WHO guideline, respectively (Figure 4.1). The highest level of $PM_{2.5}$ recorded at Adabraka relative to the other sites could be attributed to the various emitting activities carried out in that area, including traffic congestion and use of biomass for cooking and heating by commercial food vendors. Activities from the Agbogbloshie e-waste burning site (about 700 m north-easterly away from the site) could also impact the $PM_{2.5}$ levels recorded at the AD sampling site. The level of $PM_{2.5}$ recorded at the DA

sampling site was above both the limit recommended by the Ghana Standard and WHO guideline. This could result from vehicular emissions (the site is near to a road) in addition to biomass burning for heating and cooking from households and commercial food vendors. The UG site recorded the lowest $PM_{2.5}$ levels relative to the other sites, and this could be attributed to the vegetation in the vicinity of the sampling location. However, the PM levels were above the limits recommended by the Ghana Standard (35 μm^{-3}) and the WHO guidelines (15 μm^{-3}). This could be attributed to vehicular emission within and around the environs of the sampling site. According to Awokola et al. (2022) (200) and SOGA-Africa (2022) (201), particulate matter levels in sub-Saharan Africa ranged between 40 $\mu g\, m^{-3}$ and 260 $\mu g\, m^{-3}$ and these levels substantially exceeded WHO guidelines.

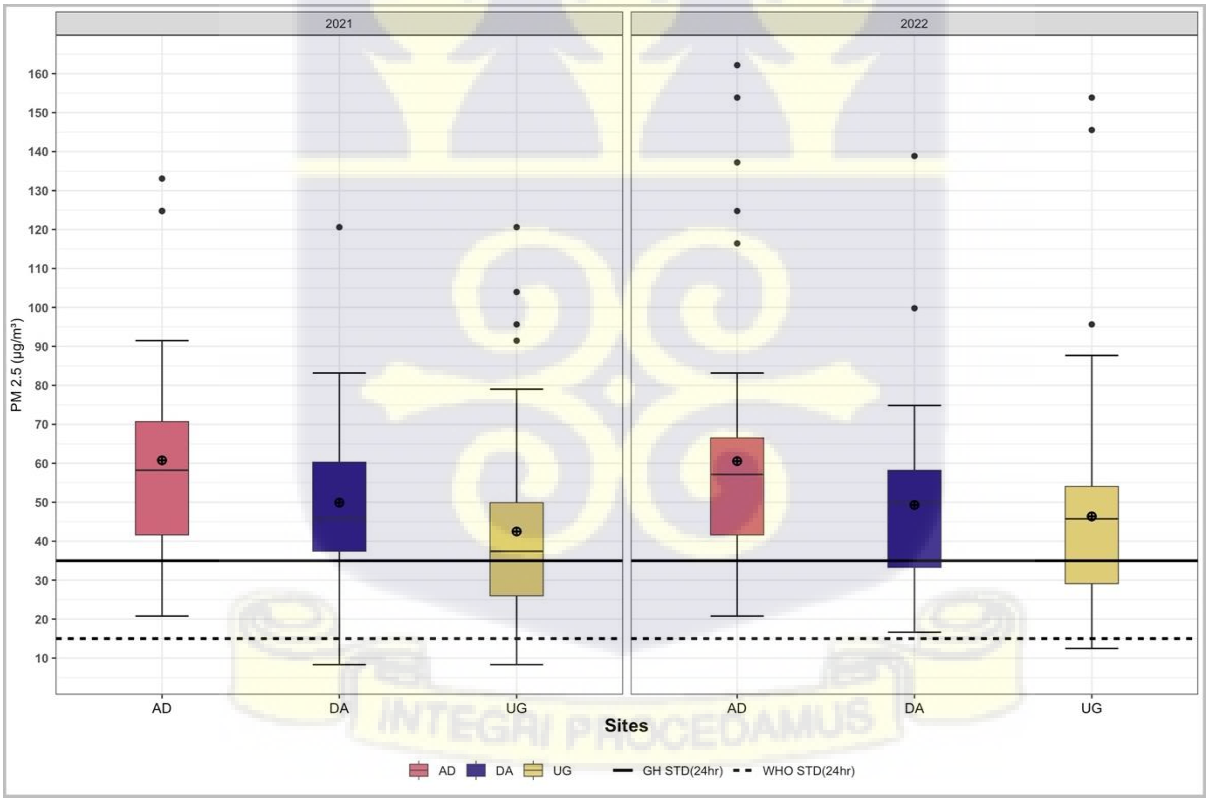

Figure 4.1 Box plots of $PM_{2.5}$ mass concentration ($\mu g\, m^{-3}$) during the entire study period (2021-2022).

The time series plot below (Figure 4.2) depicts the diurnal trend of $PM_{2.5}$ during the period of study. The $PM_{2.5}$ levels were high in the months of November–February, which is the dry season for all the sampling sites in both 2021 and 2022. All sampling locations in both 2021 and 2022 recorded relatively low levels of $PM_{2.5}$ between the months of April and October. Compared to daily levels at UG, the majority of the daily $PM_{2.5}$ levels for sites AD and DA in 2021 exceeded the Ghana Standard's prescribed limit, with a similar trend observed in 2022. Considerably, all $PM_{2.5}$ levels exceeded WHO air quality guideline and this is in congruence with the outcome of results obtained by Kwarteng et al., 2020 (202).

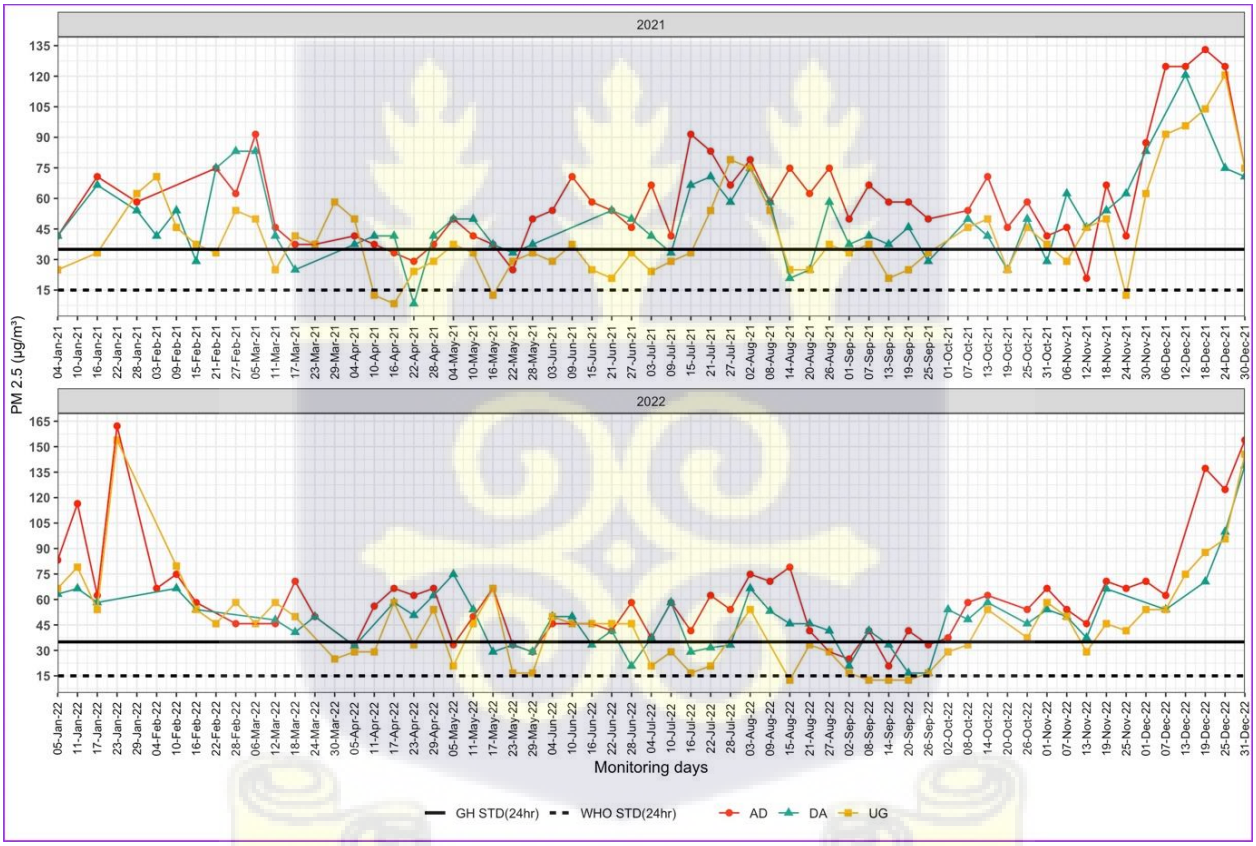

Figure 4.2 Time series plots of $PM_{2.5}$ mass concentration($\mu g\, m^{-3}$), (gravimetric) for the entire study period (2021 and 2022).

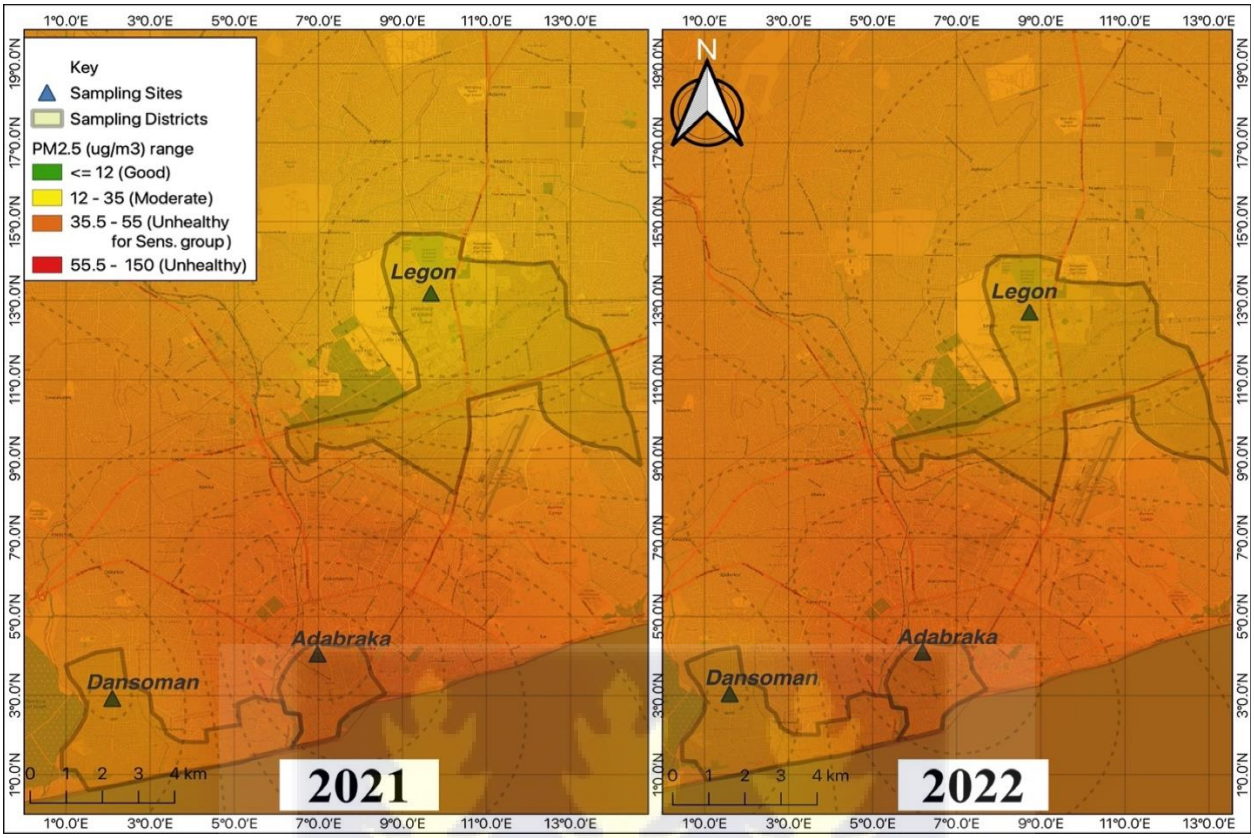

Figure 4.3 Spatial plot of $PM_{2.5}$ mass concentration, ($\mu g\, m^{-3}$) (gravimetric) for the entire study period (2021 and 2022).

From Figures. 4.1, 4.2, and 4.3, the $PM_{2.5}$ concentration at the AD site was relatively higher in both years as compared to the other sites (UG and DA) under study. The high levels found at AD could be because of the large amounts of $PM_{2.5}$ emissions caused by human activities, such as the widespread use of biomass fuels like firewood for cooking and heating in homes and small businesses, as well as emissions from traffic, industry, sea spray, road and soil dust, trash burning, and tyre and brake pad wear in the area. Comparatively, UG recorded the lowest $PM_{2.5}$ levels among the three sites (AD, DA, and UG). This site is within an academic environment, characterized by a tarred and paved road network connecting the university community, a vast plantation of mature trees and green grasses covering top soils, and significantly reduced numbers of vehicles (cars, buses, and taxis) during the morning and evening commuting times than at other

locations. Vegetation that intercepts and absorbs particulate matter could also be the reason for the lower pollution levels observed in UG. Furthermore, the pollution levels of all the sites in 2021 were not significantly different from the pollution levels in 2022 (a 2% increase from 2021).

Table 4.2 Inferential table of $PM_{2.5}$ mass concentrations during the study period in 2021 and 2022.

	Site	$PM_{2.5}$ ($\mu g\, m^{-3}$) Pollution level				Kruskal Wallis test	
		Mean	SD	**Min**	**Max**	*H*	*p-value*
2021	Adabraka	51.05	22.71	12.47	124.75	6.8786	0.03209
	UG						
	Dansoman						
2022	Adabraka	52.06	26.19	16.63	151.63	7.1912	0.02744
	UG						
	Dansoman						

A test of significance was conducted on the trend of particulate matter emissions from the three sites to see if there was a big difference in the amount of pollution at each site. The Shapiro-Wilk test of normality conducted revealed significant differences within the data; hence, there is no evidence that the data follows a normal distribution (*p-value* < 0.05). Therefore, the Kruskal-Wallis test of significance was used to ascertain whether there was statistical significance within the means of the pollution level in 2021 and 2022 for the various sampling locations. The test results showed that the daily trend of $PM_{2.5}$ concentration across the study period (2021 and 2022) was statistically different across the different sampling sites (Table 4.2). Dunn's test results, adjusted with the Benjamin-Hochberg correction, indicate a statistically significant disparity in $PM_{2.5}$ pollution levels between Adabraka and UG over both years. Notwithstanding the considerable gap, the reference to trends implies that both sites may display the same fundamental

pattern or trajectory in pollution levels, despite variations in absolute levels. This may result from common environmental conditions or human activity affecting both sites.

The site at Adabraka is characterized by both commercial and industrial (both heavy and light) activities, which are higher contributors of particulate matter. The Dansoman site is a residential area coupled with some commercial activities. The levels of pollution could be attributed to the frequency of vehicular movement and traffic congestion within the area. This could also be attributed to similar activities within the sampling site on the UG campus.

4.2 COMPARISON BETWEEN DATA FROM GRAVIMETRIC AND REFERENCE MONITORS

To verify and evaluate the data from this study, data was obtained from continuous (real-time) monitoring instruments that are co-located at two of the monitoring sites (AD and UG). Data from the continuous instruments (Teledyne T640 and BAM1020), which are Federal Equivalent Methods/Federal Reference Methods (FEM/FRM), were obtained during the same study period. The data obtained were averaged to 24-hour levels on the same sampling days as the data from the gravimetric samplers to ensure comparison. The continuous monitors (Teledyne T640) recorded mean $PM_{2.5}$ mass concentrations ranging from 53 $\mu g\ m^{-3}$ to 60 $\mu g\ m^{-3}$ in 2021 and 55 $\mu g\ m^{-3}$ to 56 $\mu g\ m^{-3}$ in 2022.

Table 4.3 Statistical summary of $PM_{2.5}$ mass concentration ($\mu g\ m^{-3}$) of gravimetric and reference monitors

Year	Site	n	Mean	SD	Min	Q1	Median	Q3	Max
2021	AD	54	60.76	25.06	20.79	41.58	58.22	70.69	133.07
	DA	51	49.90	19.96	8.32	37.43	45.74	60.30	120.59
	UG	58	42.49	23.10	8.32	25.99	37.43	49.90	120.59
	*UGT640	53	29.03	19.20	11.06	16.70	23.25	31.69	118.39
	*ADT640	59	37.82	16.17	19.61	25.48	35.37	46.45	110.51
	*BAM1020	60	26.30	13.68	9.15	18.08	23.15	29.23	94.58
2022	AD	56	60.54	29.14	20.79	41.58	57.14	66.53	162.18
	DA	49	49.28	20.84	16.63	33.27	49.90	58.22	138.86
	UG	55	46.37	28.60	12.48	29.11	45.74	54.06	153.86
	*UGT640	55	30.96	29.16	5.97	12.94	22.18	27.99	151.75
	*ADT640	56	35.45	26.72	5.41	22.55	25.66	36.03	152.63
	*BAM1020	55	26.45	20.74	6.70	14.00	20.46	27.44	103.88

* = Optical reference monitors Q1 = First quarter Q3 = Third quarter

$PM_{2.5}$ concentrations from the gravimetric monitors ranged from 51 $\mu g\ m^{-3}$ to 58 $\mu g\ m^{-3}$ in 2021 and 49 $\mu g\ m^{-3}$ to 60 $\mu g\ m^{-3}$ in 2022. $PM_{2.5}$ concentrations from the reference monitors ranged from 26.30 $\mu g\ m^{-3}$ to 37.82 $\mu g\ m^{-3}$ in 2021 and from 26.45 $\mu g\ m^{-3}$ to 35.45 $\mu g\ m^{-3}$ in 2022. The results from this study are comparable to those from a study conducted by Odoi and Kleiman in 2021 (203). The corresponding concentration from the gravimetric sampling ranged from 42.49 $\mu g\ m^{-3}$ to 60.76 $\mu g\ m^{-3}$ in 2021 and 46.36 $\mu g\ m^{-3}$ to 60.54 $\mu g\ m^{-3}$ in 2022. The concentration from the reference monitors differs significantly from the concentration from gravimetric sampling (Mann-Whitney U = 21822, p-value < 2.2e-16). The $PM_{2.5}$ concentrations recorded from the continuous monitors (FRM/FEM) were almost twice as low as the concentrations recorded from the gravimetric monitors. This could be the result of the sampling method. The gravimetric monitors collect $PM_{2.5}$ on a filter paper for the entire 24-hour period, and the cumulative $PM_{2.5}$ on

the filter paper is weighed, whereas the optical monitors use spectrometry to record real-time $PM_{2.5}$ data. Notwithstanding the significant difference in mean levels, the daily trends in pollution levels shown in Figure 4.3 are not significantly different (R^2 = 0.52 and 0.74 for 2021 and 2022, respectively). Previous analysis conducted by Kwarteng et al (202) to compare $PM_{2.5}$ levels using gravimetric monitors to continuous monitors (FRM/FEM) revealed a moderate to high-significant relationship with a 0.47–0.75 R^2 value. The Figure 4.4 shows the comparison of the air-quality monitors across the study period.

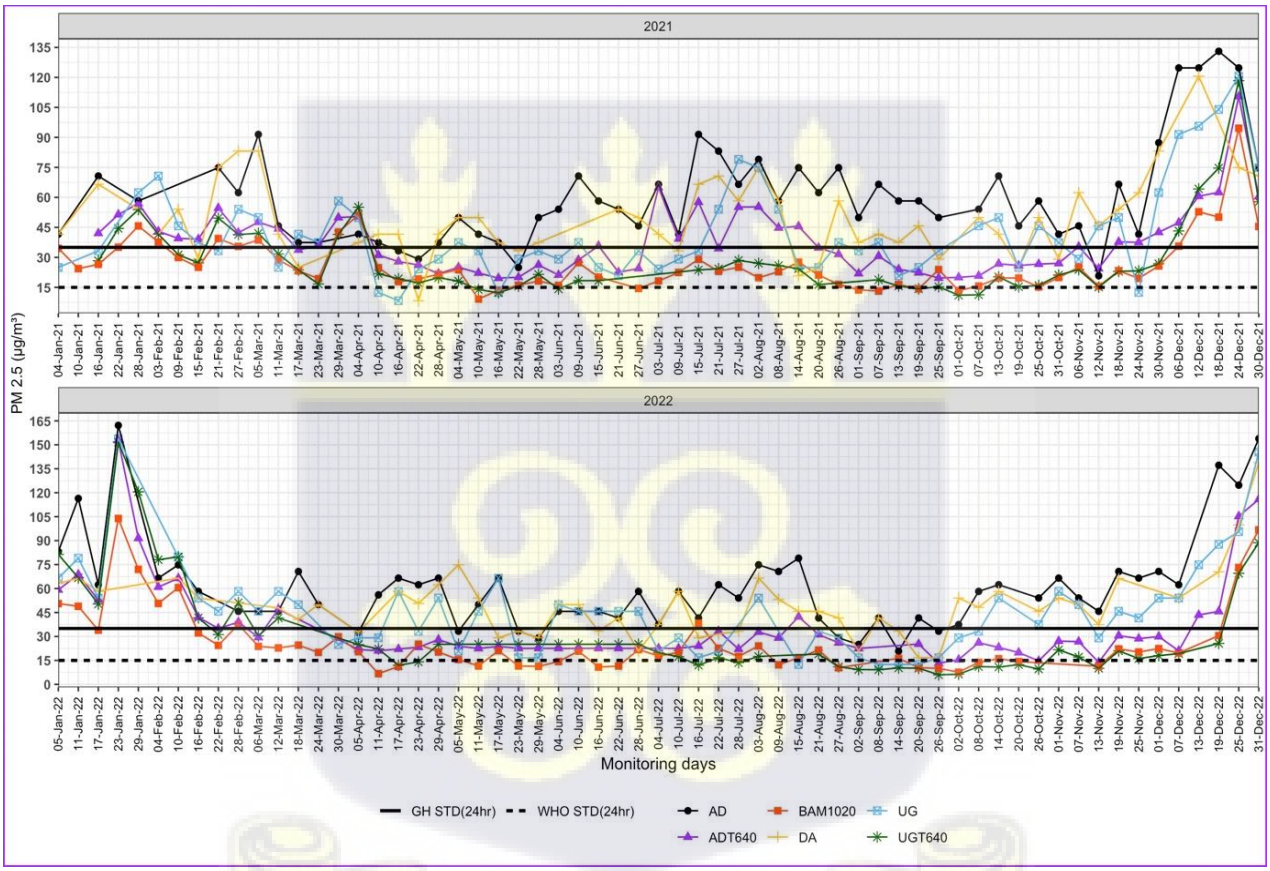

Figure 4.4 Time series plots showing pollution levels of $PM_{2.5}$ mass concentration ($\mu g\ m^{-3}$) of gravimetric and reference monitors.

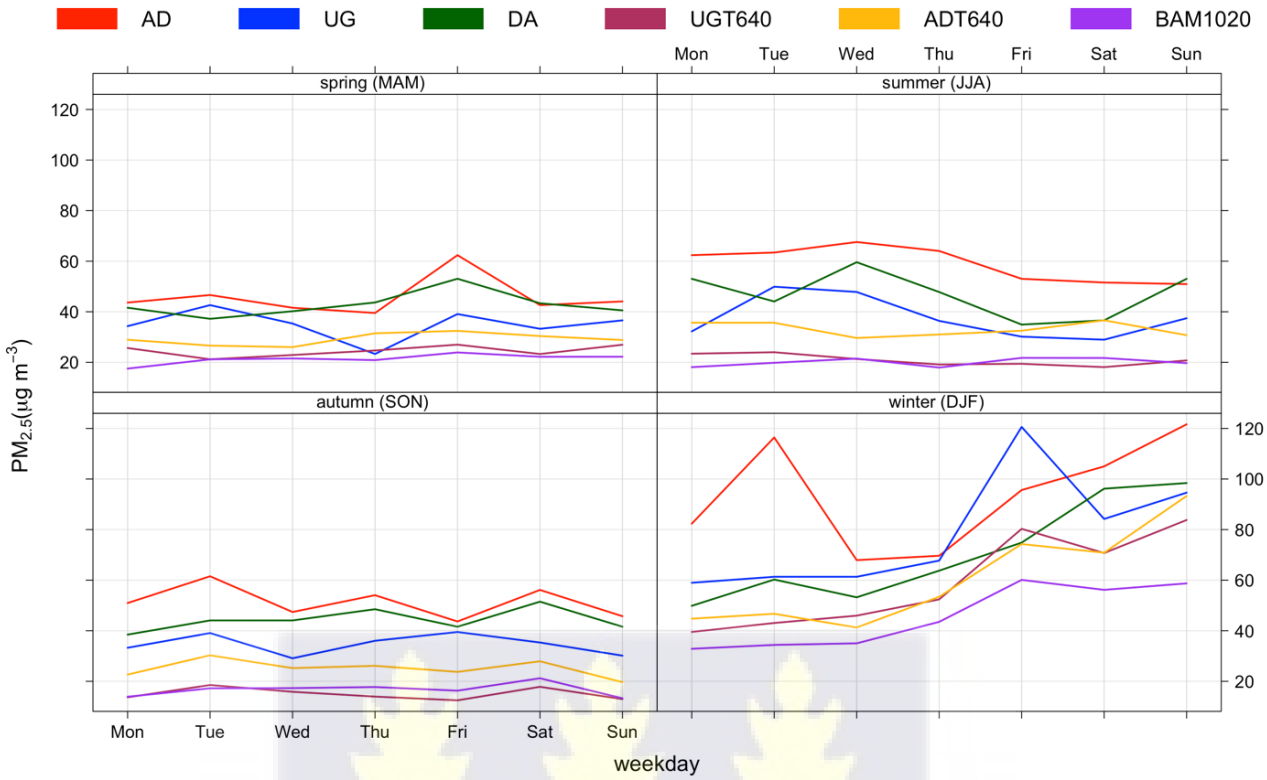

Figure 4.5 Seasonal variations of $PM_{2.5}$ ($\mu g\ m^{-3}$) between the three sites and reference monitors (2021-2022).

Table 4.4 Monthly $PM_{2.5}$ ($\mu g\ m^{-3}$) variations between sampling sites and reference monitors during the entire study period in 2021 and 2022

Month	AD		DA		UG		UGT640		ADT640		BAM1020	
	2021	2022	2021	2022	2021	2022	2021	2022	2021	2022	2021	2022
January	56.83	116.43	54.06	88.71	40.2	97.3	42.22	71.65	50.12	68.28	33.24	55.7
February	68.61	106.04	56.55	62.61	48.24	88.36	38.25	94.15	43.71	84.98	33.5	61.85
March	53.02	61.34	49.9	60.3	42.42	59.43	31.13	56.38	42.27	48.68	30.56	41.08
April	35.76	53.02	34.1	46.16	24.79	44.7	26.67	35.95	31.5	38.26	26.93	24.18
May	40.75	56.82	41.58	50.97	29.11	40.75	16.28	19.63	22.63	23.25	16.16	16.74
June	56.55	42.42	51.98	44.08	29.11	33.27	16.98	25.11	26.53	23.06	19.48	14.18
July	69.86	47.4	54.06	39.09	43.92	46.57	25.5	25.11	50.29	22.55	23.54	15.82
August	69.86	50.73	47.41	37.9	43.25	21.83	23.41	15.88	42.38	24.92	21.57	23.19
September	56.55	59.05	38.26	50.55	29.94	32.23	16.02	15.84	23.73	32.3	16.3	16.97
October	54.06	32.44	39.09	25.78	40.75	14.14	15.84	8.96	24.52	20.33	17.25	12.25
November	52.39	53.03	61.54	51.56	39.92	38.47	22.41	10.04	35.51	19.85	21.82	12.91
December	116.43	60.72	88.71	51.92	97.3	44.91	71.65	17.18	68.28	25.37	55.7	17.92

Monthly pollution trends assessed in 2021 and 2022 at all three sites revealed some usual spikes in January, December, and February (dry season). The dusty Harmattan winds that infiltrate the country from the Sahara desert significantly influenced the peaks in particulate matter concentrations during the dry season. According to Awokola, 2022 (200) monthly $PM_{2.5}$ levels peak in December through February (dry season) in West African countries.

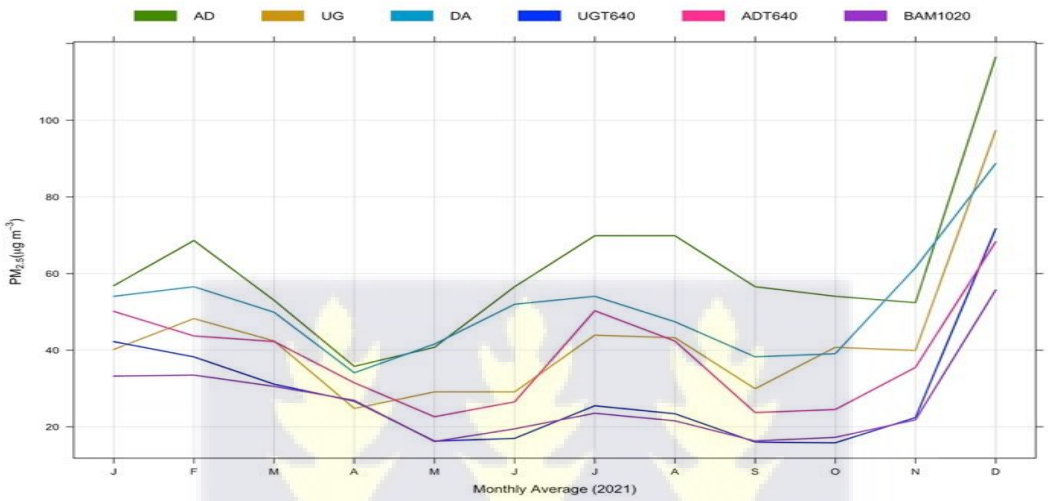

Figure 4.6 Time series plot showing monthly mean $PM_{2.5}$ concentration trend for both gravimetric and optical monitors (2021)

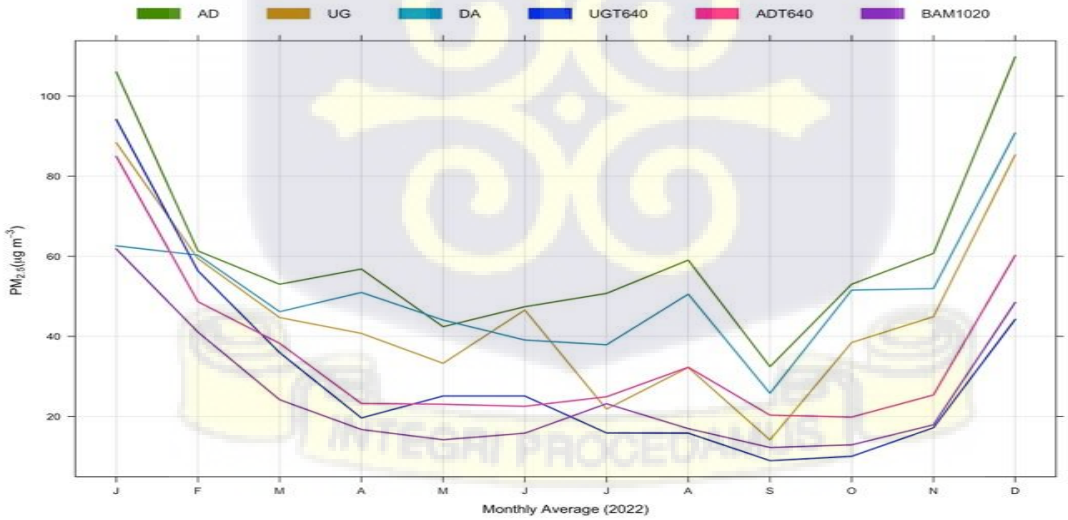

Figure 4.7 Time series plot showing monthly mean $PM_{2.5}$ concentration trend for both gravimetric and optical monitors (2022)

Calendar plots (Figure 4.8) were used to further analyze trends from the monthly variation. In 2021, the plots showed significant colour (red) similarities for the months in the dry season (December, January, and February) and August, with some minimum variation across the three sites. This further explained the unusual spike in pollution levels in August 2021. Out of the 10 data points for July and August, 9 were within the unhealthy (55.5 µg m^{-3}– 250.4 µg m^{-3}) range, and 1 was within the unhealthy range for the sensitive group (35.4 µg m^{-3}– 55.4 µg m^{-3}).

For the same month in Dansoman, 6 out of the 10 data points were within the unhealthy range (55.5 µg m^{-3}– 250.4 µg m^{-3}), 1 was in the unhealthy range for the sensitive group, and 3 were in the moderate range (12 µg m^{-3}-35 µg m^{-3}). At the University of Ghana campus in Legon, only 2 out of the 10 data points were in the unhealthy range, 3 were within the unhealthy range for sensitive groups, and 5 were in the moderate range.

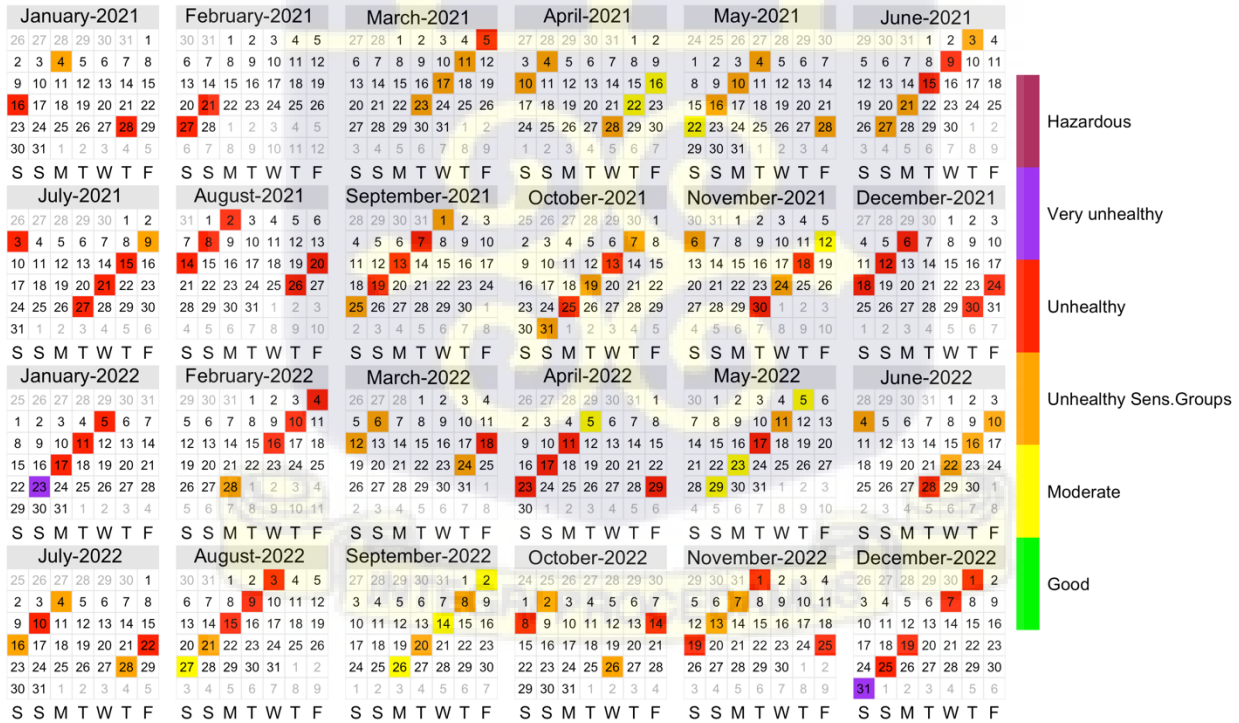

UG

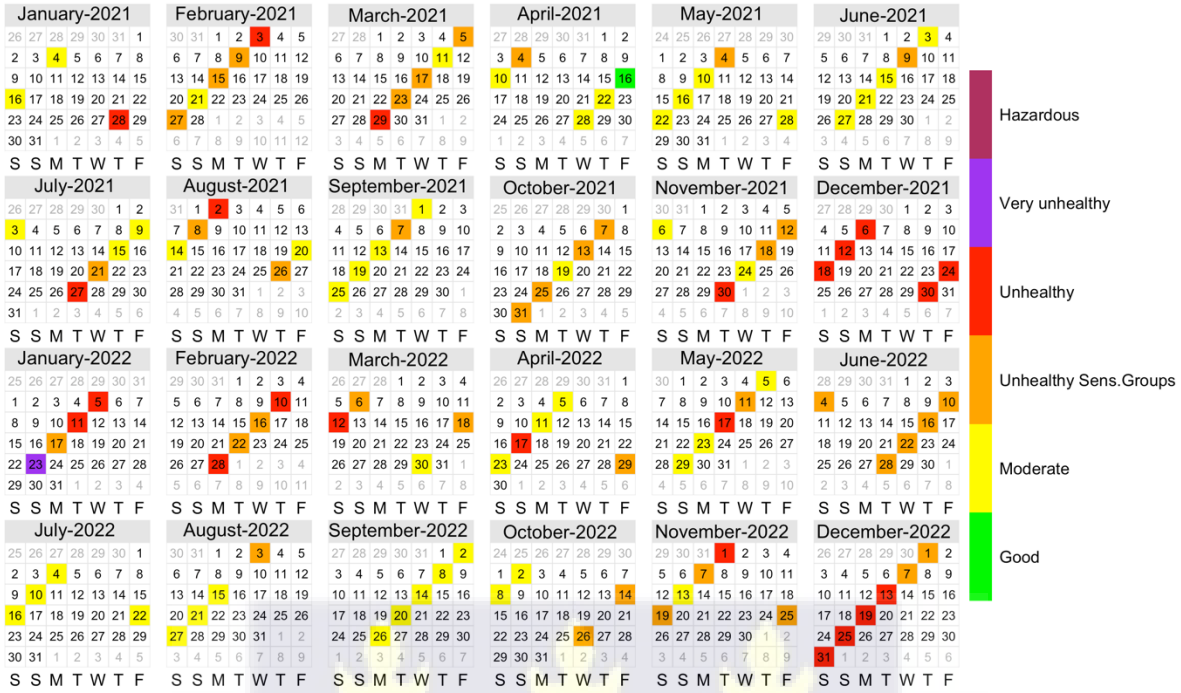

DA

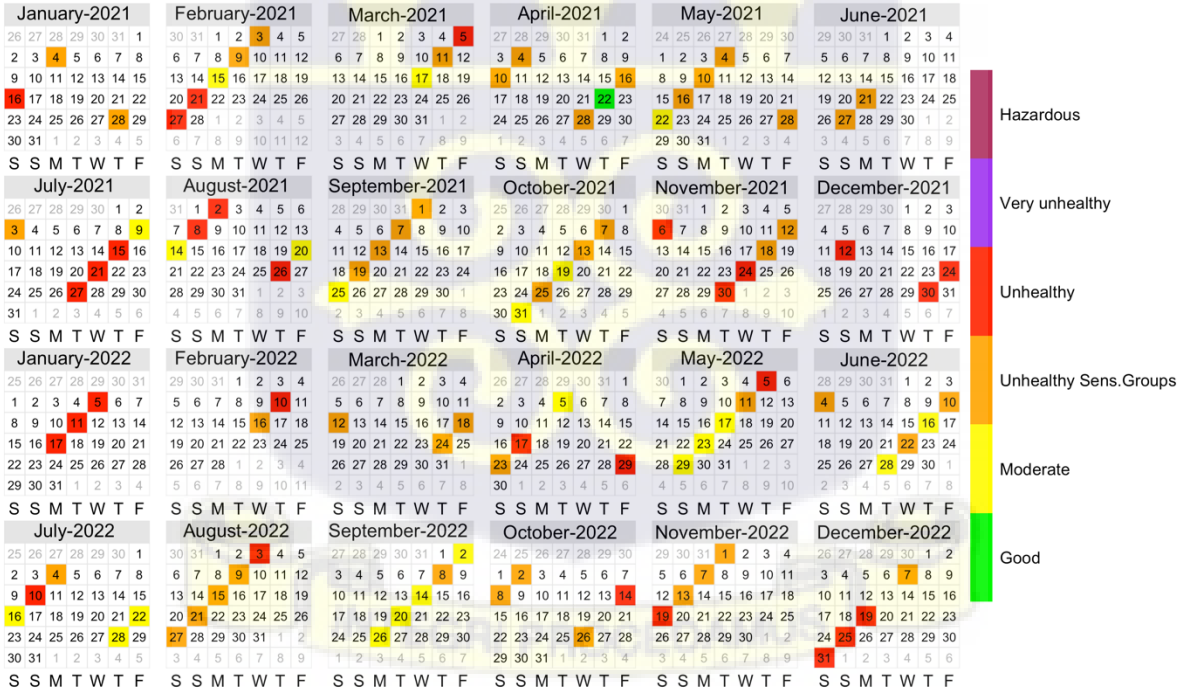

UGT640

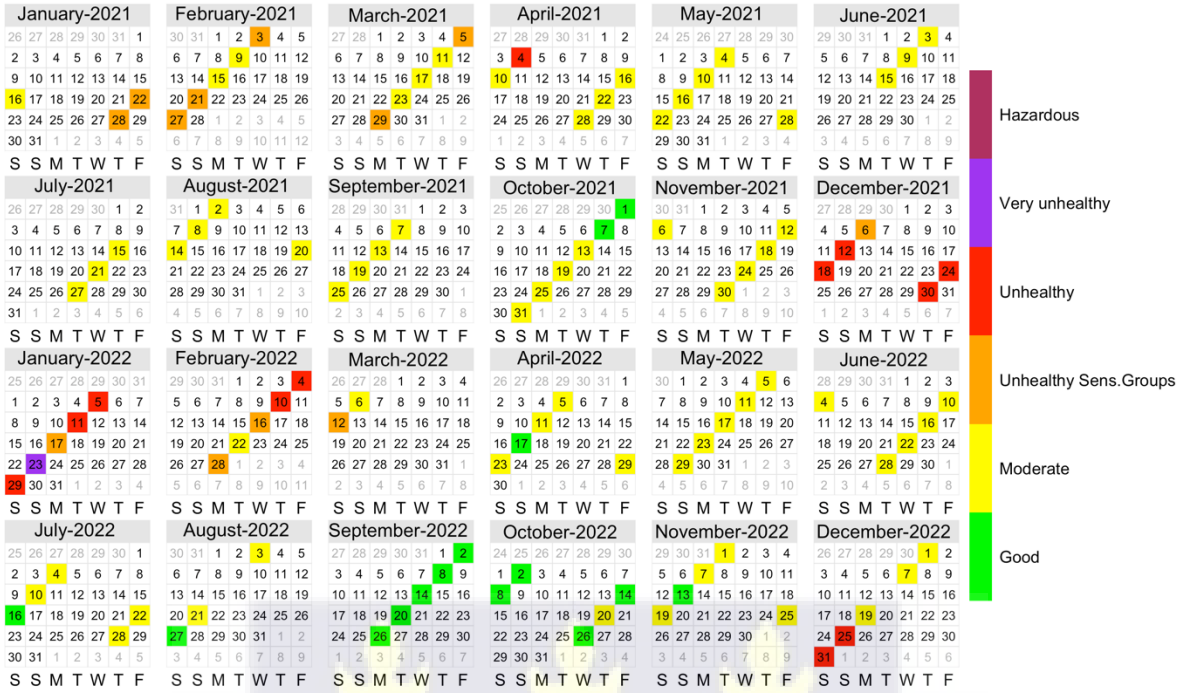

ADT640

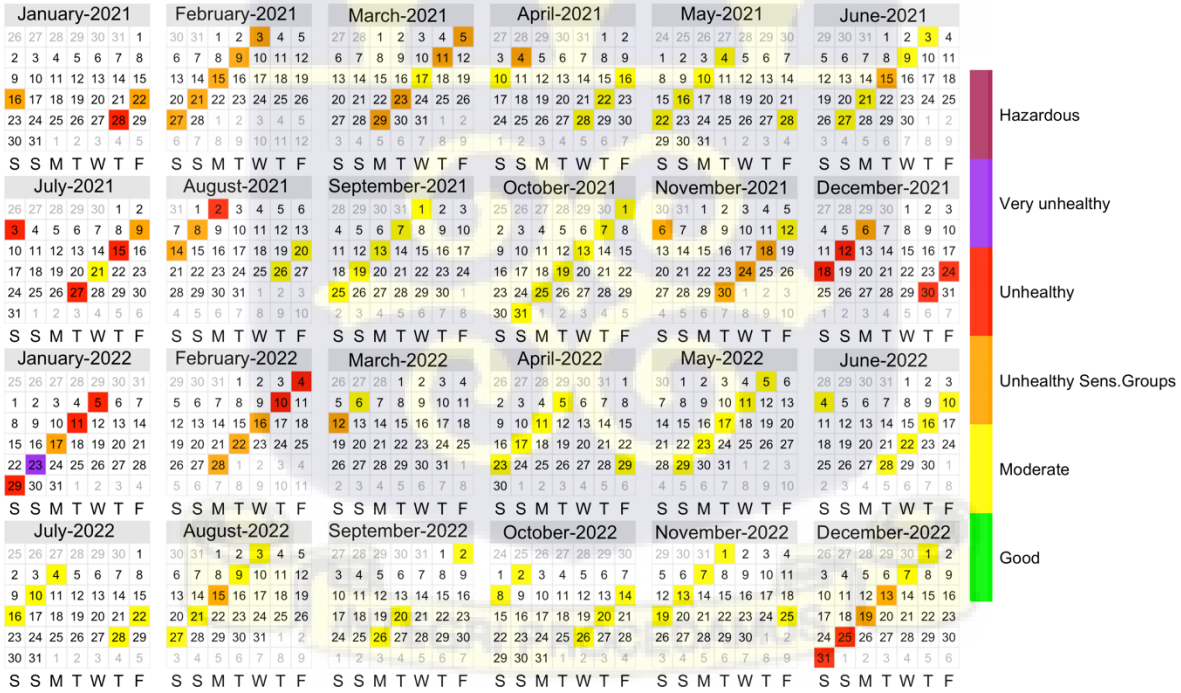

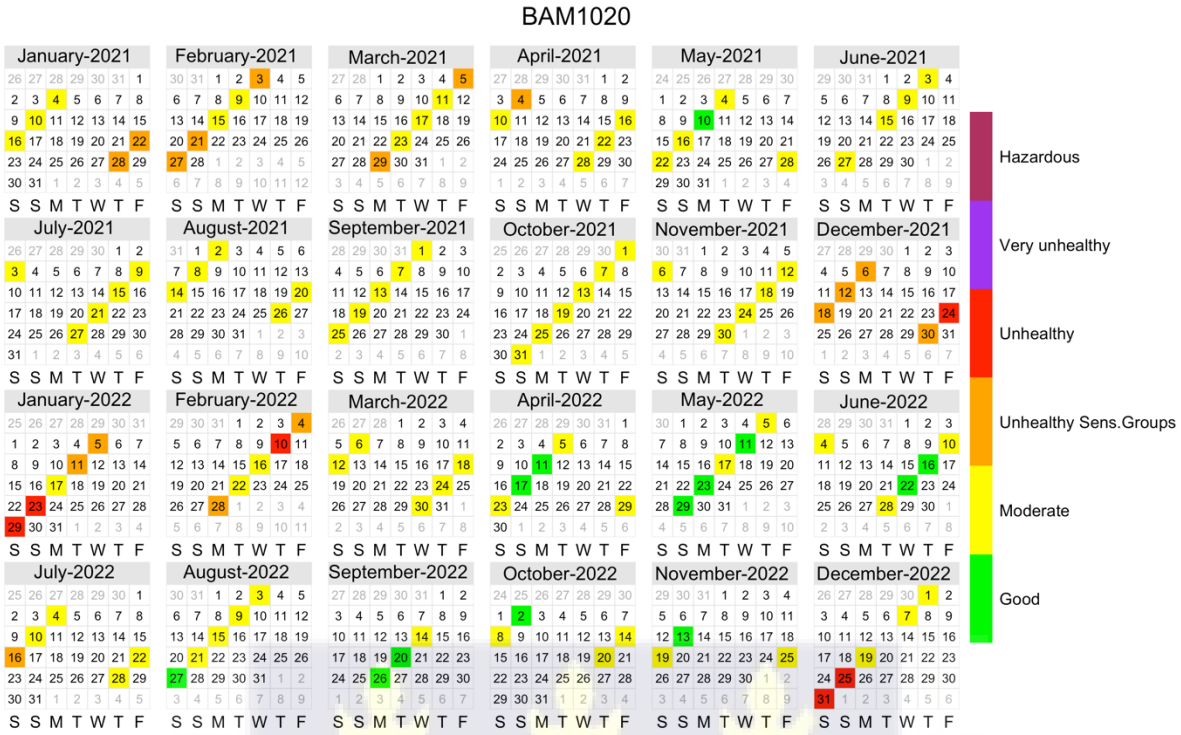

Figure 4.8 Calendar plots of the three sites and the optical monitors during the study period (2021-2022).

4.3 METEOROLOGICAL FACTORS AFFECTING PARTICULATE MATTER CONCENTRATION

4.3.1 Meteorology impact on $PM_{2.5}$ Mass

Meteorological parameters within the southern belt (precisely Accra) were used to ascertain the dynamics of particulate matter emissions within the study area. Findings from the literature show that prevailing weather conditions greatly impact emissions, transport, formation, and deposition of particulate matter (204).

These climatic parameters affect the production of secondary pollutants and the release of aerosols from the ground surface, as well as the duration they remain in the atmosphere. Therefore, it is important to comprehend the physical processes that result in the observed concentration of $PM_{2.5}$

at a particular place. One of the causes of the non-Harmattan season's low aerosol particle levels is precipitation, which washes out the particles. One of the main methods for removing aerosols from the atmosphere is moist deposition by rainfall or wet removal (205).

There were low rainfall in Accra during the Harmattan season when this study was conducted. Moreover, the average local ambient temperature showed minimal variation between the two seasons. During the harmattan and non-harmattan seasons, the relative humidity ranged from 18% to 92% and 57% to 91%, respectively (Tables 4.6 and 4.7). For the days with particulate sample collection, the average monthly values for precipitation, relative humidity, and temperature are shown in comparison to monthly averages (Figures 4.9 and 4.10). The link between temperature and rainfall and relative humidity was direct. Over the course of the sampling period, the mean wind speed varied, with the highest speed recorded in March (9.0 m/s) and the lowest recorded in September (6.2 m/s) for 2021. The highest speed recorded in 2022 was in March (9.6 m/s) and the lowest in recorded in December (5.1 m/s) (69).

Table 4.5 Mean of climatic variables measured during the sampling intervals in Accra, Ghana in 2021.

Month	Rainfall (mm)	RH (%)	Temp/°C	wind speed (m/s)	max temp/°C	min temp/°C
Jan	2	80.1	29.1	7.4	32.7	25.5
Feb	3.5	79.0	29.8	8.8	33.4	26.2
Mar	2.8	75.3	29.6	9.0	33.1	26.0
Apr	7.1	72.5	30.0	8.8	33.4	26.6
May	10.2	73.0	29.5	8.9	32.9	26.1
Jun	20	75.5	28.1	7.3	31.5	24.7
Jul	32.4	78.0	27.1	8.3	30.0	24.1
Aug	23.3	79.7	27.0	7.4	29.8	24.2
Sep	13.9	78.3	27.3	6.2	30.5	24.1
Oct	17.2	73.1	29.9	-	33.5	26.2
Nov	13.7	75.3	29.1	-	32.9	25.3
Dec	11.5	73.1	29.9	6.5	33.5	26.2

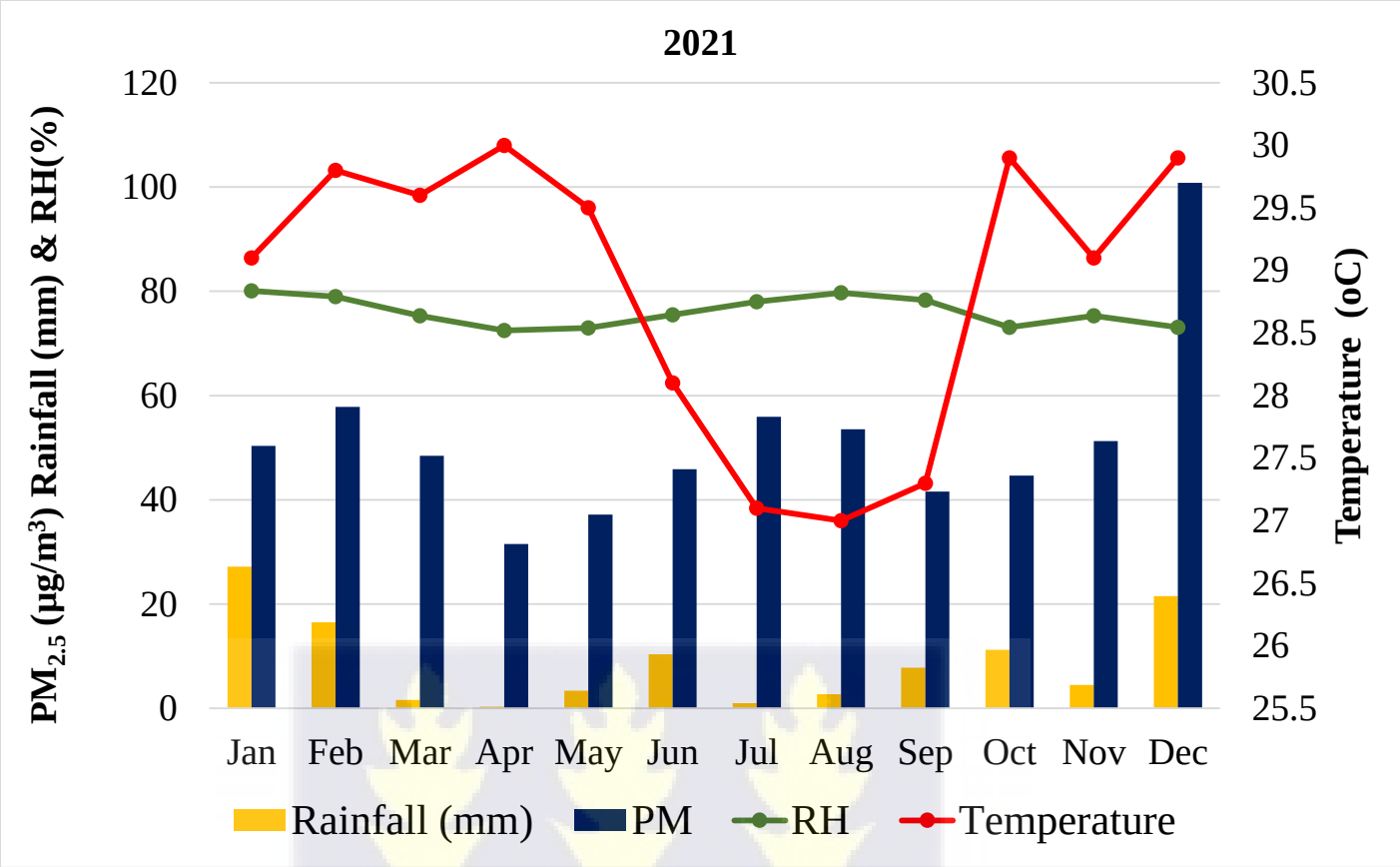

Figure 4.9 Monthly mean of atmospheric temperature (°C), relative humidity (RH, in %) and rainfall (mm) against mean $PM_{2.5}$ mass concentration for January 2021 – December 2021 in Greater Accra Metropolitan Area (69).

Table 4.6 Average of meteorological parameters during the sampling periods in Accra, Ghana in 2022.

Month	Rainfall (mm)	RH (%)	Temp/°C	wind speed (m/s)	max temp/°C	min temp/°C
Jan	No data	71.0	29.7	5.5	33.7	25.7
Feb	No data	77.4	29.8	7.9	33.3	26.4
Mar	0.5	74.6	30.1	9.6	33.4	26.8
Apr	17.8	75.0	28.8	7.6	32.4	25.2
May	26.9	77.9	28.6	7.1	32.2	25.1
Jun	11.7	79.6	27.3	6.3	30.5	24.1
Jul	28.2	78.8	26.4	7.3	28.9	23.8
Aug	3.1	82.2	25.5	7.5	28.1	23.0
Sep	10.0	83.0	26.2	7.3	28.9	23.5
Oct	16.3	77.1	27.8	5.7	31.2	24.4
Nov	42.3	76.2	28.8	5.3	32.6	24.9
Dec	7.9	73.7	29.2	5.1	33.2	25.2

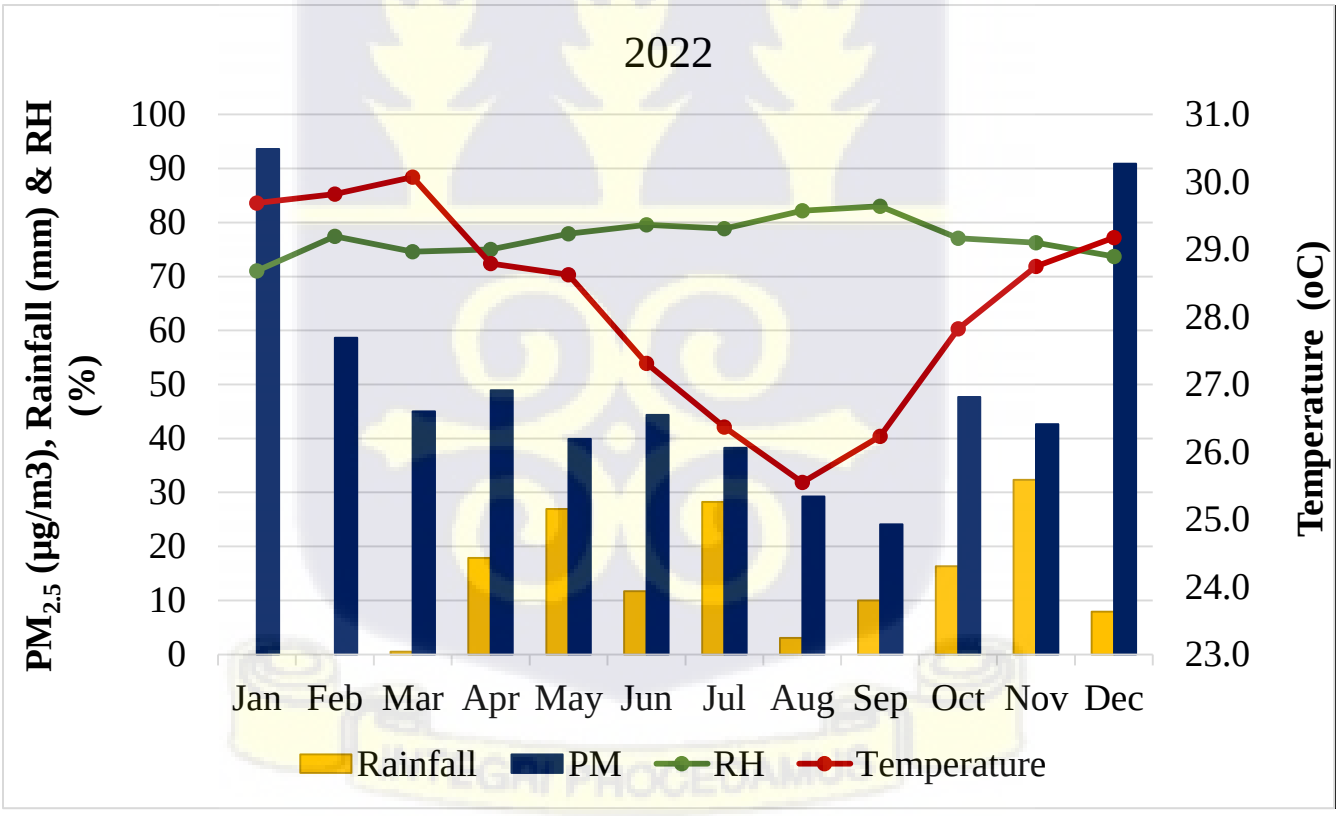

Figure 4.10 Monthly average of atmospheric temperature (°C), relative humidity (RH, in %) and rainfall (mm) against mean $PM_{2.5}$ mass concentration for January 2022 – December 2022 in Greater Accra Metropolitan Area (69).

Tables 4.6 and 4.7 provide an overview of the summary statistics for rainfall, relative humidity, temperature, and wind direction and speed for the entire study period. In 2021, the summary (mean and standard deviation) for temperatures averaged 28.9 ± 1.2 °C, relative humidity (RH) averaged 76.1 ± 2.8%, and rainfall averaged 9.0 ± 8.9 mm. Additionally, the summary for 2022 showed temperatures averaged 28.2 ± 1.5 °C relative humidity (RH) averaged 77.2 ± 3.4 %, and rainfall averaged 16.5 ± 12.9 mm (Figures 4.9 and 4.10).

Generally, Accra is expected to experience a predominant south-westerly wind direction originating from the Gulf of Guinea (Atlantic Ocean) (202). This experience is common during the non-Harmattan period, and it is accompanied by some level of variation in temperature and relative humidity. Numerous studies have demonstrated that several meteorological factors, such as rainfall, temperature, wind speed, and relative humidity, have an impact on particulate matter mass concentrations (205–207). During the Harmattan period, trade winds from the Saharan desert (North East) influx the country with dusty winds. Both wet and dry seasons have a great impact on particulate matter emissions.

The wind rose (Figure 4.11) describes the characteristics of wind in Accra. Wind velocities ranged from 12.1m/s to 17.5 m/s and 9.9 m/s to 18.7 m/s for the 1st and 99th percentiles in the 2021 and 2022 study periods, respectively. Wind directions were predominantly SW and S, whereas winds

from other directions were rare. The wind speed for 2021 averaged 15.002 m/s (calm = 4.1%).

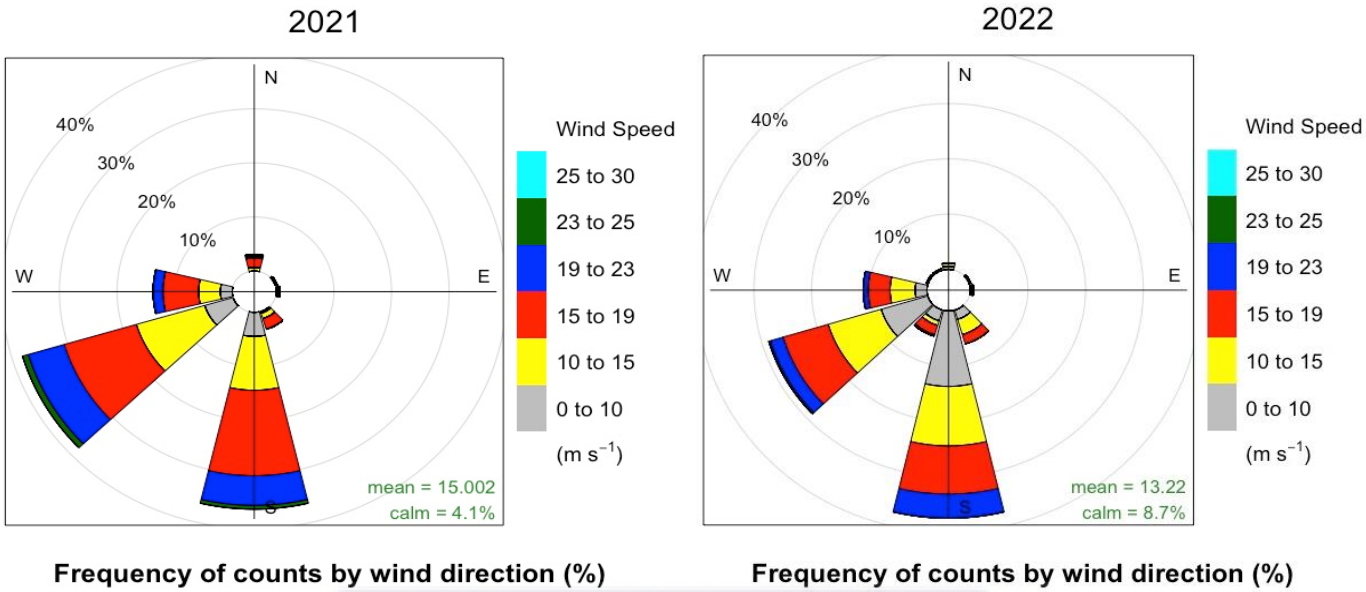

Similarly, wind speed for 2022 averaged 13.22 m/s (calm = 8.7%).

Figure 4.11 Wind rose plots for 2021 and 2022.

Throughout the entire study period, the daily average wind speed varied between 12.1 m/s and 17.5 m/s and 9.9m/s to 18.7 m/s for 2021 and 2022, respectively, while the daily average temperature varied between 27.1 °C and 30 °C and 25.5 °C to 30.1 °C for 2021 and 2022, respectively.

4.3.2 Relationship between Weather Parameters and $PM_{2.5}$

Meteorology data obtained during the study period was compared to the $PM_{2.5}$ results. Meteorological factors such as wind speed, wind direction, temperature, atmospheric stability, and mixing height exert a substantial influence on pollutant concentrations in a given region. Numerous scientific studies have explored the critical role played by meteorological parameters, directly or indirectly, in the dispersion, transformation, and removal of particulate matter from the lower atmosphere.

Table 4.8 Pearson's Correlation Matrix of $PM_{2.5}$ and weather parameter

	Relative Humidity	Temperature	Rainfall	Wind Speed	$PM_{2.5}$
$PM_{2.5}$	**-0.35**	**0.35**	**-0.18**	**-0.30**	**1**
Wind speed	0.05	0.06	-0.31	1	
Rainfall	-0.19	0.02	1		
Temperature	-0.59	1			
Relative Humidity	1				

4.3.2.1 Relationship between Rainfall and $PM_{2.5}$

Whenever there was rainfall (precipitation), the bulk concentration of $PM_{2.5}$ was consistently low (Figure 4.12). Rainfall eliminates air particulates, and moisture prevents soil particles from being re-suspended by making the soil wet; therefore, there will be a lower mass concentration of particulate matter in the atmosphere. $PM_{2.5}$ mass concentrations exhibited a negative correlation against rainfall during the study period; however, it was not statistically significant (218).

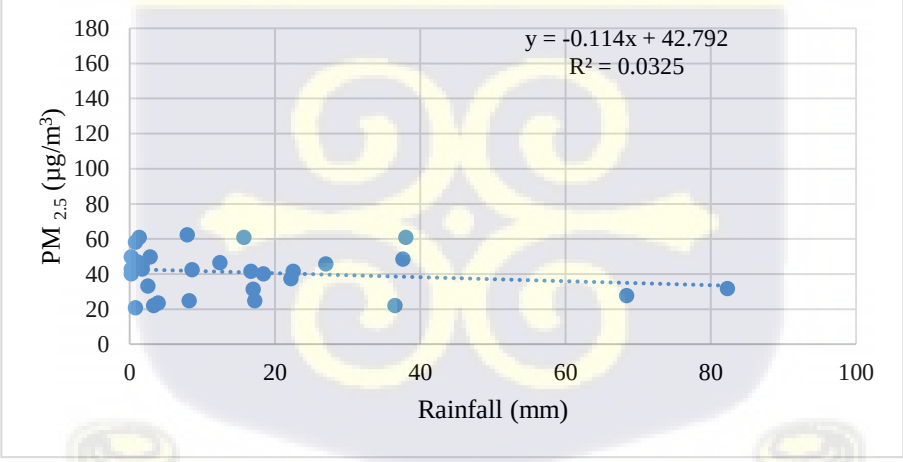

Figure 4.12 Relationship between mean $PM_{2.5}$ mass concentrations and total daily cumulative rainfall.

4.3.2.2 Relationship between Temperature and $PM_{2.5}$

The variation of mass concentration of $PM_{2.5}$ versus temperature is depicted by Figure 4.13 for the entire investigation period. It was found that pollution levels spread across the temperature range. Although this association is more tenuous in 2021, $PM_{2.5}$ mass concentration and temperature were positively correlated during the entire period of study in 2021 and 2022. This indicates that $PM_{2.5}$ rises or falls as the temperature changes. The relationship between temperature and $PM_{2.5}$ is explained by the fact that warm air masses have better atmospheric dispersion conditions than cold air masses (208,209).

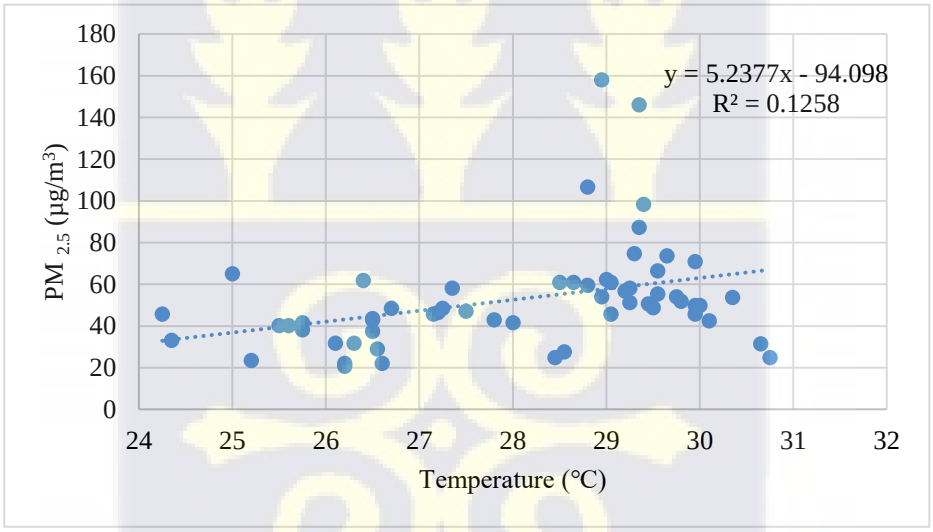

Figure 4.13 Relationship between mean $PM_{2.5}$ mass concentrations and total daily average temperature

4.3.2.3 Relationship between Relative Humidity and $PM_{2.5}$

An inverse connection between $PM_{2.5}$ mass concentration and relative humidity was observed during the investigation periods (Figure 4.14). The negative correlation could possibly be due to some climatic changes during the study period. The relative humidity factor often leads to the accumulation and settling of particles on the ground rather than their suspension in the atmosphere. As a result, high relative humidity significantly reduces air pollution.

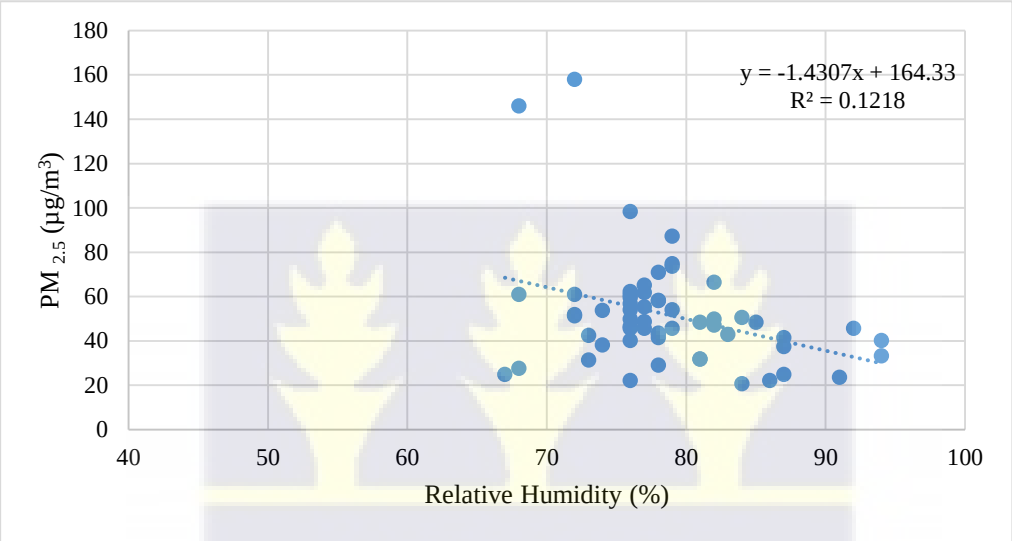

Figure 4.14 Relationship between mean $PM_{2.5}$ mass concentrations and relative humidity

4.3.2.4 Relationship between Wind Speed and $PM_{2.5}$

There was a negative correlation between wind speed and $PM_{2.5}$ (Figure 4.15). The negative connection between $PM_{2.5}$ and wind speed suggests that local sources are more prevalent (210). When it comes to removing particulate matter from the atmosphere and moving it from one place to another, wind speed is crucial. It also has an impact on the turbulence close to the ground. Low winds allow particulate levels to rise, whereas strong winds remove particulate matter from the atmosphere.

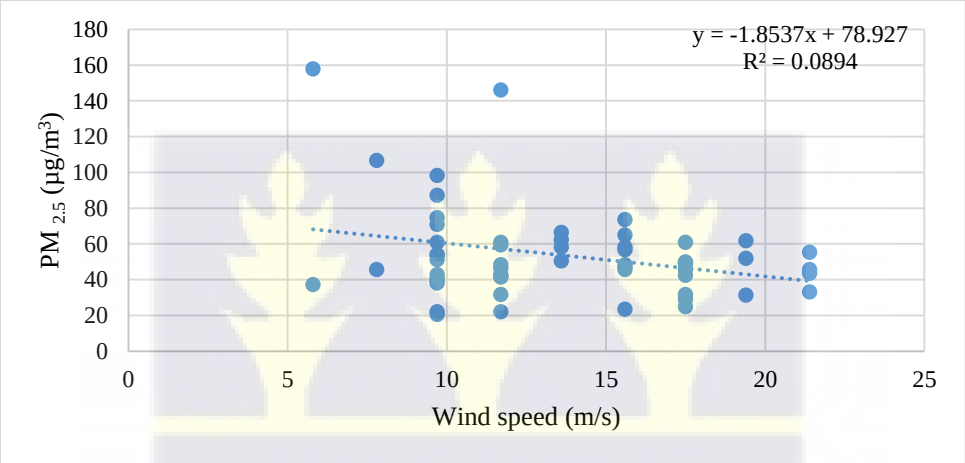

Figure 4.15 Relationship between mean $PM_{2.5}$ mass concentrations and daily wind speed

4.4: CHARACTERIZATION OF ATMOSPHERIC PARTICULATE MATTER $PM_{2.5}$

Characterizing $PM_{2.5}$ entails examining the composition, distribution of sizes, and sources of emission of fine particles. Chemical analysis is used to identify the different components present in a substance, whereas size distribution studies provide information on the sizes of particles. Source apportionment techniques assist in assigning $PM_{2.5}$ to specific sources, facilitating the reduction of environmental and health consequences. The EDXRF analysis of the atmospheric particulate matter $PM_{2.5}$ from the sampling sites revealed the following elements: Al, Br, Ca, Ce, Cl, Co, Cr, K, Fe, Cu, Ni, P, Pb, Rb, S, Sc, Si, Ti, V, Zn, and Zr. Table 4.8 below shows the concentrations of elemental composition from the various particulate matter sampled.

Table 4.8 Mean concentration of total $PM_{2.5}$ ($\mu g\ m^{-3}$) and its elemental concentration ($ng\ m^{-3}$) at the three sites (2021 and 2022).

Elements	**DA21**		**DA22**		**AD21**		**AD22**		**UG21**		**UG22**	
	Mean	SD	Mean	SD	Mean	SD	Mean	SD	Mean	SD	Mean	SD
Total $PM_{2.5}$	**49.90**	**19.96**	**49.28**	**20.84**	**60.76**	**25.00**	**60.54**	**29.14**	**42.49**	**23.10**	**46.37**	**28.60**
Al	**71.60**	0.02	78.90	0.01	1.26	0.79	2.03	1.79	-	-	-	-
Br	**0.36**	1.57	0.02	0.04	0.08	0.09	0.09	0.18	0.37	1.60	0.02	0.02
Ca	**56.25**	33.13	13.42	18.43	0.24	6.61	0.38	0.07	56.25	30.13	19.61	66.83
Ce	**2.94**	4.12	0.40	1.19	2.33	3.17	2.02	2.12	2.94	4.12	0.88	1.17
Cl	**737.77**	442.91	170.94	121.74	33.72	130.11	9.51	26.55	737.77	4342.91	168.04	674.38
Co	**0.13**	0.20	0.01	0.03	0.07	0.11	0.09	0.14	0.13	0.19	0.03	0.02
Cr	**12.33**	18.92	0.02	0.10	-	-	-	-	-	-	0.13	0.17
K	**252.99**	134.85	146.8	81.33	94.63	45.33	137.12	59.40	127.05	120.39	58.22	18.19
Fe	**22.80**	61.04	3.62	7.47	2.34	3.32	1.44	1.54	22.80	61.04	3.54	7.61
Cu	-	-	0.04	0.09	0.41	0.69	0.23	0.42	1.63	2.85	0.37	1.40
Ni	**3.33**	6.18	0.17	0.26	2.14	2.95	0.00	0.00	3.33	6.10	1.17	4.89

P	**62.27**	54.75	20.00	29.10	0.13	0.11	0.17	0.11	62.27	54.75	74.31	86.20
Pb	**0.20**	0.35	0.05	0.07	0.16	0.15	0.07	0.13	0.20	0.33	0.37	1.38
Rb	**0.03**	0.04	0.02	0.06	0.11	0.13	0.05	0.05	0.03	0.04	0.06	0.20
S	**15.74**	10.69	24.04	18.09	32.52	19.30	15.41	43.96	15.59	12.57	12.69	13.35
Sc	-	-	-	-	0.65	1.20	0.42	0.69	-	-	-	-
Si	**665.2**	387.4	569.6	225.4	529.9	495.52	555.92	202.38	665.21	387.44	609.83	891.12
Ti	**2.53**	3.17	1.45	2.14	1.40	1.41	0.98	1.68	2.53	3.17	1.93	3.71
V	**0.32**	0.34	0.09	0.25	0.42	0.51	0.15	0.14	0.32	0.34	0.27	0.36
Zn	**0.03**	0.02	0.07	0.24	0.11	0.17	0.08	0.12	0.03	0.01	0.20	0.24
Zr	**0.19**	0.96	0.02	0.03	0.07	0.07	0.04	0.05	0.19	0.96	0.01	0.00

4.5 ENRICHMENT FACTOR (EF) ANALYSIS

Enrichment factor (EF) analysis was used to determine the indication of the degree of anthropogenic contributions to the elemental composition of $PM_{2.5}$ observed at the three urban sites. The enrichment factor is calculated by comparing the concentration of a specific element in a sample (e.g., air, soil, or water) to its natural background concentration. EFs were computed using the mean concentrations of all elements found in the $PM_{2.5}$ samples. According to convention, elements with an EF < 10 are typically assumed to come from a crustal or natural source, whereas elements with an EF > 10 are typically thought to have a large contribution from non-crustal or anthropogenic sources (211–213).

The enrichment factors were calculated using equation 3.17, with silicon (Si) chosen as the reference element due to its high abundance in the earth's crust and its resilience to human-induced interferences. This information may be found in section 3.5 (194,196,214). Table 4.9 displays the results of the enrichment factor computerization for the elements found in $PM_{2.5}$ at each of the three sampling locations (AD, DA, and UG).

Table 4.9 Determined enrichment factors (EFs) for each of the examined $PM_{2.5}$ elements, (using Si as a reference).

ELEMENT	DA 21	DA 22	AD 21	AD 22	UG21	UG22
Al	2.27	1.52	0.14	0.12	-	-
Br	24.33	4.55	316.64	181.82	25.03	2.71
Ca	0.23	0.16	0.19	0.12	0.23	0.22
Ce	7.52	2.98	332.15	154.37	7.52	6.16
Cl	959.37	650.46	2438.65	368.34	959.37	596.67
Co	0.87	0.24	27.98	18.32	0.87	0.46
Cr	20.84	0.10	5.16	4.29	-	0.58
Cu	-	0.40	69.50	21.06	5.00	3.12
K	2.05	1.11	2.08	0.51	2.08	1.29
Fe	0.07	0.03	0.39	0.13	0.07	0.03
Ni	5.63	0.83	201.54	-	5.63	5.41
P	10.03	9.42	12.01	11.24	10.03	32.67
Pb	2.71	1.87	121.09	29.16	2.71	13.71
Rb	0.06	0.09	11.47	2.71	0.06	0.31
S	535.7	489.3	452.59	298.30	1001.01	989.8
Sc	-	-	278.62	96.28	-	-
Si	1.00	1.00	1.00	1.00	1.00	1.00
Ti	0.08	0.13	2.31	0.86	0.08	0.16
V	0.40	0.33	29.14	5.59	0.40	0.93
Zn	0.08	0.52	15.03	5.40	0.08	1.32
Zr	0.20	0.06	3.71	1.06	0.20	0.05

The mean concentration of all samples from every site was used to compute EFs (see equation 3.4). Source of crustal concentrations is Taylor and McLennan (28,199).

Table 4.9 shows the average EFs of elements in $PM_{2.5}$ for all Accra sample sites over the course of the study period (2012–2022). Al, Si, P, K, Ca, Ti, V, Fe, Co, Ni, Zn, Rb, and Zr are the

categories of EF<10 for $PM_{2.5}$ in 2021 and 2022 across all sample sites. Nearly same values were shown in the EF results at every sampling location. These characteristics are typical of crustal origin, or soil dust. While most of these components originated from natural sources, anthropogenic contributions must also be considered. K is released when wood and biomass are burned; Ca is released when motor vehicles run on detergents that are used to lubricate engines; Fe is released when brake pads wear down and other automobile components (215). In $PM_{2.5}$ fractions, Ce, Zn, Cu, and Fe are also linked to vehicle exhaust emissions, tyre and brake wear (216,217).

The lowest EF value was 0.07 for Fe, which was shown at DA 21 and while the highest EF value was 7.52 at DA 21 and UG21 respectively. The group with EF > 10 but less than 100 were the elements Br, Co, Cr, Cu, P, Pb, Sc, V, and Zn at almost all sites. It showed that there was a moderate enrichment of Br, Co, Cr, Cu, P, Pb, Sc, V, and Zn. Traditional vehicle emission tracers include V, Cu, Co, Cr, Pb, and Zn. Their EF values indicated a significant contribution from vehicle emissions.

It has been reported earlier that in addition to the combustion of fuel and motor oil, other potential sources of Pb pollution include brake wear, industrial emissions, dust carried over long distances, and re-suspended soil that has been exposed to particles from previously emitted leaded petrol (218,219). Zinc compounds have found widespread application as dispersion or detergent enhancers for lubricating oils, as well as antioxidants (e.g. zinc carboxylate complexes and zinc sulphonates).

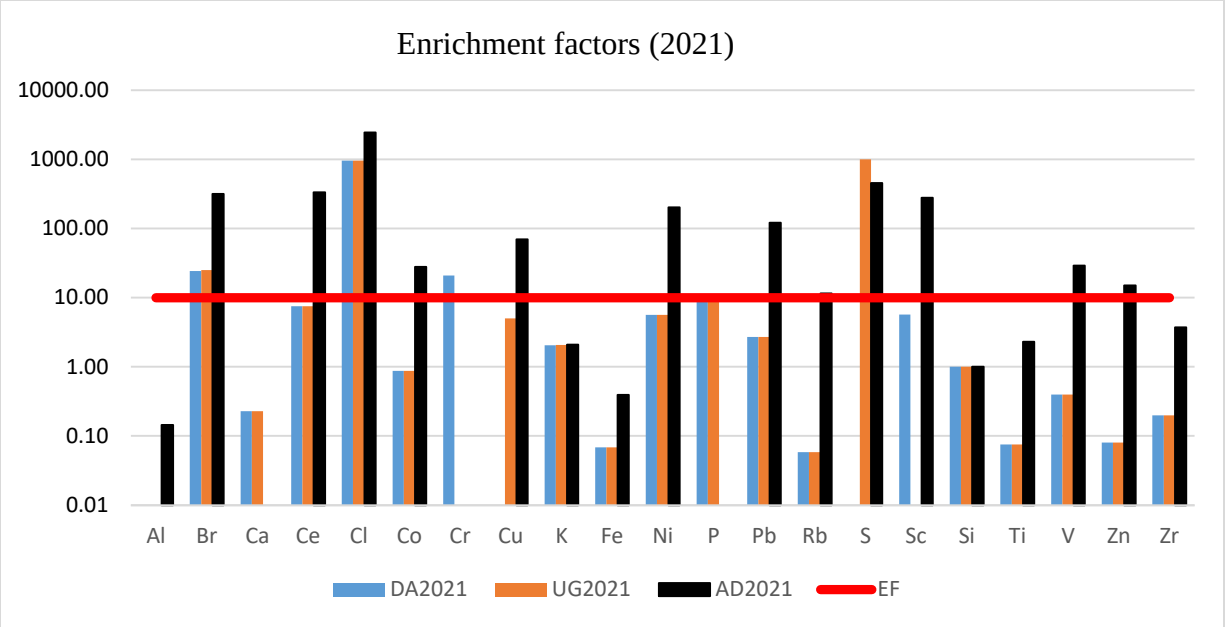

Figure 4.16 Enrichment factor for $PM_{2.5}$ chemical components of all sites in Greater Accra Metropolitan Area (2021)

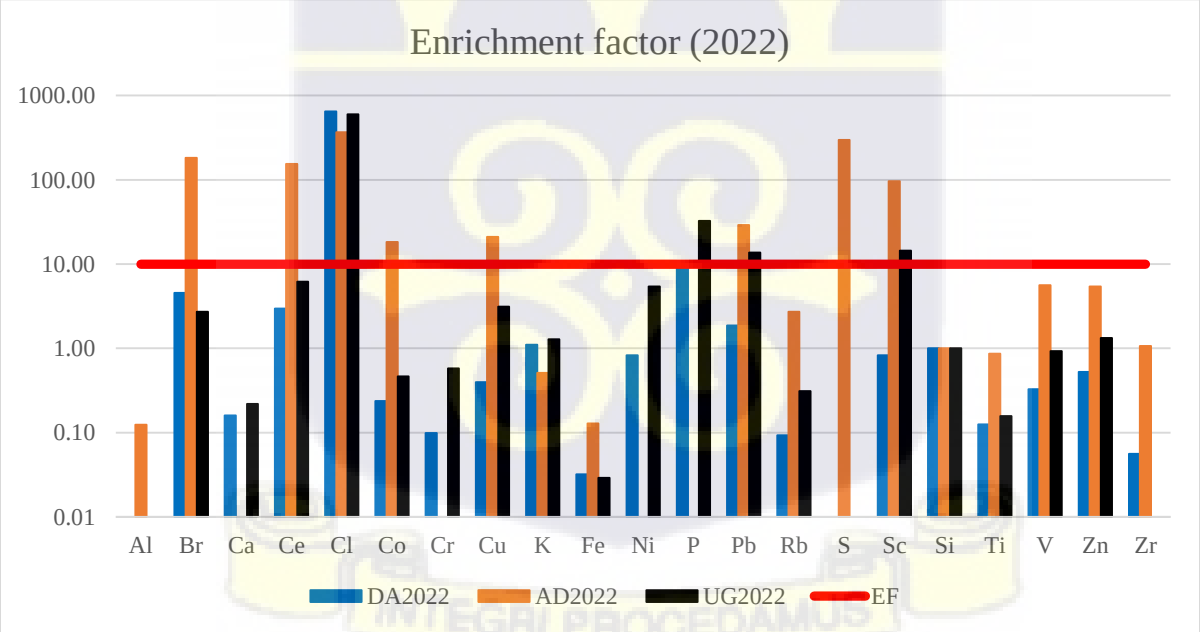

Figure 4.17 Enrichment factor for $PM_{2.5}$ chemical components of all sites in Greater Accra Metropolitan Area (2022)

Zn of urban dust can be greatly increased by mechanical vehicle abrasion, industrial metal processing, and tyre wear and tear on vulcanized cars (220,221).

Species with EF > 100 included S, Br, Sc, Ce, Cl, and Pb. These components have substantial levels of enrichment, and the emission sources are probably from burning garbage and traffic, respectively. Since most hazardous trace metals are found in the environment as Sulphates or nitrates, the S content is significant since it contains Sulphates. The species Cl at the AD site and S at the UG were in the group with EF>1000. Given that the AD location is about 2.75 km to the Atlantic Ocean, the highly enriched Cl there is not surprising. The primary source of Cl is sea salt. Tailpipe emissions of vehicles on UG campus is the main source of S, due to transport activities.

4.6 SOURCE IDENTIFICATION AND APPORTIONMENT USING POSITIVE MATRIX FACTORIZATION

The U. S. EPA's Positive Matrix Factorization (PMF) version 5.0 modeling software was used to identify and allocate the source of APM (197). Six sources were identified by PMF in the $PM_{2.5}$ fractions. The PMF model study used the observed $PM_{2.5}$ mass concentrations as an independent variable to directly determine the mass apportionment, eliminating the need for the traditional multilinear regression. In the model study, the PM mass values were adjusted by reducing the weights of the uncertainty to four times the mass concentrations.

Table 4.10 S/N values for the $PM_{2.5}$ data at the three sites during the study (2021 and 2022)

Species	AD21	AD22	UG21	UG22	DA21	DA22
Al	2.6	4.2	-	-	2.4	2.7
Br	2.1	2.6	3.1	2.3	5.2	4.1
Ca	2.8	4.5	3.7	2.7	2.2	3.3
Cl	7.3	9.2	2.2	2.5	6.1	2.9
Co	2.1	2.7	2.7	2.3	2.4	3.1
Cr	2.8	2.2	2.6	2.6	2.7	2.4
Cu	2.1	2.5	2.1	2.5	2.2	2.6
Fe	2.9	2.2	5.2	3.5	4.4	3.7
K	3.1	2.7	2.8	2.9	4.2	3.9
Ni	2.5	3.1	2.2	2.4	2.6	3.1
P	-	-	5.2	5.7	4.5	3.2
Pb	2.1	2.9	2.9	2.6	2.4	2.7
Rb	2.5	2.2	3.4	3.2	2.6	2.3
S	3.3	4.8	2.8	2.4	4.9	4.1
Sc	2.2	2.1	2.6	2.9	-	-
Si	3.1	7.1	2.2	4.4	2.5	2.1
Ti	2.7	3.1	3.5	3.1	2.7	2.1
V	2.1	2.7	2.5	2.8	2.9	2.7
Zn	2.8	2.2	2.4	2.5	2.3	2.4
Zr	2.8	2.0	2.4	3.5	2.2	2.8

Table 4.11 Average contributions of identified sources of $PM_{2.5}$ concentrations ($\mu g\ m^{-3}$) (2021 - 2022)

	AD 2021	AD 2022	DA 2021	DA 2022	UG 2021	UG 2022
Biomass burning	0.01801	0.032885	0.006781	0.01482	0.003848	0.004409
Solid waste burning	0.015022	0.02251	0.002546	0.004645	0.004332	0.004302
Sea salt spray	0.007519	0.01077	0.003523	0.00574	0.001561	0.00128
Vehicular/industry	0.02211	0.046562	0.009892	0.024719	0.005382	0.004986
Soil dust	0.01191	0.02050	0.005307	0.007873	0.003303	0.003256
Re-suspended Dust	0.01374	0.02985	0.006061	0.013567	0.004238	0.004423

Source 1: In this fine fraction, Figure 4.18a and 4.18b show the source profile with high loadings of S, and K while Figure 4.18c displays the time series of concentrations. K is a very effective indicator of a biomass burning source, since it is generally recognized (3,28,222,223). From the source contributions, concentration of K was highest at AD, followed by DA with the least at UG. However, compared to Dansoman and University of Ghana campus, Adabraka has substantially larger household densities of biomass fuel users, meaning that in absolute terms, biomass burning caused greater particle pollution in this location (224).

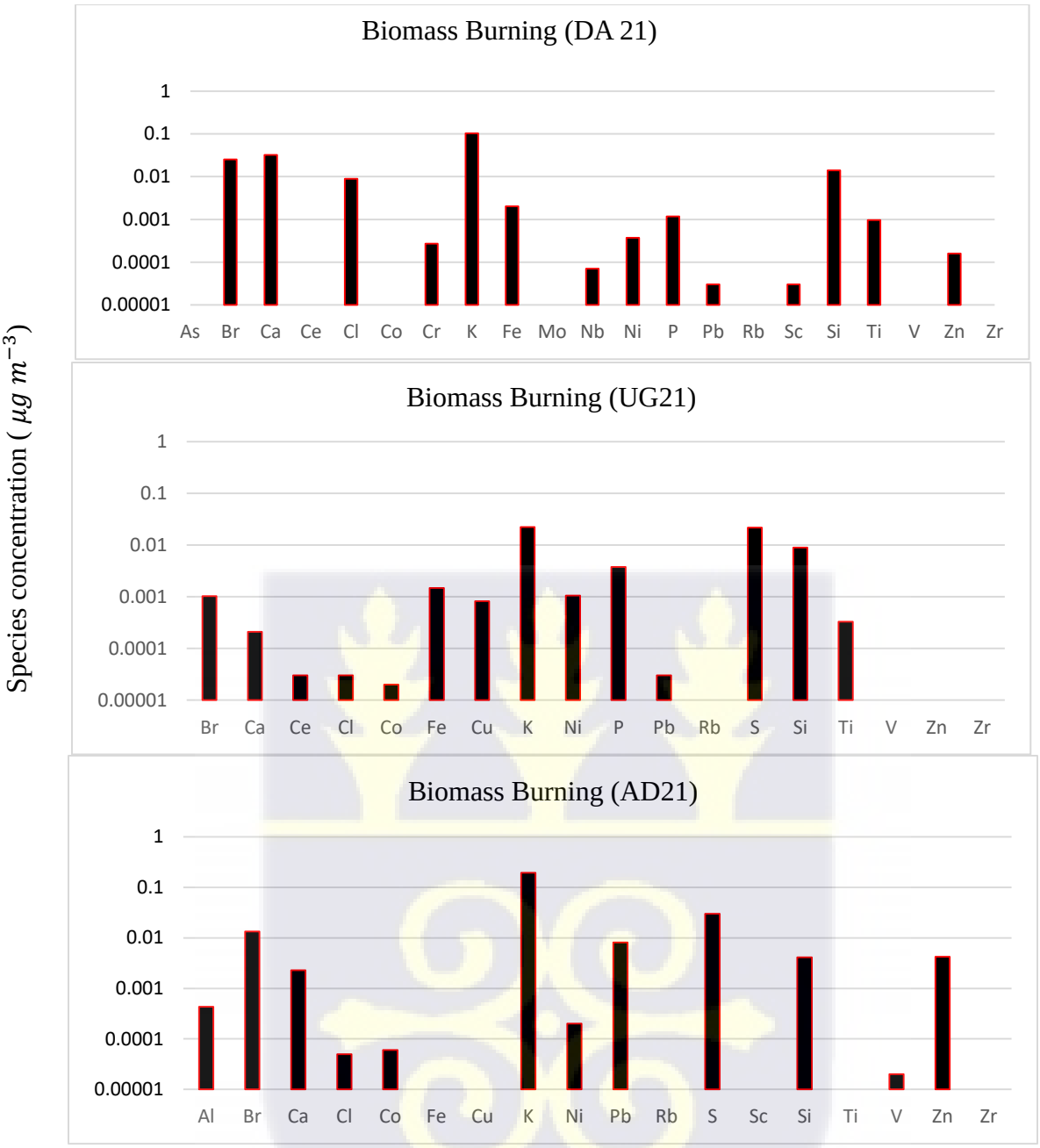

Figure 4.18a $PM_{2.5}$ source profiles for biomass factors (2021)

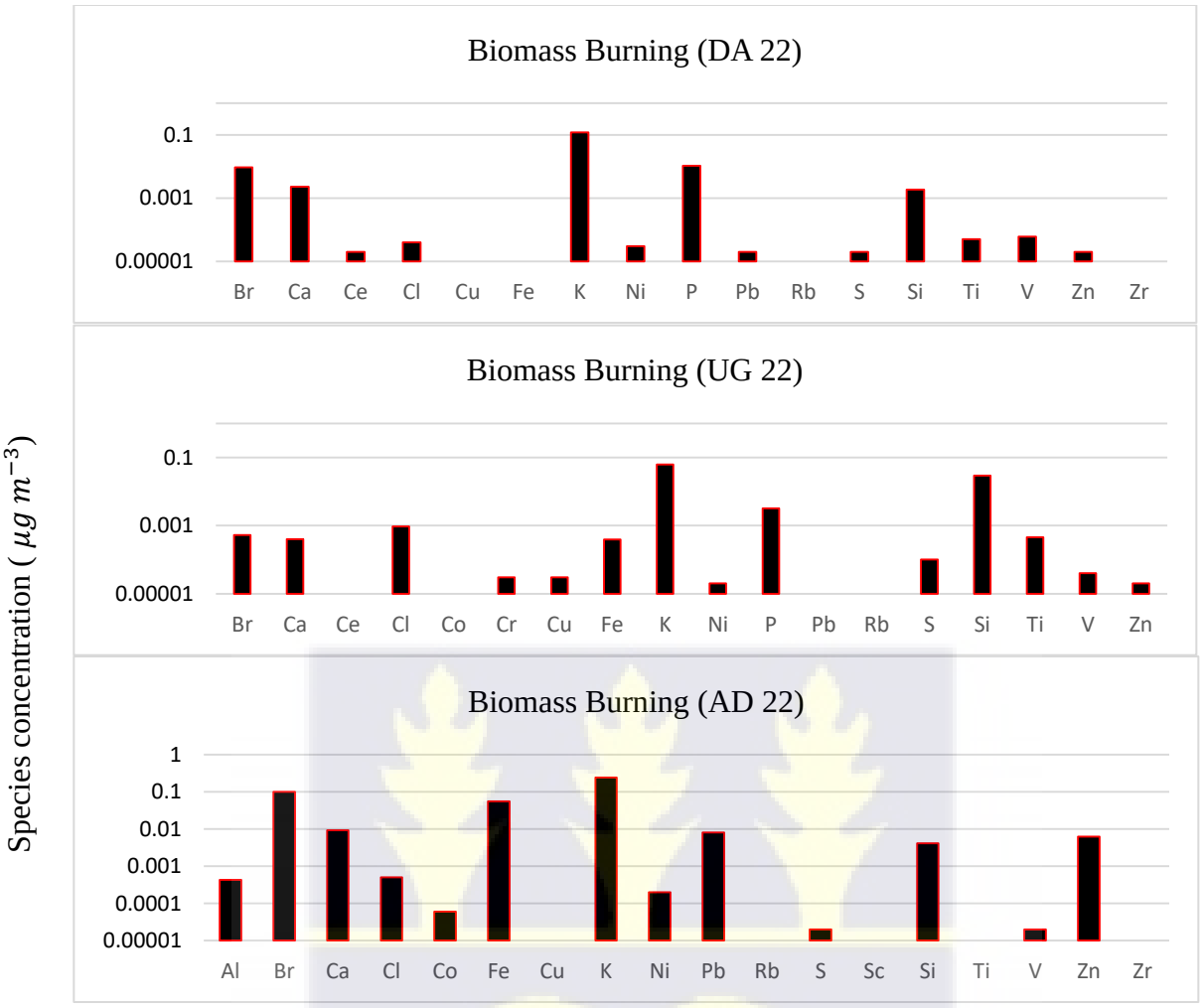

Figure 4.18b $PM_{2.5}$ source profiles for biomass factors (2022)

In densely populated metropolitan areas such as Adabraka and Dansoman, a significant number of individuals rely on wood, particularly wood charcoal, for the purpose of cooking and providing heat inside their residences. Additionally, some people in the nearby areas use these biomass fuels for local commercial cooking (12,225,226). Burning grass, wood and trash is a widespread practice. In Accra, burning biomass is a significant contributor to $PM_{2.5}$ (37). Majority of the sources' contributions (Figures 4.18a and 4.18b) is due to the regular bushfires that happen during the dry season in August and December.

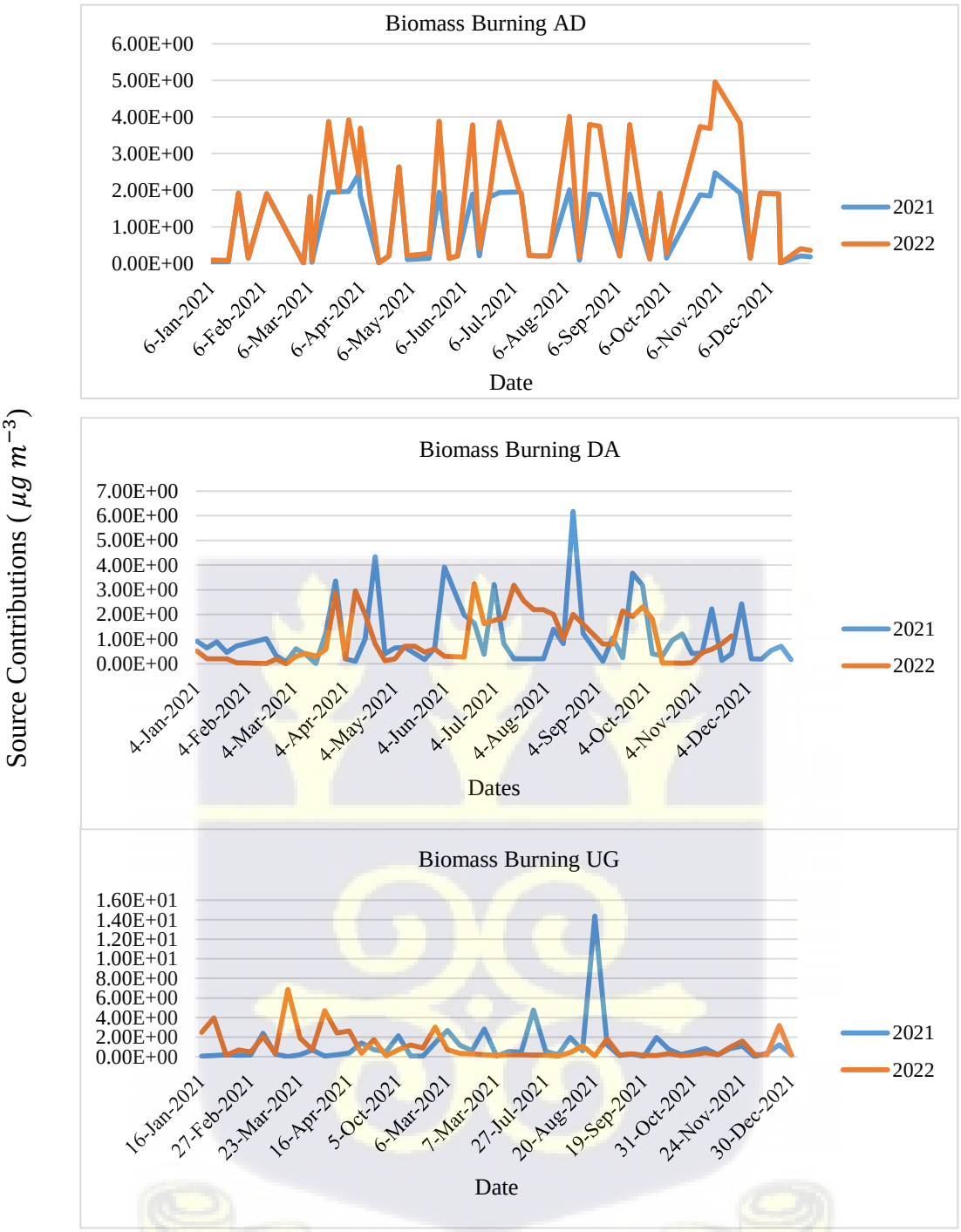

Figure 4.18c Time series of $PM_{2.5}$ source contribution for biomass factors

Source 2: A source exhibiting notable amounts of K, Ti, Fe, Ca, and Zn was detected at AD, DA, and UG, as seen in Figures 4.19a and 4.19b. The source has been identified as re-suspended dust. In 2021, the re-suspended dust source made contributions of 10%, 18%, and 24% to the mass of

$PM_{2.5}$ at AD, DA and UG respectively. Similarly, in 2022, the re-suspended dust source contributed AD (18%), DA (35%), and UG (24%) respectively. The resuspension of road dust often comprises the accumulation of vehicle exhaust emissions, industrial emissions, tyre and brake abrasion, dust originating from paved roads or potholes, and dust generated from building sites.

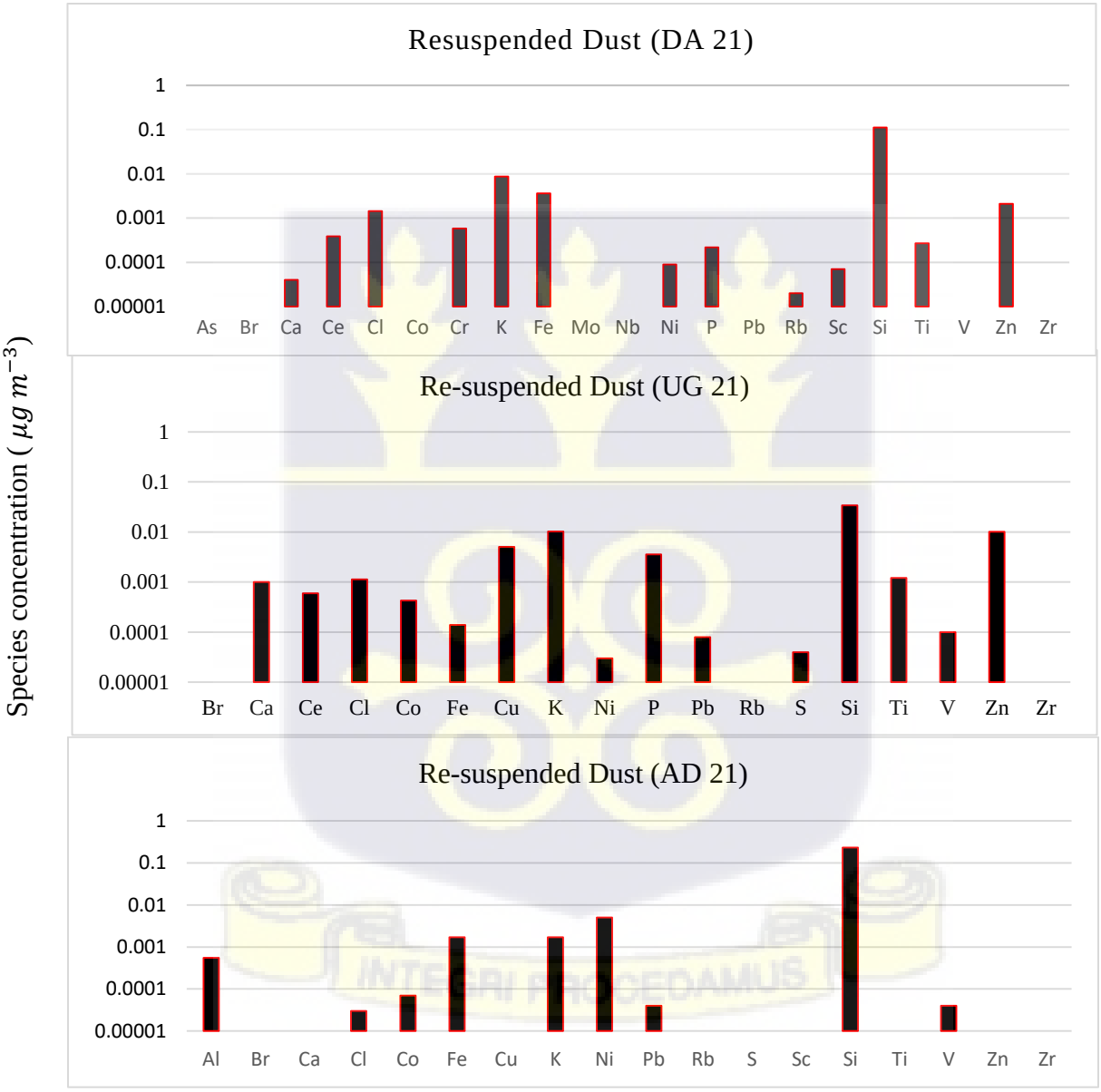

Figure 4.19a $PM_{2.5}$ source profiles for re-suspended dust (2021)

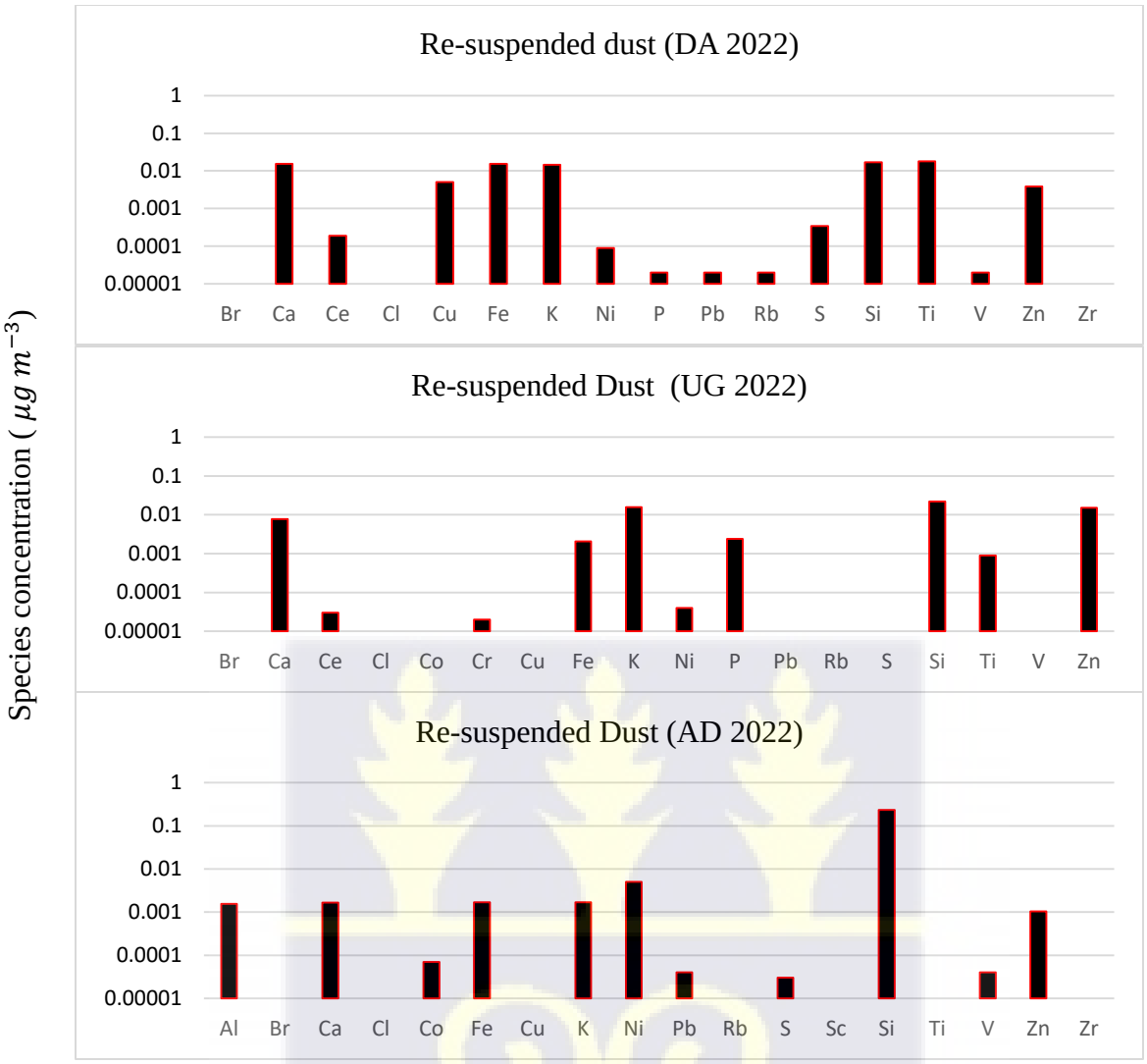

Figure 4.19b $PM_{2.5}$ source profiles for re-suspended dust (2022)

Iron (Fe) emissions occur due to the mechanical degradation of brake pads and other components in vehicles. Zinc (Zn) may possibly come from automotive sources, such as the breakdown of vulcanized rubber tyres, lubricating oil, and the rusting of galvanized vehicle parts (227). The element K has also been used as a tracer for the analysis of paved road dust (228,229). The time series plots (Figure 4.19c) show elevated concentration throughout the months of November, December, January, and February, which correspond to the dry season period.

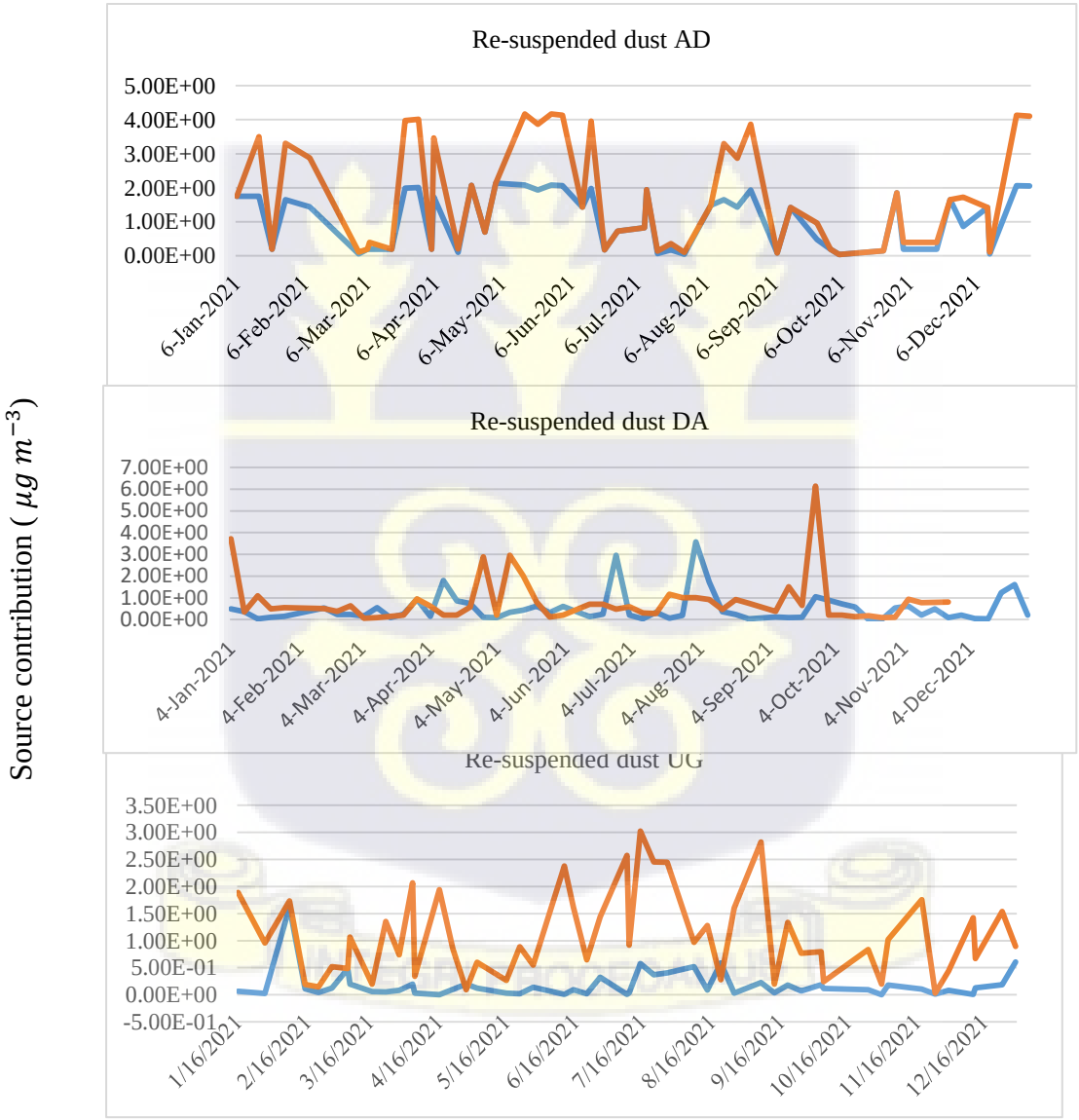

Figure 4.19c Time series of $PM_{2.5}$ source contribution for re-suspended dust (2021)

Source 3: The PMF model identified a source that had significant mass fractions of chlorine (Cl) and Sulphur (S) at all sites, with the greatest contribution seen at site DA. Figures 4.20a and 4.20c, display the source profiles, and Figure 4.20b, with the display of source contributions. The sea salt spray contributions to $PM_{2.5}$ mass were AD (9%), DA (10%), and UG (6%) in 2021, and AD (7%), DA (8%) and UG (6%) in 2022. According to several source apportionment studies, sea salt with a high chloride (Cl) content is the main source profile in coastal areas (230–232). Aerosols containing sea salt can also contain Sulphur. Due to its location along the Atlantic Ocean coast, Accra is vulnerable to the widespread influence of sea salt aerosols (233). The monitoring locations' separations from the ocean's coast are: AD 2.75 km, DA 2.65 km and UG 11.9 km. Source 3 was labelled as “sea salt spray”.

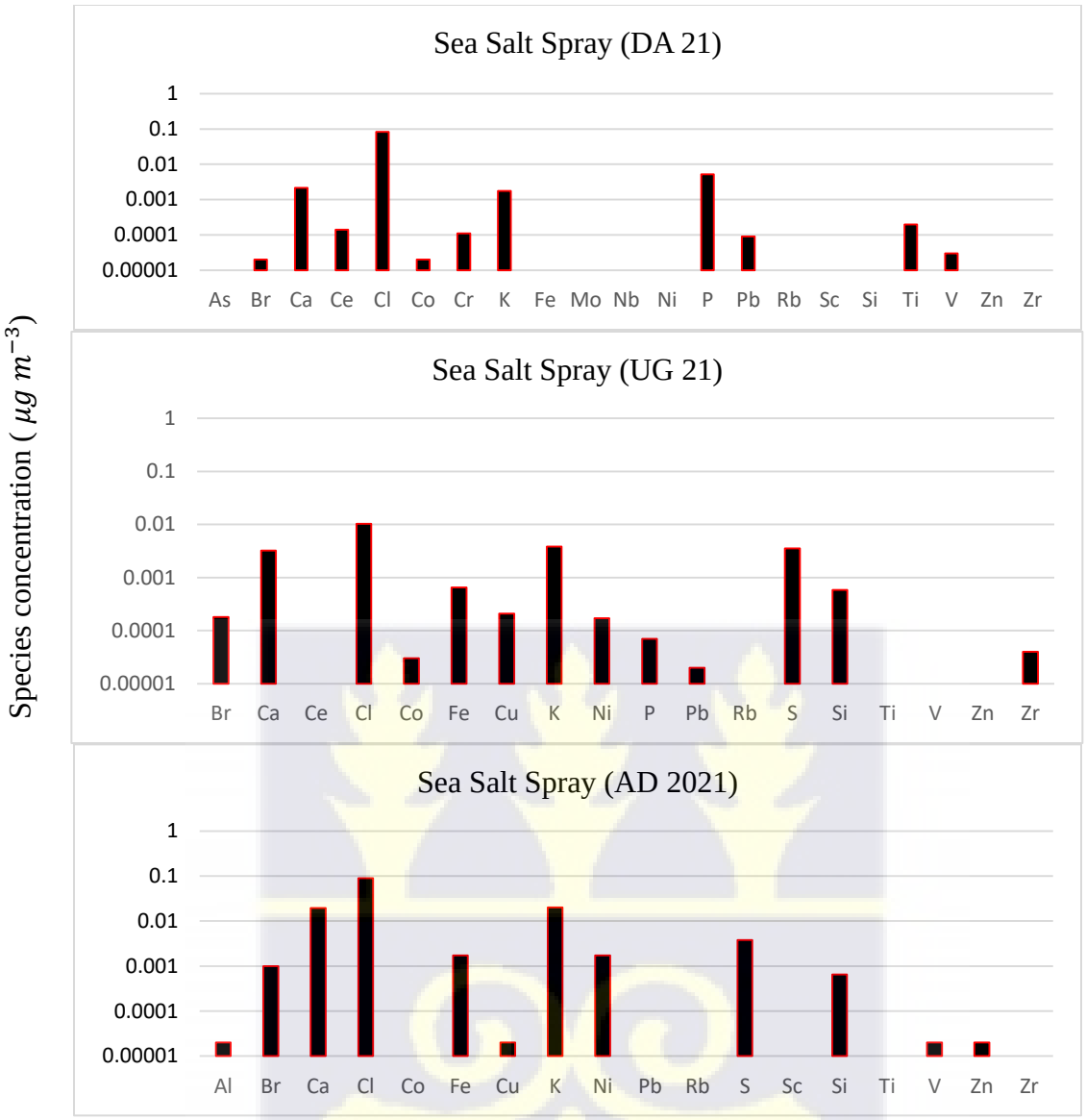

Figure 4.20a $PM_{2.5}$ source profiles for sea salt spray (2021)

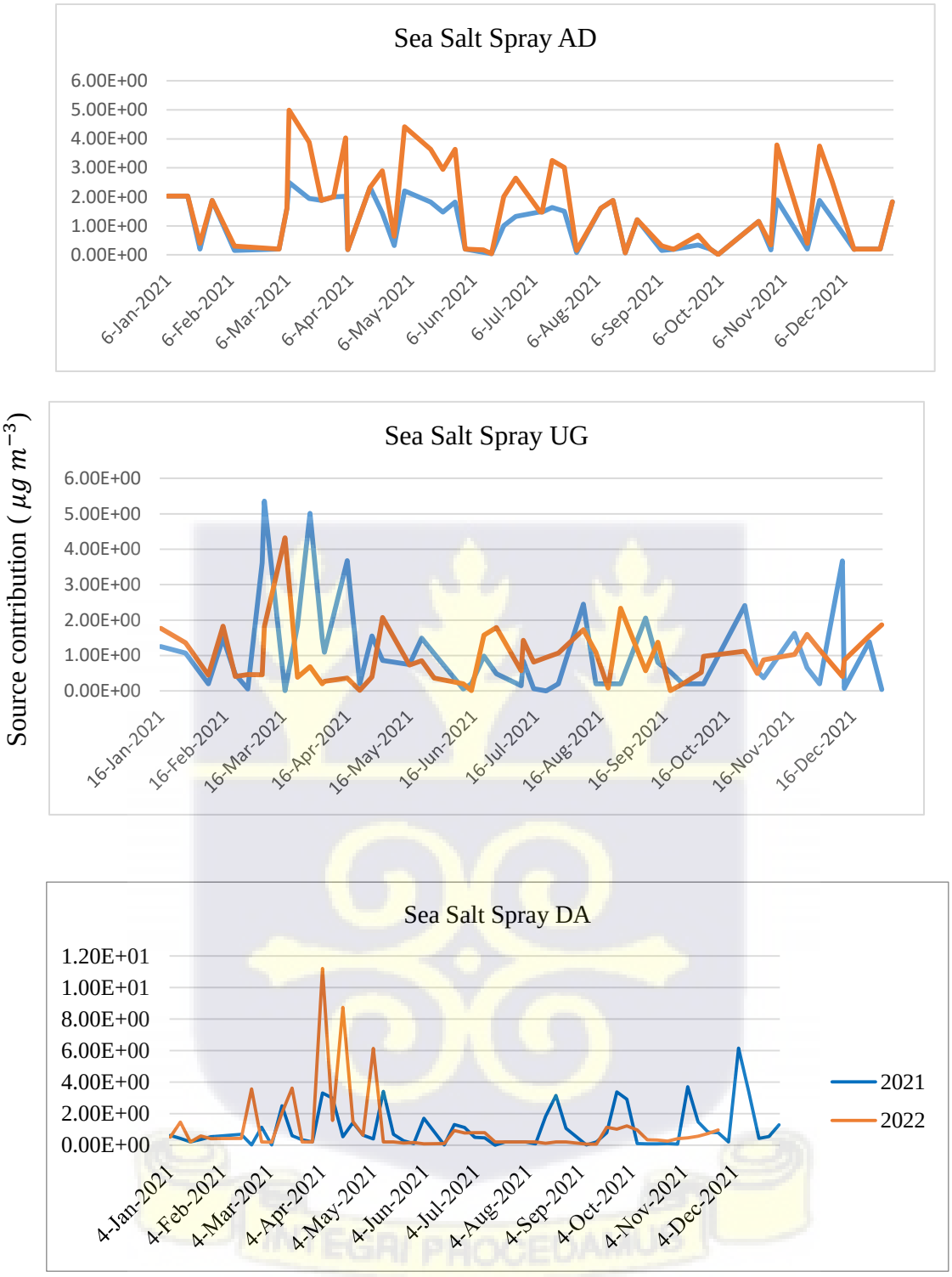

Figure 4.20b Time series of $PM_{2.5}$ source contribution for sea salt spray (2021-2022)

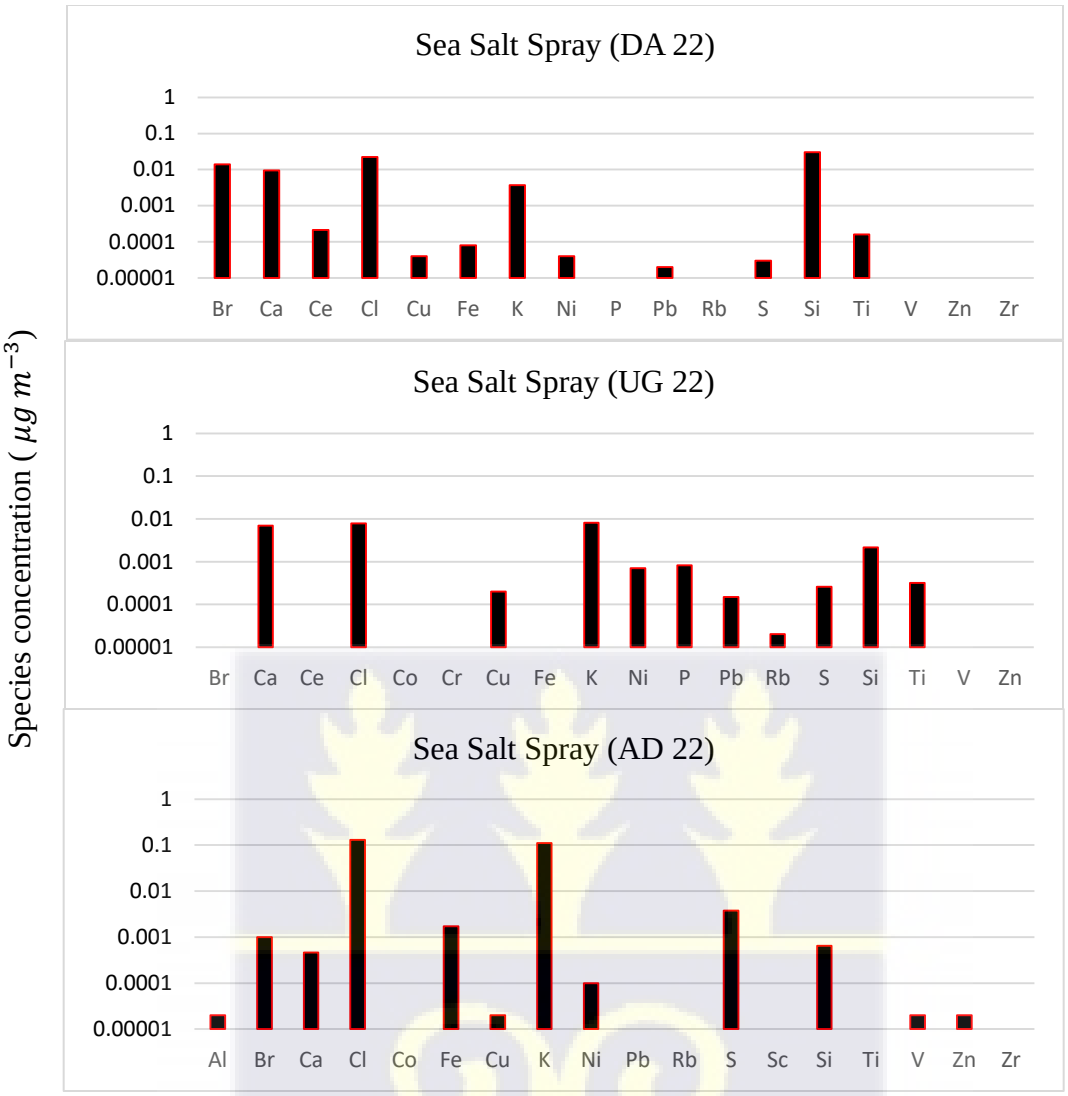

Figure 4.20c $PM_{2.5}$ source profiles for sea salt spray (2022)

Source 4: The profile below, species concentrations (Figures 4.21a and 4.21c) and their contributions (Figure 4.21b) revealed a higher loading for Br, Pb, K, Si, Zn, and Fe. These species are prominent tracers for solid waste incineration. Brominated flame retardants (BFRs) are component in waste electrical and electronic equipment (WEEE) hence Br in this profile could be attributed to burning of plastic and electrical waste (234,235). The presence of K could be attributed to wood base waste burning. The presence of residual Pb in airborne particulate matter may be attributed to many factors, including the re-suspension of dust, the persistence in

combustion of oil and solid waste (236,237). The percentage contribution of solid waste was high in AD (17%), UG (16%) followed by DA (7%). The activities at the E-waste site could impact on the high percentage contribution at AD as compared to the other sites in 2021. However, the percentage contribution at AD declined to 14% in 2022, which could be attributed to the closure of the e-waste site at Agbogbloshie in 2022, besides other pollution sources (3).

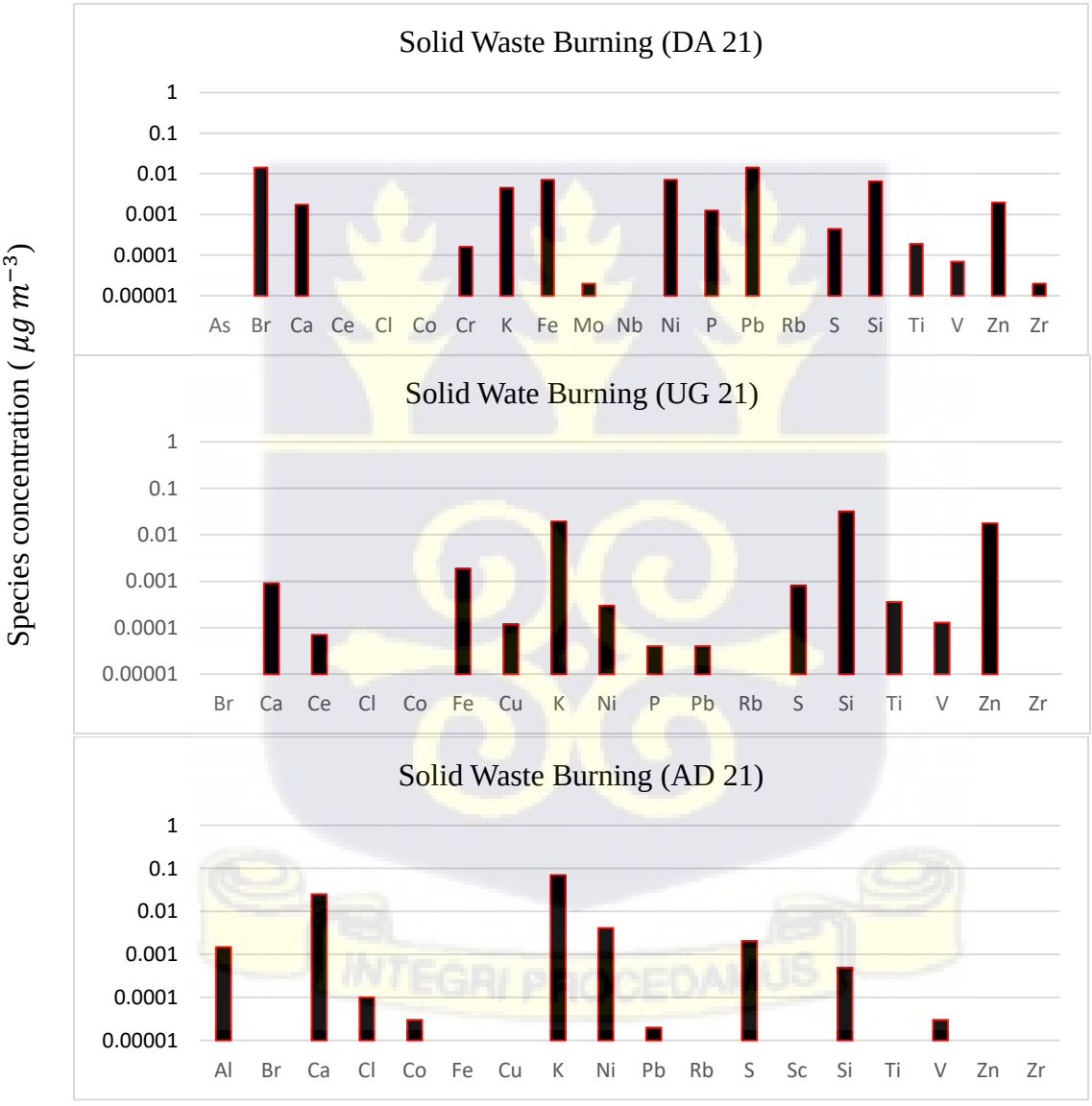

Figure 4.21a $PM_{2.5}$ source profiles for solid waste burning (2021)

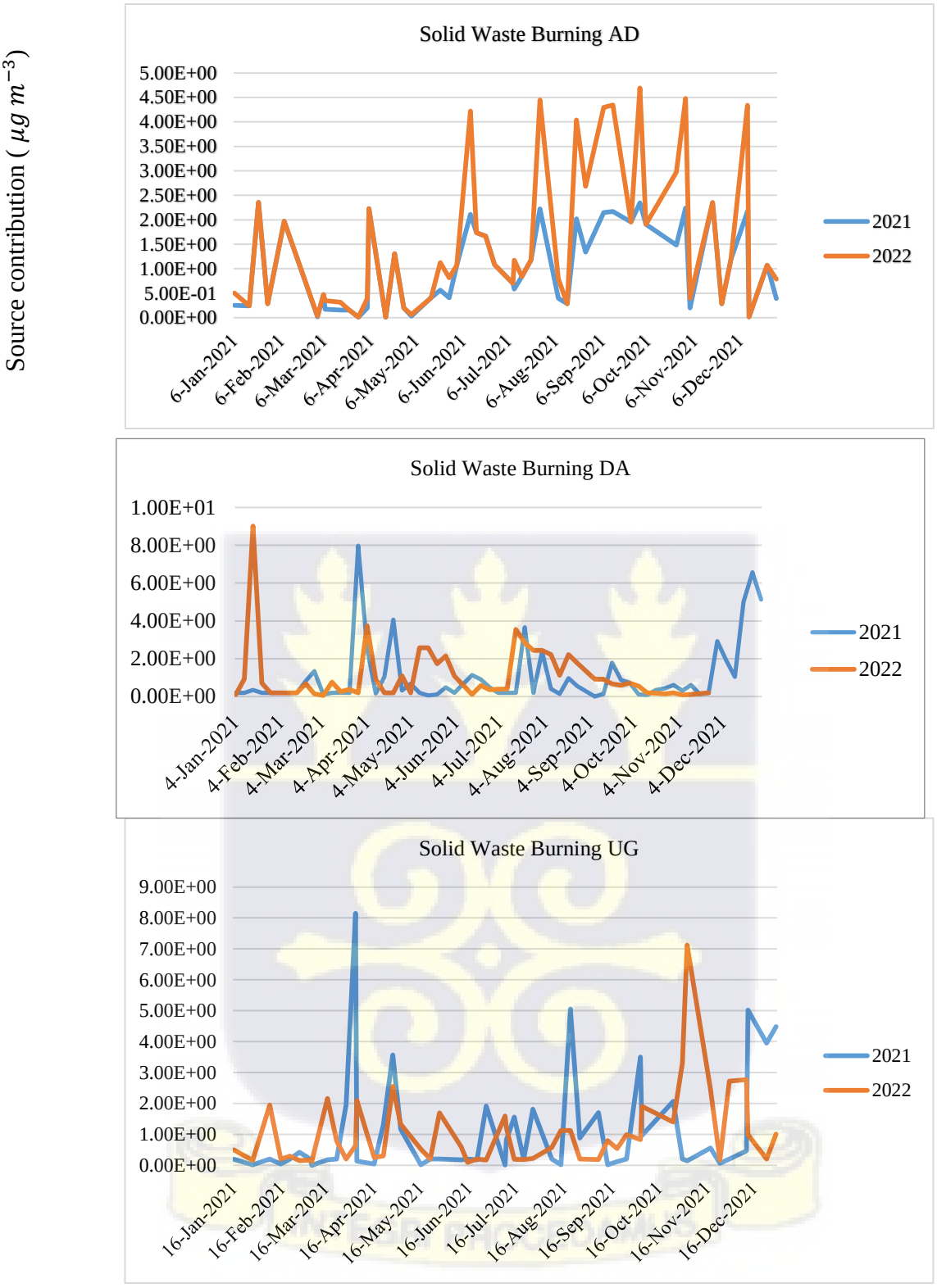

Figure 4.21b Time series of $PM_{2.5}$ source contribution for sea salt spray (2021-2022)

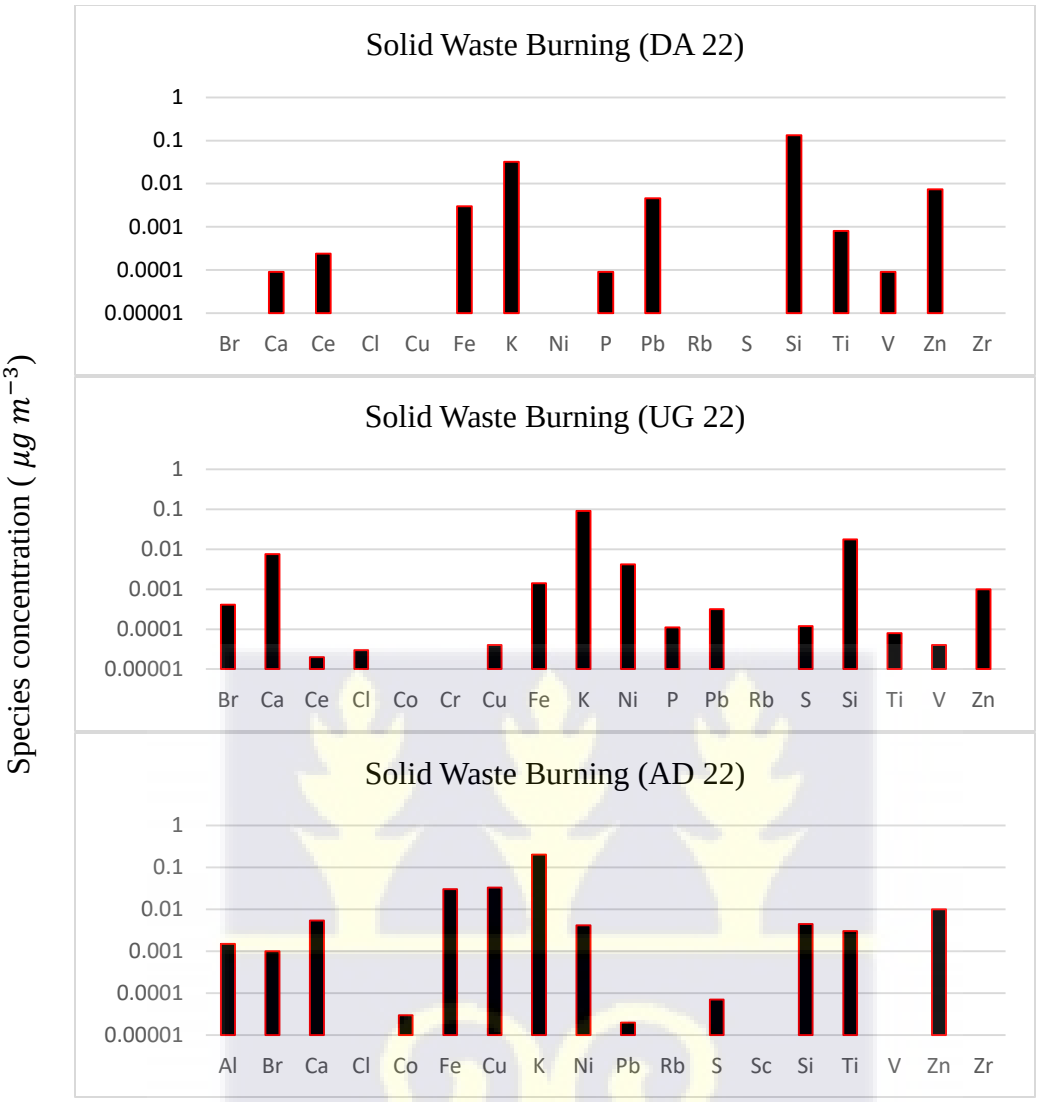

Figure 4.21c $PM_{2.5}$ source profiles for solid waste burning (2022)

Source 5: The primary constituents in the concentrations profiles below (Figures 4.22a and 4.22c) are silicon (Si), sulphur (S), aluminium (Al), iron (Fe), calcium (Ca), and potassium (K). Likewise, these elements are abundant in the Earth's crustal composition (28). Hence, the origin of this source may be attributed to soil dust. This phenomenon often arises from airborne particulate matter, including dust particles carried by wind and dust particles generated by vehicular traffic (238–240). The Figure shown (Figure 4.22b) displays the contribution plot, which indicates the highest concentration levels observed throughout the harmattan season, spanning from November to

February. The occurrence of calcium (Ca) in the profile may be ascribed to construction activities such as building or road construction, specifically in relation to the presence of calcium in concrete materials. The percentage contribution of soil dust in $PM_{2.5}$ mass ranged from 13 to 16% in 2021 and 11 to 14% in 2022.

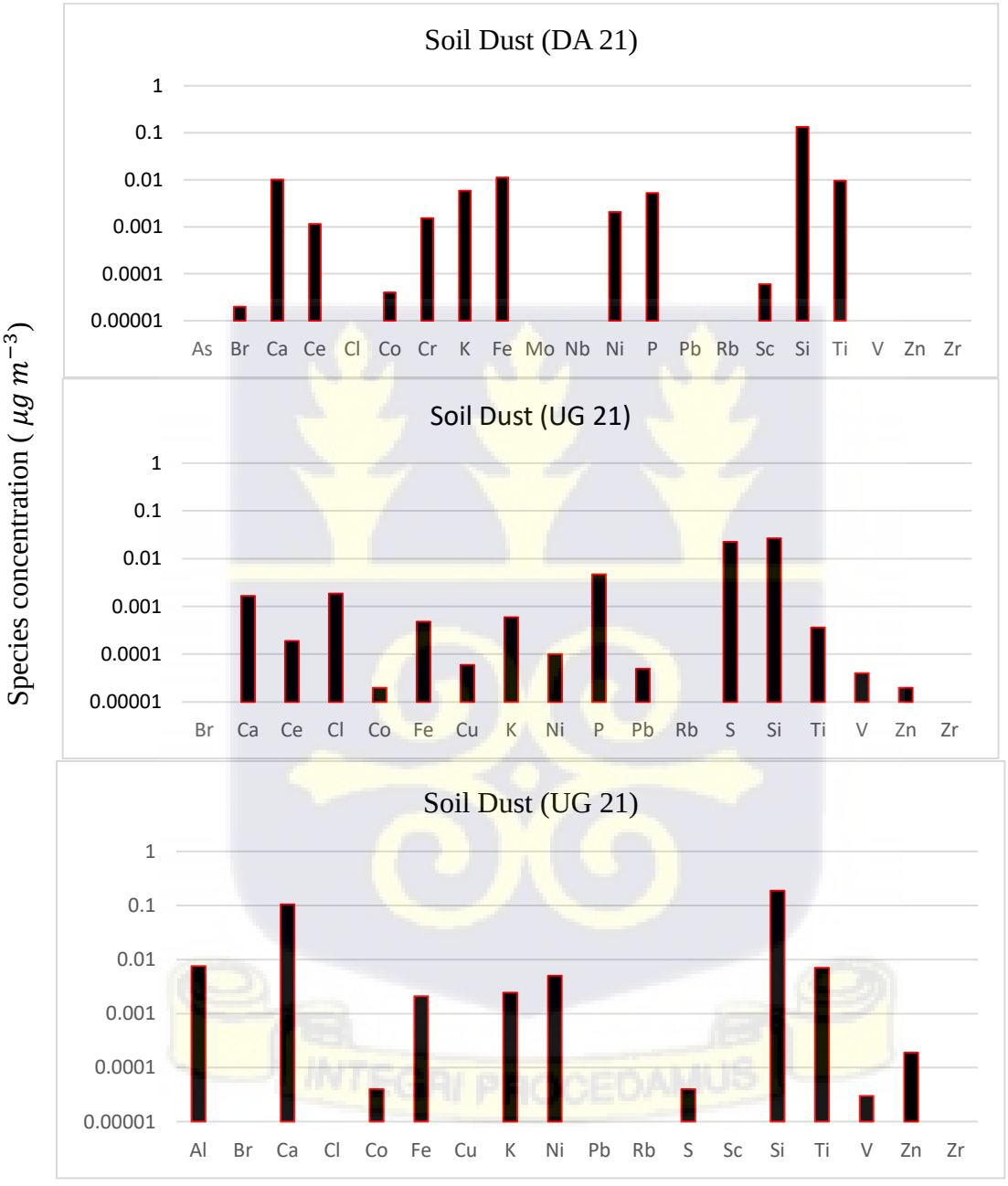

Figure 4.22a $PM_{2.5}$ source profiles for soil dust (2021)

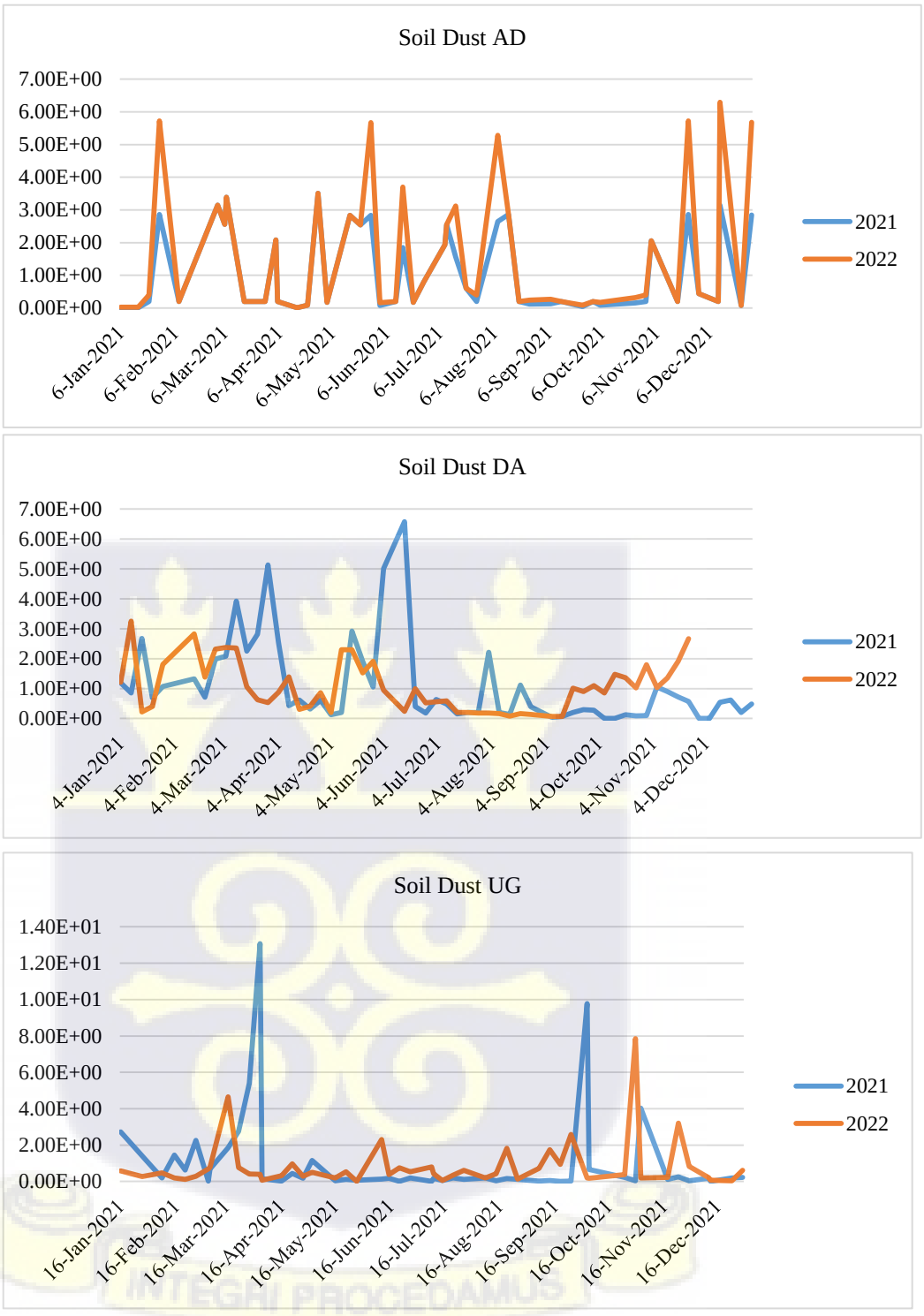

Figure 4.22b Time series of $PM_{2.5}$ source contribution for soil dust (2021-2022)

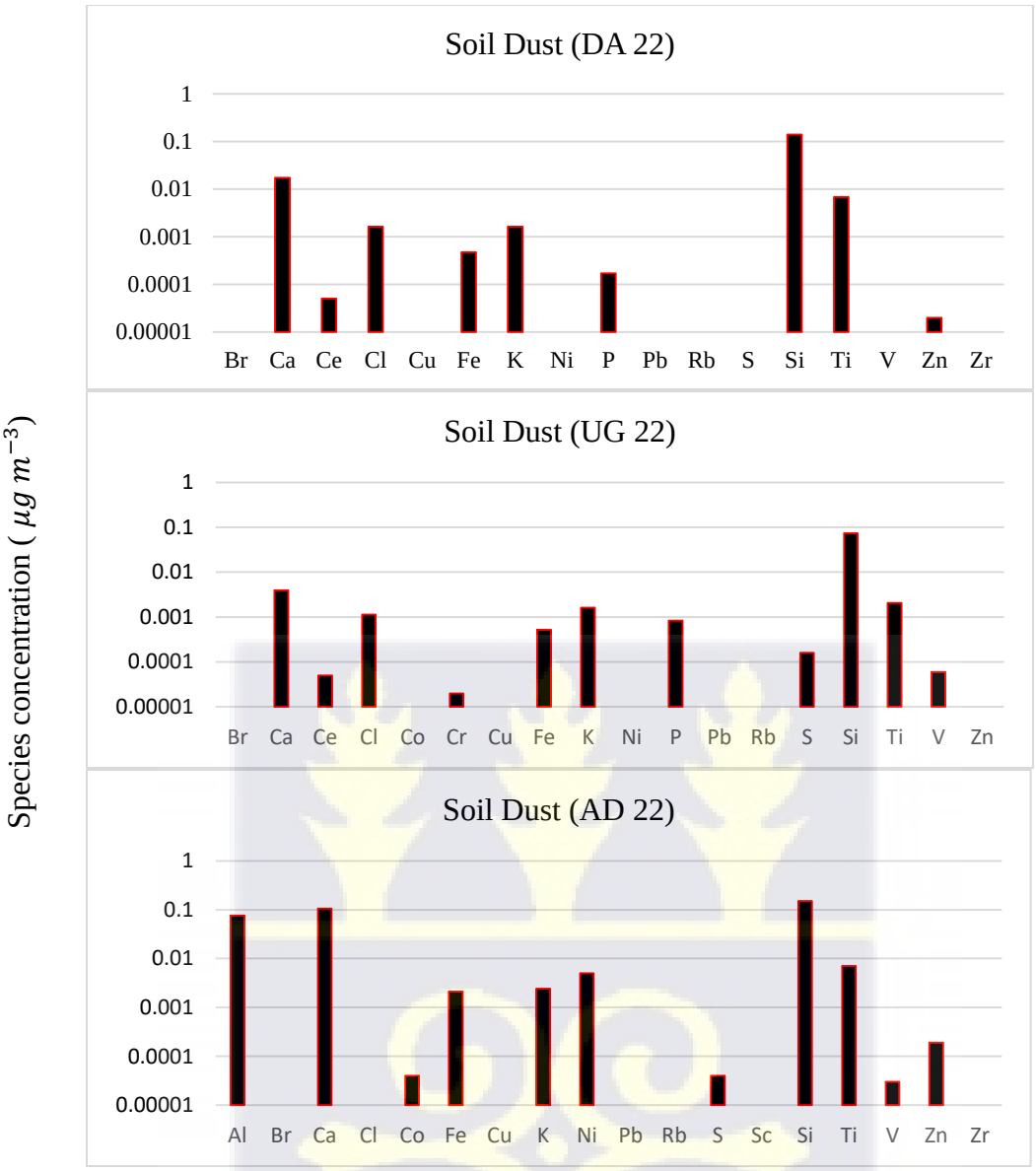

Figure 4.22c $PM_{2.5}$ source profiles for soil dust (2022)

Source 6: The findings from source three indicated a comparatively elevated level of Sulphur (S) in conjunction with zinc (Zn), copper (Cu), iron (Fe), and lead (Pb). The marker elements present in zinc (Zn) and copper (Cu) are associated with the abrasion of brakes and tyre bearings, respectively. In a study conducted by Fayad et al. (2022) (241), combination and combustion of gasoline and lubricant inside the piston chambers of engines results in the emission of Zn. The

primary constituents found in automobile exhaust emissions are zinc (Zn), lead (Pb), iron (Fe), nickel (Ni), organic carbon (OC), and copper (Cu) (99,242).

Furthermore, it has been shown that these constituents have a significant presence in the context of industrial emissions, as highlighted by Sharma et al (243). The presence of lead (Pb) in the environment may be attributed to industrial emissions, since lead has been used in incinerators (244). The detection of the element S within the tracer elements used for automotive emissions serves as an indicator of the utilization of fuel that is abundant in Sulphur. Consequently, these elements can be used as marker element for vehicular and industrial emission. The Figures below (Figures 4.23a and 4.23c) visualize the marker elements prominent in vehicular and industrial emission. Notably, levels of S in 2021 (Figure 4.23a) were lower than in 2022 (Figure 4.23c). These spikes in Sulphur levels in 2022 could be attributed to the waiver on Sulphur levels limit in fuel in 2022, with the limit raised from 50 ppm to 1500 ppm (NPA, 2022). Vehicular/industrial emission was highest in DA and UG (29%), followed by AD (25%) in 2021. In 2022, vehicular/industrial emissions increased in DA (35%) and AD (28%) where contribution in UG reduced (26%) and this is consistent with work conducted by Fayad et al., (2022). This could be largely attributed to the waiver in Sulphur levels in fuel (241).

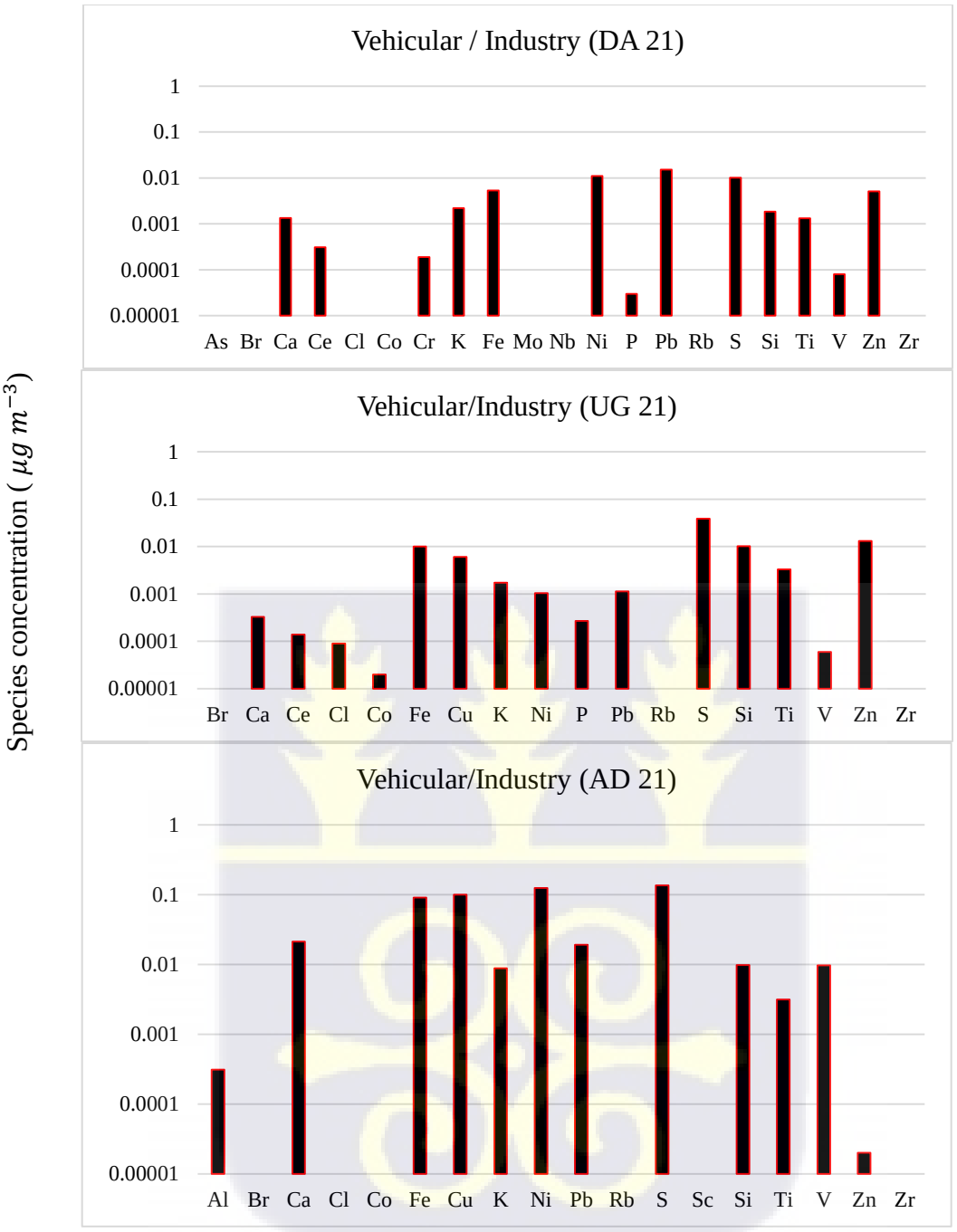

Figure 4.23a $PM_{2.5}$ source profiles for vehicular/ industry (2021)

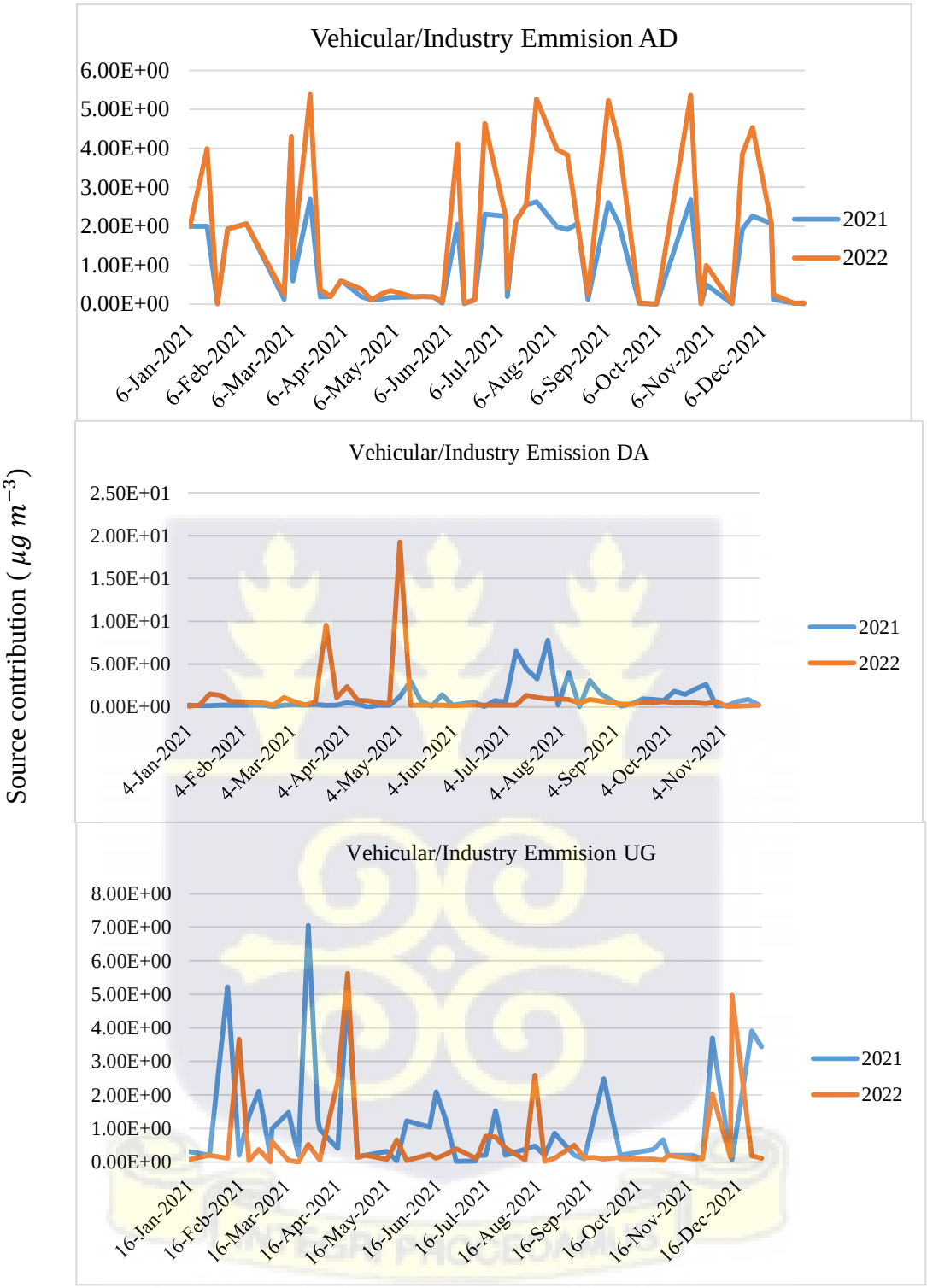

Figure 4.23b Time series of $PM_{2.5}$ source contribution for vehicular/ industry (2021-2022)

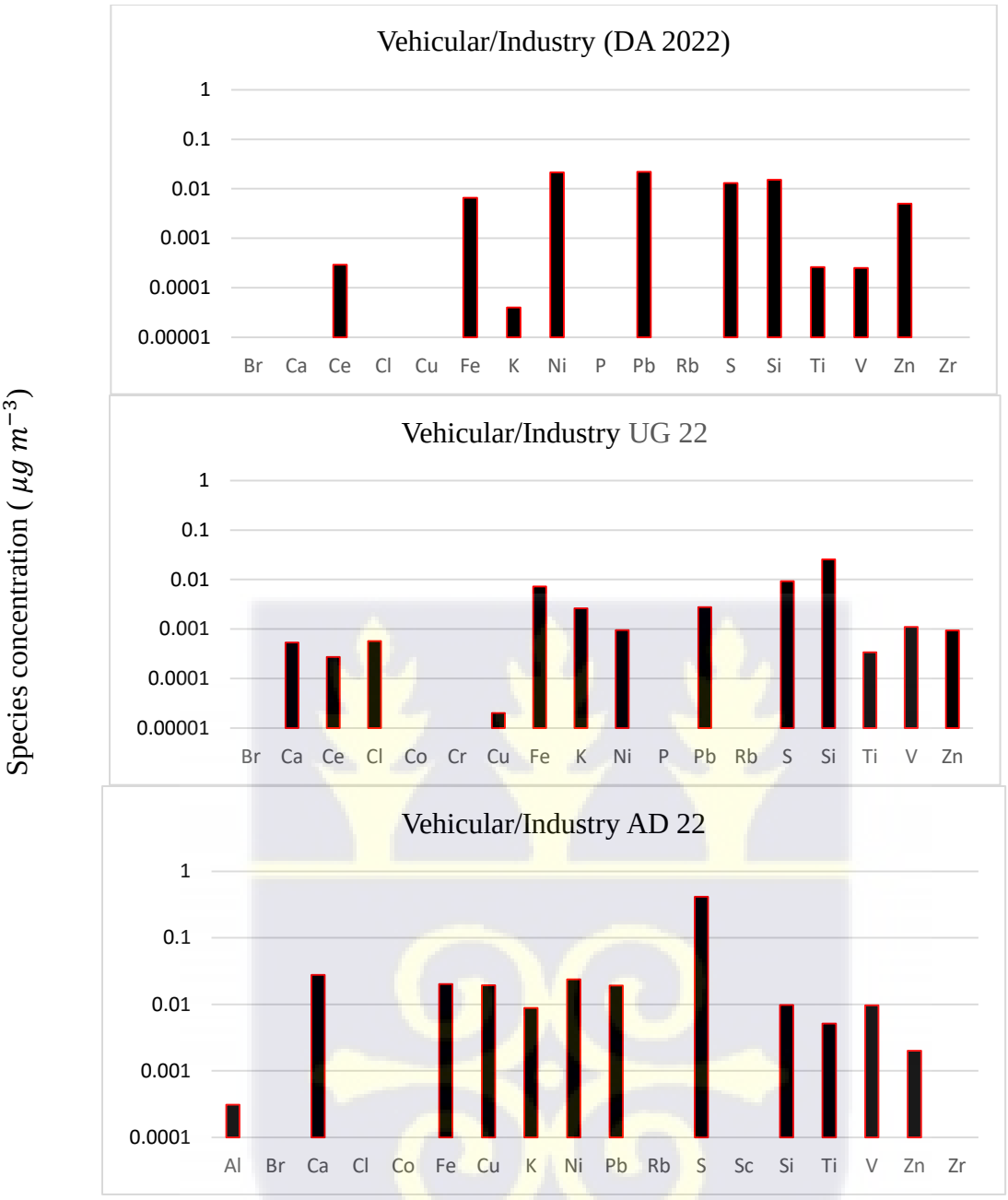

Figure 4.23c $PM_{2.5}$ source profiles for vehicular/ industry (2022)

4.7 PERCENTAGE SOURCE CONTRIBUTION OF $PM_{2.5}$ MASS

Pie charts have been used to reveal the percent source contribution of particulate matter at Adabraka (AD), Dansoman (DA) and University of Ghana (UG) sites in 2021 and 2022. Biomass burning and soil dust resulted as the predominant contributing factors of particulate matter at the three sites in 2021 (27% and 28% respectively).

The results from PMF revealed six different sources contributing to $PM_{2.5}$ at all three sites. The plots below indicated the percentage of source contribution of particulate matter for the three monitoring sites. In AD, the largest contributing factor of particulate matter was vehicular/industrial emission in both years of study (25% in 2021 and 28% in 2022).

The second-largest source of particulate matter is biomass burning (20% for both years). This could emanate from various commercial and domestic cooking activities (usage of firewood and charcoal) in the environs of the monitoring location. Vehicular emissions and biomass burning contributed about 50% of the particulate matter recorded at AD in both years. This is an indication of how anthropogenic activity impacts pollution in AD. Solid waste burning, re-suspended dust particles, soil dust, and sea salt contribute the remaining 50% of particulate matter. Solid waste burning was higher in AD than at the other sites. This could result from particles transported from the e-waste site at Agbogbloshie.

Similarly, at DA, the highest source contributor of $PM_{2.5}$ is vehicular/industrial emissions (29% in 2021 and 35% in 2022), followed by biomass burning (20% in 2021 and 21% in 2022). Both sites are characterized by heavy traffic congestion as well as commercial cooking activities. It could be inferred that similarly, anthropogenic activities heavily impact $PM_{2.5}$ since the loading from solid waste and biomass burning contributes to half of the particulate matter. Sea salt in DA was

relatively higher as compared to AD and UG. This could be attributed to the proximity of the site with respect to the sea. The sea is approximately 2.6 km from DA, 2.7 km from AD, and 11.7 km from UG. At UG, vehicular/industrial emissions were the highest contributing factor to $PM_{2.5}$, followed by re-suspended dust particles. Sea salt was obviously the least contributing factor to $PM_{2.5}$ at UG. Re-suspended dust and solid waste burning at UG sites could emanate from sources within the environs of the University of Ghana, Legon campus.

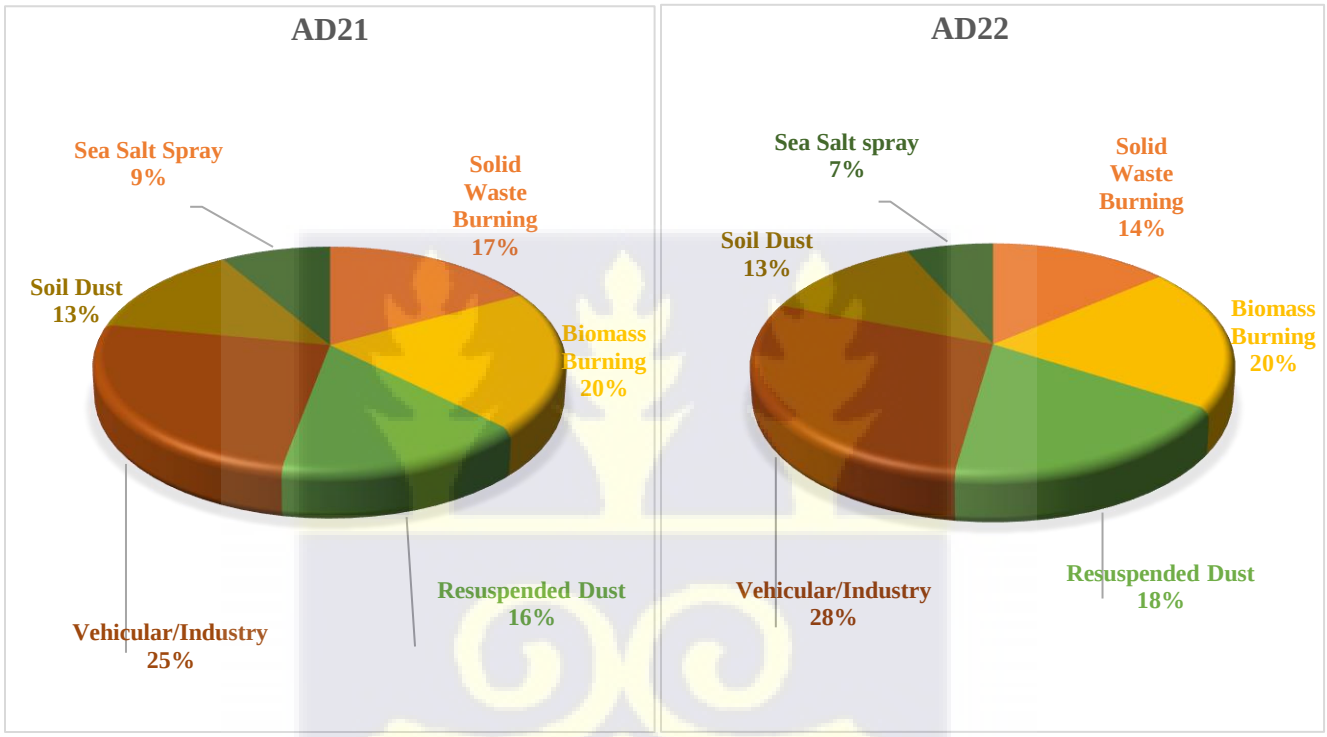

Figure 4.24 $PM_{2.5}$ source contribution for AD (2021-2022)

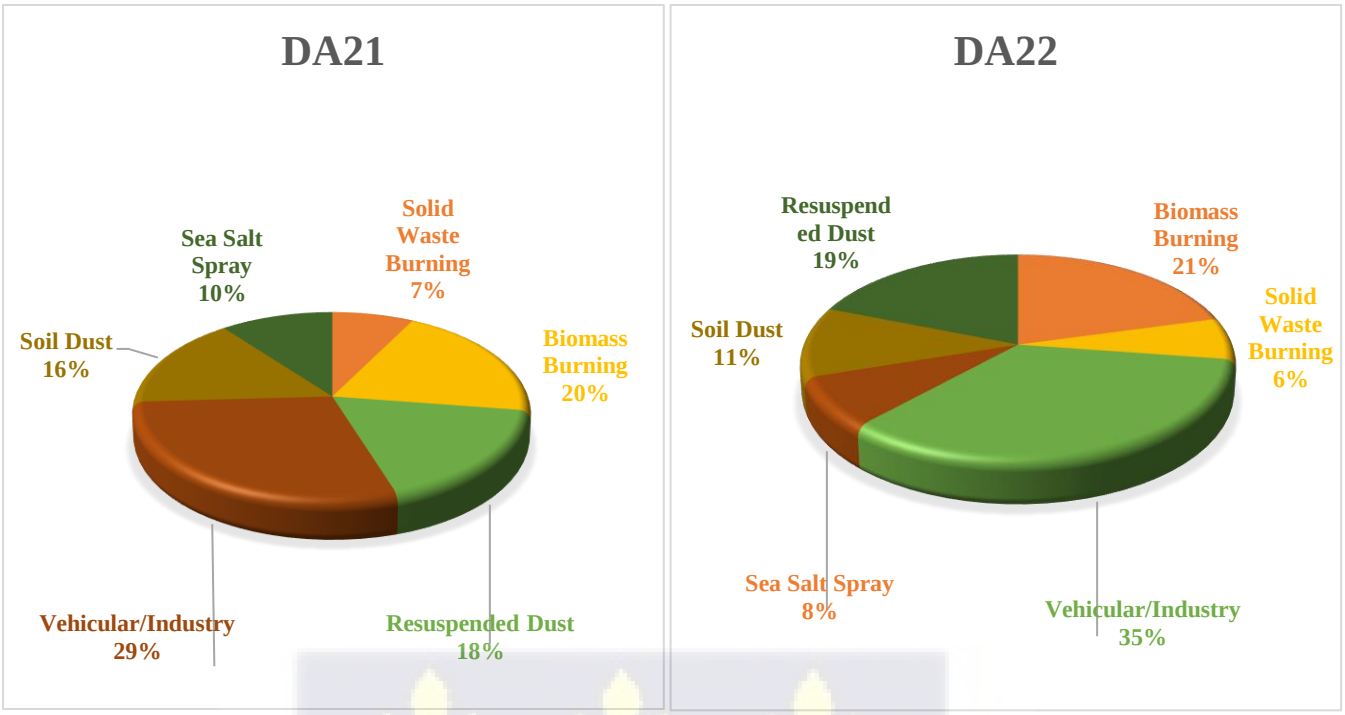

Figure 4.25 $PM_{2.5}$ source contribution for DA (2021-2022)

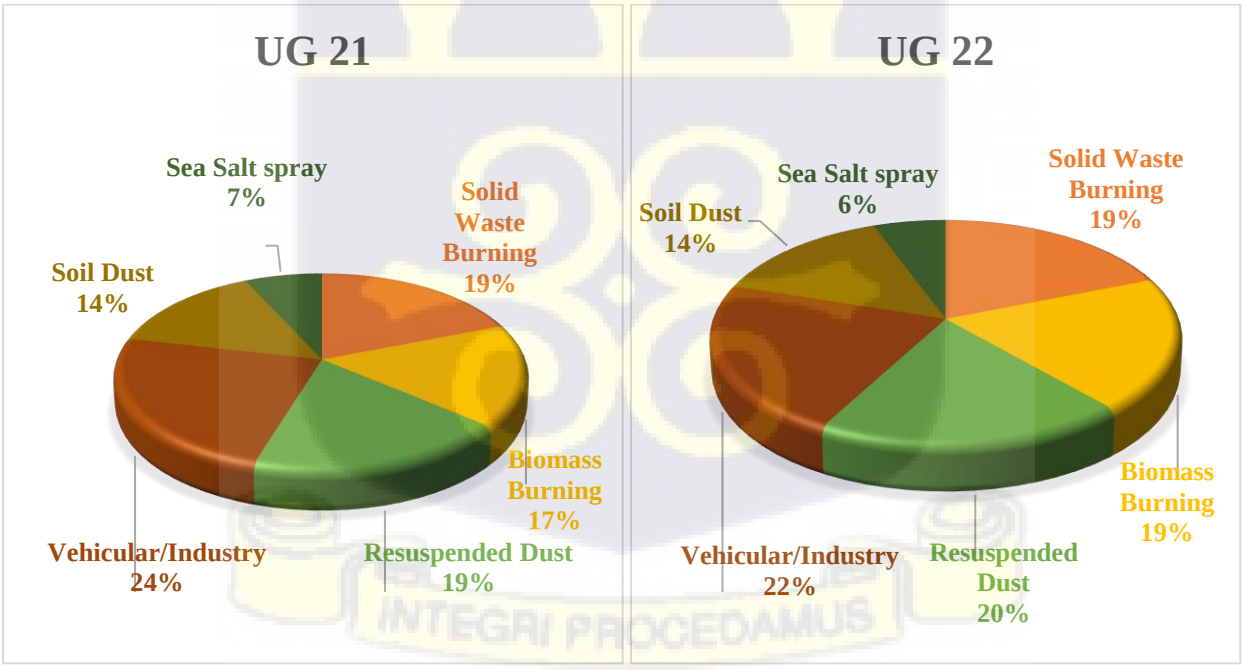

Figure 4.26 $PM_{2.5}$ source contribution for UG (2021-2022)

CHAPTER 5
CONCLUSIONS AND RECOMMENDATIONS

5.1 CONCLUSIONS

In this thesis, the concentrations, elemental composition, and origins of airborne particulate matter ($PM_{2.5}$) across different sampling locations within three distinct districts of Accra, Ghana, were studied. The investigation stands as one of the pioneering efforts to explore the nexus between meteorological conditions and $PM_{2.5}$ mass from gravimetric analysis and reference monitors over a two-year span in Accra, Ghana, considering seasonal fluctuations.

Through meticulous measurements conducted every six days within the 2 years using advanced air sampling techniques, significant average mass concentration values for $PM_{2.5}$ across all locations throughout the research period were observed. Notably, these concentrations exceeded air quality standards set by Ghana, the World Health Organization (WHO), the United States Environmental Protection Agency (USEPA), and the European Union (EU). The findings closely align with prior research conducted across sub-Saharan Africa, underscoring the severity of $PM_{2.5}$ pollution in urban centers across the region.

Furthermore, the utilization of the Energy Dispersive X-ray Fluorescence (EDXRF) technique revealed a diverse array of trace elements present in the examined particulate matter samples. These variations in elemental composition suggest distinct local and regional influences on air quality at the receptor locations.

Employing the U.S. EPA's Positive Matrix Factorization (PMF) 5.0 model enabled the identification of six primary sources of $PM_{2.5}$ pollution, including biomass combustion, solid waste burning, sea salt aerosols, automobile emissions, soil dust, and re-suspended dust. Notably, anthropogenic sources emerged as the predominant contributors to air pollution across all study

locations, particularly along traffic routes, emphasizing the urgent need for targeted interventions to mitigate vehicular and industrial emissions, as well as biomass burning and waste disposal practices.

In summary, this study sheds light on the intricate dynamics of airborne particulate matter in Accra, Ghana, providing valuable insights for policymakers, urban planners, and environmentalists to devise effective strategies aimed at improving air quality and safeguarding public health in rapidly growing urban environments. Continued research and concerted efforts are needed to address the multifaceted challenges posed by air pollution and foster sustainable development in Accra and beyond.

5.2 RECOMMENDATIONS

The study's findings highlight several key recommendations for addressing air pollution in Accra, Ghana, and similar urban settings. Firstly, establishing monitoring sites across diverse regions is crucial for continuous assessment of particulate matter levels, enabling authorities to identify pollution hotspots and implement targeted interventions. Additionally, integrating low-cost air sensors alongside traditional monitoring methods can enhance data collection efforts, providing a more comprehensive understanding of air quality dynamics. Regular $PM_{2.5}$ estimation studies across different cities and seasons in Ghana are essential for tracking pollution trends and informing policy decisions aimed at mitigating health risks associated with poor air quality.

Furthermore, expanding research to analyze additional air pollutants beyond $PM_{2.5}$, such as black carbon and Sulphates, is imperative for a more holistic understanding of air pollution's health impacts. Investigating the intricate relationship between climatic conditions and particulate matter can provide valuable insights into the factors driving air pollution levels, facilitating the development of targeted mitigation strategies. Additionally, implementing source-oriented control

measures and policies to curb anthropogenic activities contributing to poor air quality is essential, along with regulations aimed at reducing emissions from old automobiles and engines.

Finally, promoting environmentally friendly transportation options, subsidizing cleaner cooking technologies, and encouraging the use of renewable energy sources are critical steps towards reducing dependency on fossil fuels and mitigating air pollution. This should be done in addition to educating communities about the health risks associated with air pollution, and promoting efficient waste management practices to prevent open burning measures aimed at improving air quality and safeguarding public health. By implementing these recommendations, policymakers can work toward achieving sustainable development goals while protecting the well-being of urban populations.

References

1. Manisalidis I, Stavropoulou E, Stavropoulos A, Bezirtzoglou E. Environmental and Health Impacts of Air Pollution: A Review. Front Public Heal. 2020;8(February):1–13.
2. Timilsina GR, Dulal HB. Regulatory instruments to control environmental externalities from the transport sector. 2009;41(March):80–112.
3. Ahiamadjie H. Characterization of Atmospheric Particulate Matter at E-waste Landfill Site. Semant Sch. 2017;1–186.
4. Aboh IJK. Characterization and sources of air particulate matter at Kwabenya, near Accra, Ghana (PhD Thesis). 2009;(May):211.
5. Zheng F, Laucks ML, Davis EJ. AERODYNAMIC PARTICLE SIZE MEASUREMENT BY ELECTRODYNAMIC OSCILLATION TECHNIQUES. 2000;31(10):1173–85.
6. Hester RE, Harrison RM, Clark C, Sbihi H, Tamburic L, Brauer M, et al. Vol. 80, The Lancet. 2017. p. 1819–20 Environmental Impacts of Road Vehicles: Past, Present and Future.
7. World Health Organization. WHO Global Air Quality Guidelines. Particulate matter (PM2.5 and PM10), ozone, nitrogen dioxide, sulfur dioxide and carbon monoxide. 2021. 1–300 p.
8. Shaddick G, Thomas ML, Mudu P, Ruggeri G, Gumy S. Half the world's population are exposed to increasing air pollution. npj Clim Atmos Sci. 2020;3(1):1–5.
9. World Bank. World Bank. 2021. World {Bank} {Group} - {International} {Development}, {Poverty}, & {Sustainability}.
10. WEF. Www.Weforum.Org. 2018. p. 2020 African cities will double in populatio by 2050. 4 ways to mnake sure they thrive.
11. Lahariya C. The State of the World Population 2007: Unleashing the potential of urban growth. Indian Pediatr. 2008;45(6):481–2.
12. Dionisio KL, Rooney MS, Arku RE, Friedman AB, Hughes AF, Vallarino J, et al. Within-neighborhood patterns and sources of particle pollution: Mobile monitoring and

geographic information system analysis in four communities in Accra, Ghana. Environ Health Perspect. 2010;118(5):607–13.

13. WHO. World Health Organisation Geneva. 2018. p. 6–8 Ambient (outdoor) air pollution.

14. Revesz RL. Air Pollution and Environmental Justice. Ecol Law Q. 2022;49(1):187–252.

15. UNEP. Unep. 2019. p. 9 pant. Air Pollution Note .

16. Rahman MM, Begum BA, Hopke PK, Nahar K, Newman J, Thurston GD. Cardiovascular morbidity and mortality associations with biomass-and fossil-fuel-combustion fine-particulate-matter exposures in Dhaka, Bangladesh. Int J Epidemiol. 2021;50(4):1172–83.

17. Avik Sinha. Carbon Emissions and Mortality Rates: A Causal Analysis for India (1971-2010). Munich Pers RePEc Arch. 2014;1–7.

18. Bailis R, Ezzati M, Kammen DM. Mortality and greenhouse gas impacts of biomass and petroleum energy futures in Africa. Science (80-). 2005;308(5718):98–103.

19. Bauer SE, Im U, Mezuman K, Gao CY. Desert Dust, Industrialization, and Agricultural Fires: Health Impacts of Outdoor Air Pollution in Africa. J Geophys Res Atmos. 2019;124(7):4104–20.

20. Max Roser. Global death toll from air pollution . 2021. Data Review: How many people die from air pollution? - Our World in Data.

21. Krzyżanowski M, Kuna-Dibbert B, Schneider J. Health Effects of Transport-Related Air Pollution. 2005. p. 190.

22. HEI. Traffic-Related Air Pollution:A Critical Review of the Literature on Emissions, Exposure, and Health Effects. 2010.

23. Arku RE, Vallarino J, Dionisio KL, Willis R, Choi H, Wilson JG, et al. Characterizing air pollution in two low-income neighborhoods in Accra, Ghana. Sci Total Environ. 2008;402(2–3):217–31.

24. Kermani M, Dowlati M, Jafari AJ, Kalantari RR. Health risks attributed to particulate matter of 2 . 5 microns or less in Tehran air 2005-2014. 2016;20(99):99–105.

25. Asia AEI, Wang G, Wang H, Yu Y, Gao S, Feng J, et al. Chemical characterization of water-soluble components of PM 10 and PM 2 . 5 atmospheric aerosols in five locations of. 2003;37:2893–902.

26. Agyei-Mensah S, Bawah AA, Gyeabour EK. Challenges of monitoring and developing environmental policy in Sub-Saharan Africa: the case of air pollution and biofuels in Ghana. Toxic News 2018. 2018;(September).

27. Amegah AK, Dakuu G, Mudu P, Jaakkola JJK. Particulate matter pollution at traffic hotspots of Accra, Ghana: levels, exposure experiences of street traders, and associated respiratory and cardiovascular symptoms. J Expo Sci Environ Epidemiol. 2022;32(2):333–42.

28. Hughes AF. Characterization and Source Apportionment of Airborne Particulate Matter in Some Urban Neighbourhoods of Accra, Ghana. 2014;(July).

29. Obioh IB, Ezeh GC, Abiye OE, Alpha A, Ojo EO, Ganiyu AK. Atmospheric particulate matter in Nigerian megacities. Toxicol Environ Chem. 2013;95(3):379–85.

30. Kinney PL, Gatari M, Volavka-close N, Ngo N, Ndiba PK, Law A, et al. Traffic impacts on PM 2 . 5 air quality in Nairobi , Kenya. Environ Sci Policy. 2011;14(4):369–78.

31. Abera A, Mattisson K, Eriksson A, Ahlberg E, Sahilu G, Mengistie B, et al. Air pollution measurements and land-use regression in urban sub-saharan Africa using low-cost sensors—possibilities and pitfalls. Atmosphere (Basel). 2020;11(12):1–21.

32. Benjamin D. Horne et al. Short-Term Elevation of Fine Particulate Matter Air Pollution and Acute Lower Respiratory Infection. 2014;(979):1–39.

33. Pope CA, Coleman N, Pond ZA, Burnett RT. Fine particulate air pollution and human mortality: 25+ years of cohort studies. Environ Res. 2020;183:108924.

34. de Jesus AL, Rahman MM, Mazaheri M, Thompson H, Knibbs LD, Jeong C, et al. Ultrafine particles and PM2.5 in the air of cities around the world: Are they representative of each other? Environ Int. 2019;129(May):118–35.

35. Friend AJ, Ayoko GA, Jayaratne ER, Jamriska M, Hopke PK, Morawska L. Source

apportionment of ultrafine and fine particle concentrations in Brisbane, Australia. Environ Sci Pollut Res. 2012;19(7):2942–50.

36. Zhou Z, Dionisio K, States U, Protection E, Arku RE. Chemical composition and sources of particle pollution in affluent and poor neighborhoods of Accra , Ghana. 2013;(January 2015).

37. Ofosu F, Aboh I, Bamford S. Ambient Air PM10 Particulate Levels at Ashaiman Near Tema in Ghana. Br J Appl Sci Technol. 2016 Jan;12(4):1–14.

38. USEPA. Revised Air Quality Standards for Particle Pollution and Updates To the Air Quality Index (AQI). United States Environ Prot Agency, Washingt DC, USA. 2012;1–5.

39. Spengler JD, Wilson R. Particles in Our Air Exposures and Health Effects. Spengler JD, Wilson R, editors. 1996;265.

40. Stern W. (PDF) Elemental Analysis of PM2.5 Samples Collected in the Framework of the Ecrhs II Study | Willem Stern - Academia.edu.

41. Krüger O. Observational evidence for human impact on aerosol cloud-mediated processes in the Baltic region. Oceanologia. 2014;56(2):205–22.

42. Amoatey P, Omidvarborna H, Baawain MS, Al-Mamun A. Emissions and exposure assessments of SOX, NOX, PM10/2.5 and trace metals from oil industries: A review study (2000–2018). Vol. 123, Process Safety and Environmental Protection. Institution of Chemical Engineers; 2019. p. 215–28.

43. Africa's economic growth to outpace global forecast in 2023-2024 – African Development Bank biannual report | African Development Bank Group [Internet]. [cited 2024 Apr 3]. Available from: https://www.afdb.org/en/news-and-events/press-releases/africas-economic-growth-outpace-global-forecast-2023-2024-african-development-bank-biannual-report-58293

44. Ofosu FG, Hopke PK, Aboh IJK, Bamford SA. Characterization of fine particulate sources at Ashaiman in Greater Accra, Ghana. Atmos Pollut Res [Internet]. 2012;3(3):301–10. Available from: http://dx.doi.org/10.5094/APR.2012.033

45. Ghana Statistical Service. Ghana 2021 Population and Housing Census (PHC) Preliminary Report. 2021;30.

46. Schwela D. Review of Urban Air Quality in Sub-Saharan Africa Region. Rev Urban Air Qual Sub-Saharan Africa Reg. 2012;

47. Mudu P. Ambient air pollution and health in Accra, Ghana. 2021. 1–44 p.

48. Population V, Rate G. Ministry of transport, Ghana. 2016;

49. Nairametrics. Nigeria's vehicle population data reveals towering opportunities | Nairametrics.

50. DVLA | Official Website [Internet]. 2023 [cited 2024 Mar 19]. Available from: https://dvla.gov.gh/

51. Boadi KO, Kuitunen M. Municipal solid waste management in the Accra Metropolitan Area, Ghana. Environmentalist. 2003;23(3):211–8.

52. Zhou Z, Dionisio KL, Arku RE, Quaye A, Hughes AF, Vallarino J, et al. Household and community poverty, biomass use, and air pollution in Accra, Ghana. Proc Natl Acad Sci U S A. 2011;108(27):11028–33.

53. Ghana GE. Environmental Statistical Compendium. 2020;(September):32.

54. Hayward DF. Climatology of West Africa. Climatol West Africa. 2019 Oct;

55. Schwanghart W, Schütt B. Meteorological causes of Harmattan dust in West Africa. 2008;95:412–28.

56. GHStudents. Map of Ghana Showing the 16 Regions and Their Capital Cities. 2020.

57. Lyngsie G, Olsen JL, Awadzi TW, Fensholt R, Breuning-Madsen H. Influence of the inter tropical discontinuity on Harmattan dust deposition in Ghana. Geochemistry, Geophys Geosystems. 2013;14(9):3425–35.

58. Antwi EK, Otsuki K, Saito O, Obeng F, Gyekye K, Boakye-Danquah J, et al. Developing a Community-Based Resilience Assessment Model with reference to Northern Ghana. J Integr Disaster Risk Manag. 2014;4(1):73–92.

59. Resch F, Sunnu A, Afeti G. Saharan dust flux and deposition rate near the Gulf of Guinea. Tellus, Ser B Chem Phys Meteorol. 2008;60 B(1):98–105.

60. Addaney M, Yegblemenawo SAM, Akudugu JA, Kodua MA. Climate change and preservation of minority languages in the upper regions of Ghana: A systematic review. Chinese J Popul Resour Environ. 2022 Jun;20(2):177–89.

61. Newman CE, Hueso R, Lemmon MT, Munguira A, Vicente-Retortillo Á, Apestigue V, et al. NASA's Perseverance Studies the Wild Winds of Jezero Crater. Sci Adv. 2022 May;8(21).

62. Ankrah J, Monteiro A, Madureira H. Extreme Temperature and Rainfall Events and Future Climate Change Projections in the Coastal Savannah Agroecological Zone of Ghana. Atmos. 2023 Feb;14(2):386.

63. Ankrah J, Monteiro A, Madureira H. Vol. 15, Water (Switzerland). 2023. Spatiotemporal Characteristics of Meteorological Drought and Wetness Events across the Coastal Savannah Agroecological Zone of Ghana.

64. Candeias C, Ávila PF, Alves C, Gama C, Sequeira C, da Silva EF, et al. Dust characterization and its potential impact during the 2014–15 fogo volcano eruption (Cape Verde). Minerals. 2021 Nov;11(11):1275.

65. Asare-Nuamah P, Botchway E. Understanding climate variability and change: analysis of temperature and rainfall across agroecological zones in Ghana. Heliyon. 2019;5(10):e02654.

66. Oppong R, Badu E. Building Material Preferences in Warm-Humid and Hot-Dry Climates in Ghana. J Sci Technol. 2013;32(3):24–37.

67. Gordon C, Nukpezah D, Tweneboah-Lawson E, Ofori BD, Yirenya-Tawiah D, Pabi O, et al. West Africa - Water Resources Vulnerability Using a Multidimensional Approach: Case Study of Volta Basin. Vol. 5, Climate Vulnerability: Understanding and Addressing Threats to Essential Resources. Elsevier; 2013. 283–309 p.

68. Klutse NAB, Ajayi VO, Gbobaniyi EO, Egbebiyi TS, Kouadio K, Nkrumah F, et al. Potential impact of 1.5 °c and 2 °c global warming on consecutive dry and wet days over

West Africa. Environ Res Lett. 2018;13(5):0–6.

69. Agency GM. Ghana Meteorological Agency.

70. Bilal M, Nichol JE, Nazeer M, Shi Y, Wang L, Raghavendra Kumar K, et al. Characteristics of fine particulate matter (PM2.5) over urban, suburban, and rural areas of Hong Kong. Atmosphere (Basel). 2019;10(9):1–15.

71. Chen L, Peng S, Liu J, Hou Q. Dry deposition velocity of total suspended particles and meteorological influence in four locations in Guangzhou, China. J Environ Sci. 2012;24(4):632–9.

72. Jayamurugan R, Kumaravel B, Palanivelraja S, Chockalingam MP. Influence of Temperature, Relative Humidity and Seasonal Variability on Ambient Air Quality in a Coastal Urban Area. Int J Atmos Sci. 2013;2013:1–7.

73. Khalis M, Toure AB, Elbadisy I, Khomsi K, Najmi H, Bouaddi O, et al. Relationship between Meteorological and Air Quality Parameters and COVID-19 in Casablanca Region, Morocco. Int J Environ Res Public Heal 2022, Vol 19, Page 4989. 2022 Apr;19(9):4989.

74. Prabhu V, Gupta SK, Madhwal S, Shridhar V. Exposure to Atmospheric Particulates and Associated Respirable Deposition Dose to Street Vendors at the Residential and Commercial Sites in Dehradun City. Saf Health Work. 2019;10(2):237–44.

75. Hussein T, Dada L, Hakala S, Petäjä T, Kulmala M. Urban aerosol particle size characterization in Eastern Mediterranean Conditions. Atmosphere (Basel). 2019;10(11):1–21.

76. Xulu NA, Piketh SJ, Feig GT, Lack DA, Garland RM. Characterizing Light-absorbing Aerosols in a Low-income Settlement in South Africa. Aerosol Air Qual Res. 2020 Aug;20(8):1812–32.

77. Bauer H, Schueller E, Weinke G, Berger A, Hitzenberger R, Marr IL, et al. Significant contributions of fungal spores to the organic carbon and to the aerosol mass balance of the urban atmospheric aerosol. Atmos Environ. 2008 Jul;42(22):5542–9.

78. Ji D, Deng Z, Sun X, Ran L, Xia X, Fu D, et al. Estimation of PM2.5 Mass Concentration from Visibility. Adv Atmos Sci. 2020;37(7):671–8.

79. Bhat TH, Jiawen G, Farzaneh H. Air Pollution Health Risk Assessment (AP-HRA), Principles and Applications. Int J Environ Res Public Heal 2021, Vol 18, Page 1935. 2021 Feb;18(4):1935.

80. Hidy GM. Atmospheric Aerosols: Some Highlights and Highlighters, 1950 to 2018. Aerosol Sci Eng 2019 31. 2019 Feb;3(1):1–20.

81. OMS OM de la S. World Health Organization. 2021. p. 300 WHO global air quality guidelines: particulate matter (PM2.5 and PM10), ozone, nitrogen dioxide, sulfur dioxide and carbon monoxide.

82. SENES Consultants Limited. Health Impacts Exposure to Outdoor Air Pollution in Hamilton, Ontario. 2012;(February).

83. Hopke PK, Dai Q, Li L, Feng Y. Global review of recent source apportionments for airborne particulate matter. Sci Total Environ. 2020;740:140091.

84. Lim CC, Thurston GD, Shamy M, Alghamdi M, Khoder M, Mohorjy AM, et al. Temporal variations of fine and coarse particulate matter sources in Jeddah, Saudi Arabia. J Air Waste Manag Assoc. 2018;68(2):123–38.

85. Hopke PK, Feng Y, Dai Q. Source apportionment of particle number concentrations: A global review. Sci Total Environ. 2022 May;819:153104.

86. Concentrations S fractionated PN, Mortality D. Size-Fractionated Particle Number Concentrations and Daily Mortality in a Chinese City. 2013;1174(10):1174–9.

87. Lorelei A, Jesus D, Rahman M, Mazaheri M, Thompson H, Knibbs LD, et al. Ultrafine particles and PM 2 . 5 in the air of cities around the world : Are they representative of each other ? 2019;129(May):118–35.

88. Kan H, Chen B, Zhao N, London SJ, Song G, Chen G, et al. Research report (Health Effects Institute). 2010. p. 17–78 Part 1. A time-series study of ambient air pollution and daily mortality in Shanghai, China.

89. Bagula H, Olaniyan T, de Hoogh K, Saucy A, Parker B, Leaner J, et al. Ambient Air Pollution and Cardiorespiratory Outcomes amongst Adults Residing in Four Informal Settlements in the Western Province of South Africa. Int J Environ Res Public Health. 2021 Dec;18(24):13306.

90. Air Quality Criteria for Particulate Matter (Final Report, 1996) | Risk Assessment Portal | US EPA.

91. Boateng O. Driving patterns as a contributing factor to light-duty vehicular emission in the Kumasi metropolis. Pollution. 2015;1(4):441–9.

92. World Health Organization. Air pollution levels rising in many of the world's poorest cities. 2016. p. 8–11 Air pollution levels rising in many of the world's poorest cities.

93. Mohd Shafie SH, Mahmud M. Urban Air Pollutant from Motor Vehicle Emissions in Kuala Lumpur, Malaysia. Aerosol Air Qual Res. 2020 Dec;20(12):2793–804.

94. Boateng FG, Klopp JM. Beyond bans: A political economy of used vehicle dependency in Africa. J Transp Land Use. 2022;15(1):651–70.

95. Zhang K, Batterman S. Air pollution and health risks due to v1. Zhang K, Batterman S. Air pollution and health risks due to vehicle traffic. Sci Total Environ. 2013;450–451:307–16. ehicle traffic. Sci Total Environ. 2013;450–451:307–16.

96. Pérez N, Pey J, Cusack M, Reche C, Querol X, Alastuey A, et al. Variability of particle number, black carbon, and PM10, PM 2.5, and PM1 Levels and Speciation: Influence of road traffic emissions on urban air quality. Aerosol Sci Technol. 2010;44(7):487–99.

97. Kam W, Liacos JW, Schauer JJ, Delfino RJ, Sioutas C. On-road emission factors of PM pollutants for light-duty vehicles (LDVs) based on urban street driving conditions. Atmos Environ. 2012;61:378–86.

98. Bukowieki N, Gehirg R, Lienemann P, Hill M, Figi R, Buchmann B, et al. Non-Exhaust Emissions from Road Traffic. A report from the Air Quality Expert Group to the Department for Environment, Food and Rural Affairs; Scottish Government; Welsh Government; and Department of the Environment in Northern Ireland. Non-Exhaust Emiss. 2013;67(August 2009):252–77.

99. Pant P, Harrison RM. Estimation of the contribution of road traffic emissions to particulate matter concentrations from field measurements: A review. Atmos Environ. 2013;77:78–97.

100. Atiemo SM, Ofosu FG, Aboh IJK, Oppon OC. Levels and sources of heavy metal contamination in road dust in selected major highways of Accra, Ghana. X-Ray Spectrom. 2012;41(2):105–10.

101. OECD. Non-exhaust Particulate Emissions from Road Transport. Non-exhaust Part Emiss from Road Transp. 2020;

102. Hicks W, Beevers S, Tremper AH, Stewart G, Priestman M, Kelly FJ, et al. Quantification of Non-Exhaust Particulate Matter Traffic Emissions and the Impact of COVID-19 Lockdown at London Marylebone Road. 2021;

103. Johansson C, Denby BR, Sundvor I, Kauhaniemi M, Kukkonen J, Karppinen A, et al. NO n-exhaust R oad TR affic I nduced Department of Applied Environmental Science. (June 2012).

104. Zhou Z, Dionisio KL, Verissimo TG, Kerr AS, Coull B, Howie S, et al. Chemical characterization and source apportionment of household fine particulate matter in rural, peri-urban, and urban West Africa. Environ Sci Technol. 2014;48(2):1343–51.

105. Alli AS, Clark SN, Hughes A, Nimo J, Bedford-Moses J, Baah S, et al. Spatial-temporal patterns of ambient fine particulate matter (PM2.5) and black carbon (BC) pollution in Accra. Environ Res Lett. 2021 Jul;16(7):74013.

106. Cachon FB, Cazier F, Verdin A, Genevray P, Ayi-fanou L, Aïssi F, et al. Physicochemical Characterization of Air Pollution Particulate. Atmosphere (Basel). 2023;

107. Arquero KD, Gerber RB, Finlayson-Pitts BJ. The Role of Oxalic Acid in New Particle Formation from Methanesulfonic Acid, Methylamine, and Water. Environ Sci Technol. 2017;51(4):2124–30.

108. Anglada JM, Martins-Costa M, Ruiz-López MF, Francisco JS. Spectroscopic signatures of ozone at the air-water interface and photochemistry implications. Proc Natl Acad Sci U S A. 2014;111(32):11618–23.

109. Fakinle BS, Uzodinma OB, Odekanle EL, Sonibare JA. Impact of elemental composition of particulate matter in the airshed of a University Farm on the local air quality. Heliyon. 2020;6(1):e03216.

110. Falaiye OA, Abiye OE, Nwabachili SC. Characterization of atmospheric particulate matter from urban traffic sources in Ilorin. 2021;11(1):15–30.

111. Novela RJ, Gitari WM, Chikoore H, Molnar P, Mudzielwana R, Wichmann J. Chemical characterization of fine particulate matter, source apportionment and long-range transport clusters in Thohoyandou, South Africa. Clean Air J. 2020;30(2):1–10.

112. Open Journal of Air Pollution [Internet]. Finlayson-Pitts, B.J. (2000) Chemistry of the Upper and Lower Atmosphere Theory, Experiments, and Applications. Academic Press, San Diego, CA - References - Scientific Research Publishing.

113. Hinds WC, Zhu Y. Aerosol Technology: Properties, Behavior, and Measurement of Airborne Particles, 3rd Edition | Wiley. 2022. p. 448.

114. Godish, T. (2004) Air Quality. Fourth Edition, CRC Press Inc., Boca Raton. - References - Scientific Research Publishing.

115. Johnson TM, Guttikunds S, Wells GJ, Paulo A, Bond TC, Russell AG, et al. Tools for Improving Air Quality Management: A Review of Top-down Source Apportionment Techniques and Their Application in Developing Countries. 2011. p. 220.

116. Steinfeld JI. Vol. 40, Environment: Science and Policy for Sustainable Development. 1998. p. 26–26 Atmospheric Chemistry and Physics: From Air Pollution to Climate Change.

117. Tsuda A, Henry FS, Butler JP. Particle transport and deposition: Basic physics of particle kinetics. Compr Physiol. 2013;3(4):1437–71.

118. Slezakova K, Morais S, Carmo Pereir M do. Indoor Air Pollutants: Relevant Aspects and Health Impacts. Environ Heal - Emerg Issues Pract. 2012;

119. Siegel K, Karlsson L, Zieger P, Baccarini A, Schmale J, Lawler M, et al. Insights into the molecular composition of semivolatile aerosols in the summertime central Arctic Ocean

using FIGAERO-CIMS. Environ Sci Atmos. 2021;1(4):161–75.

120. Rogula-Kozłowska W. Size-segregated urban particulate matter: mass closure, chemical composition, and primary and secondary matter content. Air Qual Atmos Heal. 2016 Jul;9(5):533–50.

121. Aboh IJK, Henriksson D, Laursen J, Lundin M, Ofosu FG, Pind N, et al. Identification of aerosol particle sources in semi-rural area of Kwabenya, near Accra, Ghana, by EDXRF techniques. X-Ray Spectrom. 2009;38(4):348–53.

122. Rycroft MJ. Vol. 60, Journal of Atmospheric and Solar-Terrestrial Physics. 1998. p. 141 The upper atmosphere, data analysis and interpretation.

123. Romano S, Becagli S, Lucarelli F, Rispoli G, Perrone MR. Airborne bacteria structure and chemical composition relationships in winter and spring PM10 samples over southeastern Italy. Sci Total Environ. 2020;730:138899.

124. Cao J, Chow JC, Lee FSC, Watson JG. Evolution of PM2.5 measurements and standards in the U.S. And future perspectives for China. Aerosol Air Qual Res. 2013;13(4):1197–211.

125. Jesus AL De. Urban ambient particles: Long-term spatio-temporal trends and impacts of different control measures. 2021;

126. Neely RR, Toon OB, Solomon S, Vernier JP, Alvarez C, English JM, et al. Recent anthropogenic increases in SO2 from Asia have minimal impact on stratospheric aerosol. Geophys Res Lett. 2013;40(5):999–1004.

127. McDuffie EE, Smith SJ, O'Rourke P, Tibrewal K, Venkataraman C, Marais EA, et al. A global anthropogenic emission inventory of atmospheric pollutants from sector- And fuel-specific sources (1970-2017): An application of the Community Emissions Data System (CEDS). Earth Syst Sci Data. 2020 Dec;12(4):3413–42.

128. Li S, Zhang Y, Zhao J, Sarwar G, Zhou S, Chen Y, et al. Regional and urban-scale environmental influences of oceanic DMS emissions over coastal China seas. Atmosphere (Basel). 2020;11(8):1–18.

129. World Health Organization (WHO). Air pollution. 2021. p. 1–300 New WHO Global Air Quality Guidelines aim to save millions of lives from air pollution. Available from: https://www.who.int/news/item/22-09-2021-new-who-global-air-quality-guidelines-aim-to-save-millions-of-lives-from-air-pollution

130. Wang M, Kong W, Marten R, He XC, Chen D, Pfeifer J, et al. Rapid growth of new atmospheric particles by nitric acid and ammonia condensation. Nature. 2020;581(7807):184–9.

131. Von Stackelberg K, Buonocore J, Bhave P V., Schwartz JA. Public health impacts of secondary particulate formation from aromatic hydrocarbons in gasoline. Environ Heal A Glob Access Sci Source. 2013 Feb;12(1):1–13.

132. Malaguti A, Mircea M, La Torretta TMG, Telloli C, Petralia E, Stracquadanio M, et al. Comparison of online and offline methods for measuring fine secondary inorganic ions and carbonaceous aerosols in the central mediterranean area. Aerosol Air Qual Res. 2015;15(7):2641–53.

133. Li M, Hu M, Walker J, Gao P, Fang X, Xu N, et al. Source apportionment of carbonaceous aerosols in diverse atmospheric environments of China by dual-carbon isotope method. Sci Total Environ. 2022 Feb;806:150654.

134. Sofowote UM, Rastogi AK, Debosz J, Hopke PK. Advanced receptor modeling of near–real–time, ambient PM2.5 and its associated components collected at an urban–industrial site in Toronto, Ontario. Atmos Pollut Res. 2014 Jan;5(1):13–23.

135. U.S. EPA. Compendium of Methods for the Determination of Inorganic Compounds in Ambient Air INTEGRATED SAMPLING OF SUSPENDED PARTICULATE MATTER (SPM) IN AMBIENT AIR. 1999;(June):20–56.

136. US EPA. Compendium of Methods for the Determination of Inorganic Compounds in Ambient Air DETERMINATION OF METALS IN AMBIENT PARTICULATE MATTER USING NEUTRON ACTIVATION ANALYSIS (NAA) GAMMA SPECTROMETRY Method IO-3.7 Acknowledgments. 1999;(June).

137. U.S. EPA. Compendium of Methods for the Determination of Inorganic Compounds in

Ambient Air. Determination of metals in ambient particulate matter using X-Ray Fluorescence (XRF) Spectroscopy. 1999;(June):20–56.

138. Nakao M, Ishihara Y, Kim CH, Hyun IG. The Impact of Air Pollution, Including Asian Sand Dust, on Respiratory Symptoms and Health-related Quality of Life in Outpatients With Chronic Respiratory Disease in Korea: A Panel Study. J Prev Med Public Heal. 2018 May;51(3):130.

139. Yin S, Wang X, Zhang X, Guo M, Miura M, Xiao Y. Influence of biomass burning on local air pollution in mainland Southeast Asia from 2001 to 2016. Environ Pollut. 2019;254:1–25.

140. Yli-Tuomi T, Venditte L, Hopke PK, Shamsuzzoha Basunia M, Landsberger S, Viisanen YO, et al. Composition of the Finnish Arctic aerosol: collection and analysis of historic filter samples. Atmos Environ. 2003;37:2355–64.

141. Graham B, Falkovich AH, Rudich Y, Maenhaut W, Guyon P, Andreae MO. Vol. 38, Atmospheric Environment. 2004. p. 1593–604 Local and regional contributions to the atmospheric aerosol over Tel Aviv, Israel: A case study using elemental, ionic and organic tracers.

142. Venkataraman C, Reddy CK, Josson S, Reddy MS. Aerosol size and chemical characteristics at Mumbai, India, during the INDOEX-IFP (1999). Atmos Environ. 2002;36(12):1979–91.

143. Jacques Adon A, Liousse C, Thierno Doumbia E, Baeza-Squiban A, Cachier H, Léon JF, et al. Physico-chemical characterization of urban aerosols from specific combustion sources in West Africa at Abidjan in Côte d'Ivoire and Cotonou in Benin in the frame of the DACCIWA program. Atmos Chem Phys. 2020;20(9):5327–54.

144. Mizera J, Havelcová M, Machovič V, Borecká L, Vöröš D. minerals Neutron Activation Analysis in Urban Geochemistry: Impact of Traffic Intensification after Opening the Blanka Tunnel Complex in Prague. 2022;

145. Fussell JC, Franklin M, Green DC, Gustafsson M, Harrison RM, Hicks W, et al. A Review of Road Traffic-Derived Non-Exhaust Particles: Emissions, Physicochemical

Characteristics, Health Risks, and Mitigation Measures. Environ Sci Technol. 2022 Jun;56(11):6813–35.

146. Wittenburg J. Analysis of ambient particulate concentration near a coal storage pile. 2018;

147. Manual O. ARA N-FRM Sampler. 2020;

148. Dinoi A, Donateo A, Conte M, Conte M, Belosi F. Comparison of atmospheric particle concentration measurements using different optical detectors: potentiality and limits for air quality applications. Measurement. 2017 Aug;106:274–82.

149. Bandhu HK, Puri S, Garg ML, Singh B, Shahi JS, Mehta D, et al. Elemental composition and sources of air pollution in the city of Chandigarh, India, using EDXRF and PIXE techniques. Nucl Instruments Methods Phys Res Sect B Beam Interact with Mater Atoms. 2000;160(1):126–38.

150. Joy I, Aboh K, Henriksson D, Laursen J, Lundin M, Pind N, et al. EDXRF characterisation of elemental contents in PM2 . 5 in a medium-sized Swedish city dominated by a modern waste incineration plant †. 2007;104–10.

151. Bennet C, Jonsson P, Lindgren ES. Concentrations and sources of trace elements in particulate air pollution , Dar es Salaam , Tanzania , studied by EDXRF †. 2005;(July 2004):1–6.

152. Manukure SA. Waste electrical and electronic Equipment (E-Wastes) management in Ghana: environmental impacts at Agbogbloshie, Accra Ghana. 2016.

153. Anzeimo J a, Lindsay JR, Survey USG, Geochemistry B, Rd M, Park M. topics in chemical istrumentation X-ray Fluorescence Spectrometric Analysis. 1987;84(8).

154. Pella PA. X-ray fluorescence spectrometry by Ron Jenkins Published by John Wiley & Sons, New York, 1988; ISBN 0-471-83675-3. X-Ray Spectrom. 1989;18(4):187–187.

155. Suryanarayana C. & Norton MG. X-Ray diffraction: a practical approach. Vol. 36, Springer Link. Boston, MA: Springer US; 1999. 36-3382-36–3382 p.

156. Verma HR. X-ray Fluorescence (XRF) and Particle-Induced X-ray Emission (PIXE). In: Atomic and Nuclear Analytical Methods. Berlin, Heidelberg: Springer Berlin Heidelberg;

2007. p. 1–90.

157. Krane, K. S., & Halliday D. Introductory nuclear physics. Rev Mod Phys. 1988;15(4):1–549.

158. Amptek. Complete XRF Experimenter's Kit – Amptek – X-Ray Detectors and Electronics. 2019.

159. Pant P, Harrison RM. Critical review of receptor modelling for particulate matter: A case study of India. Atmos Environ. 2012 Mar;49:1–12.

160. Belis CA, Karagulian F, Larsen BR, Hopke PK. Critical review and meta-analysis of ambient particulate matter source apportionment using receptor models in Europe. Atmos Environ. 2013 Apr;69:94–108.

161. Thurston GD, Ito K, Lall R. A source apportionment of U.S. fine particulate matter air pollution. Atmos Environ. 2011;45(24):3924–36.

162. Belis C a, Larsen BR, Amato F, Haddad I El, Favez O, Harrison RM, et al. European Guide on Air Pollution Source Apportionment with Receptor Models. JRC Ref Rep. 2014;(March):88.

163. Dominici F, Peng RD, Barr CD, Bell ML. Protecting human health from air pollution: Shifting from a single-pollutant to a multipollutant approach. Epidemiology. 2010;21(2):187–94.

164. Shang J, Khuzestani RB, Tian J, Schauer JJ, Hua J, Zhang Y, et al. Chemical characterization and source apportionment of PM2.5 personal exposure of two cohorts living in urban and suburban Beijing. Environ Pollut. 2019;246:225–36.

165. Pollice A. Recent statistical issues in multivariate receptor models. Environmetrics. 2011;22(1):35–41.

166. Rahman SA, Hamzah MS, Wood AK, Elias MS, Salim NAA, Sanuri E. Sources apportionment of fine and coarse aerosol in Klang Valley, Kuala Lumpur using positive matrix factorization. Atmos Pollut Res. 2011;2(2):197–206.

167. Chan Y chung, Hawas O, Hawker D, Vowles P, Cohen DD, Stelcer E, et al. Using

multiple type composition data and wind data in PMF analysis to apportion and locate sources of air pollutants. Atmos Environ. 2011;45(2):439–49.

168. Doumbia T, Liousse C, Galy-Lacaux C, Ndiaye SA, Gardrat E, Leumbe-Ouafo MR, et al. Source Apportionment of Ambient Particulate Matter (PM) in two Western Africa Urban Sites (Dakar in Senegal and Bamako in Mali). 2023 Mar;

169. Ang A. Non-negative Matrix Factorization with Regularization. 2017;870–9.

170. Huang S, Conte MH. Source / process apportionment of major and trace elements in sinking particles in the Sargasso sea. Geochim Cosmochim Acta. 2009;73(1):65–90.

171. Guttikunda SK, Kopakka R V., Dasari P, Gertler AW. Receptor model-based source apportionment of particulate pollution in Hyderabad, India. Environ Monit Assess. 2013;185(7):5585–93.

172. Zhang M, Zhang S, Bao Q, Yang C, Qin Y, Fu J, et al. Temporal variation and source analysis of carbonaceous aerosol in industrial cities of Northeast China during the spring festival: The case of Changchun. Atmosphere (Basel). 2020;11(9).

173. Murray KE, Thomas SM, Bodour AA. Prioritizing research for trace pollutants and emerging contaminants in the freshwater environment. Environ Pollut. 2010;158(12):3462–71.

174. James CA, Brandenberger JM, Dutch M, Hardy J, Norton D, Neill SMO, et al. Contaminants of Emerging Concern: A Prioritization Framework for Monitoring in Puget Sound. 2015;(January).

175. Basagaña X, Jacquemin B, Karanasiou A, Ostro B, Querol X, Agis D, et al. Short-term effects of particulate matter constituents on daily hospitalizations and mortality in five South-European cities: Results from the MED-PARTICLES project. Environ Int. 2015;75:151–8.

176. Chauhan PK, Kumar A, Pratap V, Singh AK. Seasonal characteristics of PM1, PM2.5, and PM10 over Varanasi during 2019–2020. Front Sustain Cities. 2022;4.

177. Krishna RK, Ghude SD, Kumar R, Beig G, Kulkarni R, Nivdange S, et al. Surface PM2.5

estimate using satellite-derived aerosol optical depth over India. Aerosol Air Qual Res. 2019;19(1):25–37.

178. Rivas I, Vicens L, Basagaña X, Tobías A, Katsouyanni K, Walton H, et al. Associations between sources of particle number and mortality in four European cities. Environ Int. 2021;155(June).

179. Hinds WC. Aerosol technology: properties, behavior, and measurement of airborne particles. John Wileys Sons. 2012;(January).

180. Verma MK, Chauhan LKS, Sultana S, Kumar S. The traffic linked urban ambient air superfine and ultrafine PM1 mass concentration, Contents of pro-oxidant chemicals, And their seasonal drifts in Lucknow, India. Atmos Pollut Res. 2014;5(4):677–85.

181. Li G, Li L, Liu D, Qin J, Zhu H. Effect of PM2.5 pollution on perinatal mortality in China. Sci Rep. 2021;11(1):1–12.

182. Zare Jeddi M, Hopf NB, Louro H, Viegas S, Galea KS, Pasanen-Kase R, et al. Developing human biomonitoring as a 21st century toolbox within the European exposure science strategy 2020–2030. Environ Int. 2022;168(August).

183. Ghana Districts: A repository of all Local Assemblies in Ghana.

184. Alaazi DA, Menon D, Stafinski T, Hodgins S, Jhangri G. Quality of life of older adults in two contrasting neighbourhoods in Accra, Ghana. Soc Sci Med. 2021;270:113659.

185. World | Ranking Web of Universities: Webometrics ranks 30000 institutions.

186. University of Ghana. Overview | University of Ghana. 2022. p. 1.

187. Allen GA, Oh JAA, Koutrakis P, Sioutas C. Techniques for High-Quality Ambient Coarse Particle Mass Measurements. J Air Waste Manag Assoc. 1999;49(9):133–41.

188. Witz S, Eden RW, Wadley MW, Dunwoody C, Papa RP, Torre KJ. Rapid Loss of Particulate Nitrate, Chloride and Ammonium on Quartz Fiber Filters During Storage. J Air Waste Manag Assoc. 1990;40(1):53–61.

189. Williams R, Brook R, Bard R, Conner T, Shin H, Burnett R. Impact of personal and

ambient-level exposures to nitrogen dioxide and particulate matter on cardiovascular function. Int J Environ Health Res. 2012 Feb;22(1):71–91.

190. Hänninen OO, Koistinen KJ, Kousa A, Keski-Karhu J, Jantunen MJ. Quantitative analysis of environmental factors in differential weighing of blank Teflon filters. J Air Waste Manag Assoc. 2002;52(2):134–9.

191. Chance R, Jickells TD, Baker AR. Atmospheric trace metal concentrations, solubility and deposition fluxes in remote marine air over the south-east Atlantic. Mar Chem. 2015;177:45–56.

192. Alani RA, Ayejuyo OO, Akinrinade OE, Badmus GO, Festus CJ, Ogunnaike BA, et al. The level PM2.5 and the elemental compositions of some potential receptor locations in Lagos, Nigeria. Air Qual Atmos Heal. 2019;12(10):1251–8.

193. Basha S, Jhala J, Thorat R, Goel S, Trivedi R, Shah K, et al. Assessment of heavy metal content in suspended particulate matter of coastal industrial town, Mithapur, Gujarat, India. Atmos Res. 2010;97(1–2):257–65.

194. Raysoni AU, Armijos RX, Margaret Weigel M, Echanique P, Racines M, Pingitore. NE, et al. Evaluation of sources and patterns of elemental composition of PM2.5at three low-income neighborhood schools and residences in Quito, Ecuador. Int J Environ Res Public Health. 2017;14(7):1–26.

195. Chimidza S, Viksna A, Lindgren ES. EDXRF and TXRF analysis of aerosol particles and the mobile fraction of soil in Botswana. X-Ray Spectrom. 2001;30(5):301–7.

196. Kothai P, Saradhi I V., Pandit GG, Markwitz A, Puranik VD. Chemical characterization and source identification of particulate matter at an urban site of Navi Mumbai, India. Aerosol Air Qual Res. 2011;11(5):560–9.

197. Norris, G.A., Duvall, R., Brown, S.G., Bai S. EPA Positive M atrix Factorization (PM F) 5 . 0 Fundamentals and User Guide. Environ Prot Agency Off Researc Dev Publushing House Whashington, DC 20460. 2014;136.

198. Paatero P, Hopke PK. Discarding or downweighting high-noise variables in factor analytic models. Anal Chim Acta. 2003;490(1–2):277–89.

199. Housh T, Bowring SA, Villeneuve M. The continental crust: Its composition and evolution. J Geol. 1985 Jan;97(6):735–47.

200. Awokola B, Okello G, Johnson O, Dobson R, Ouédraogo AR, Dibba B, et al. Longitudinal Ambient PM2.5 Measurement at Fifteen Locations in Eight Sub-Saharan African Countries Using Low-Cost Sensors. Atmosphere (Basel). 2022;13(10).

201. Health Effects Institute, IHME. The State of Air Quality and Health Impacts in Africa. 2022. p. 23.

202. Kwarteng L, Baiden EA, Fobil J, Arko-Mensah J, Robins T, Batterman S. Air Quality Impacts at an E-Waste Site in Ghana Using Flexible, Moderate-Cost and Quality-Assured Measurements. GeoHealth. 2020;4(8):0–2.

203. Kleiman G. Strengthening Air Quality Management in Accra, Ghana IMPROVED POLLUTION MANAGEMENT AND REDUCED ENVIRONMENTAL HEALTH RISK IN ACCRA-TEMA METROPOLITAN AREA (P164417). 2021;(August).

204. WHO. WHO Urban Health Initiative in Accra, Ghana; Summary of projects result. Who. 2022.

205. Bose A, Roy Chowdhury I. Investigating the association between air pollutants' concentration and meteorological parameters in a rapidly growing urban center of West Bengal, India: a statistical modeling-based approach. Model Earth Syst Environ. 2023;9(2):2877–92.

206. Yang Q, Yuan Q. The Relationships between PM 2 . 5 and Meteorological Factors in China : Seasonal and Regional Variations. 2017;5.

207. El-sharkawy MF, Zaki GR. Effect of meteorological factors on the daily average levels of particulate matter in the Eastern Province of Saudi Arabia : A cross-sectional study. Online J Sci Technol. 2015;5(1):18–29.

208. Omokungbe OR, Fawole OG, Owoade OK, Popoola OAM, Jones RL, Olise FS, et al. Analysis of the variability of airborne particulate matter with prevailing meteorological conditions across a semi-urban environment using a network of low-cost air quality sensors. Heliyon. 2020;6(6):e04207.

209. Kayes I, Shahriar SA, Hasan K, Akhter M, Kabir MM, Salam MA. The relationships between meteorological parameters and air pollutants in an urban environment. Glob J Environ Sci Manag. 2019;5(3):265–78.

210. Rahim HA, Khan MF, Ibrahim ZF, Shoaib A, Suradi H, Mohyeddin N, et al. Coastal meteorology on the dispersion of air particles at the Bachok GAW Station. Sci Total Environ. 2021;782:1–44.

211. Feinberg A. The atmospheric sulfur and selenium cycles: A global model of transport and deposition. 2020;(26816):186.

212. Jia H, Huo J, Fu Q, Duan Y, Lin Y, Jin X, et al. Insights into chemical composition, abatement mechanisms and regional transport of atmospheric pollutants in the Yangtze River Delta region, China during the COVID-19 outbreak control period. Environ Pollut. 2020;267:115612.

213. Bai L, He Z, Ni S, Chen W, Li N, Sun S. Investigation of PM2.5 absorbed with heavy metal elements, source apportionment and their health impacts in residential houses in the North-east region of China. Sustain Cities Soc. 2019;51.

214. Sinex SA, Wright DA. Distribution of trace metals in the sediments and biota of Chesapeake Bay. Mar Pollut Bull. 1988;19(9):425–31.

215. Davy PK, Ancelet T, Trompetter WJ, Markwitz A, Weatherburn DC. Composition and source contributions of air particulate matter pollution in a New Zealand suburban town. Atmos Pollut Res. 2012;3(1):143–7.

216. Liu J, Peng J, Men Z, Fang T, Zhang J, Du Z, et al. Brake wear-derived particles: Single-particle mass spectral signatures and real-world emissions. Environ Sci Ecotechnology. 2023;15:100240.

217. Liu Y, Wu S, Chen H, Federici M, Perricone G, Li Y, et al. Brake wear induced PM10 emissions during the world harmonised light-duty vehicle test procedure-brake cycle. J Clean Prod. 2022;361.

218. Subaar C, Gyan E, Osei -Owusu J, Edziah R, Dofuor A., Tandoh JB, et al. Determination of Heavy Metals Pollution in Soil and Tree Rings along Haatso- Atomic Road in Ghana.

Pollut Eff Community Heal. 2022;1(1):1–12.

219. Sun Y, Zhuang G, Zhang W, Wang Y, Zhuang Y. Characteristics and sources of lead pollution after phasing out leaded gasoline in Beijing. Atmos Environ. 2006;40(16):2973–85.

220. Guo G, Wu F, Xie F, Zhang R. Spatial distribution and pollution assessments of heavy metals in urban soils from southwest of China. 2012;24(3):410–8.

221. Kumar M, Gogoi A, Kumari D, Borah R, Das P, Mazumder P, et al. Review of Perspective, Problems, Challenges, and Future Scenario of Metal Contamination in the Urban Environment. J Hazardous, Toxic, Radioact Waste. 2017;21(4):1–16.

222. Popouen AJ, Benchrif A, Kezo PC, Agbo DDA, Koua AA, Bounakhla M, et al. Elemental Composition of PM2.5 and PM10 in the Industrial Area of Yopougon, Abidjan, Côte d'Ivoire. J Environ Prot (Irvine, Calif). 2022;13(06):385–97.

223. Song Y, Xie S, Zhang Y, Zeng L, Salmon LG, Zheng M. Source apportionment of PM2 . 5 in Beijing using principal component analysis / absolute principal component scores and UNMIX. 2006;372(September 2000):278–86.

224. Zhou Z, Dionisio KL, Verissimo TG, Kerr AS, Coull B, Arku RE, et al. Chemical composition and sources of particle pollution in affluent and poor neighborhoods of Accra, Ghana. Environ Res Lett. 2013;8(4).

225. Teye M. Assessment of Heavy Metal Residues in Hides of Goats Singed with Tyres , and the Effect of Boiling on the Heavy Metal Concentrations in the Hides Journal of Veterinary Advances Assessment of Heavy Metal Residues in Hides of Goats Singed with Tyres , and t. 2014;(May 2013).

226. Mensah NJ, Antwi-akomeah S, Akanlu S, Martin B, Sixtus B, Godfred SE. American Journal of Environmental Science & Technology Residual Levels of Heavy Metal Contaminants in Cattle Hides Singed with Scrap Tyre and Firewood Fuel Sources : a Comparative Study in the Wa Municipality of Ghana. 2019;3(1):1–11.

227. Kulshrestha MJ, Singh R, Engardt M. Ambient and Episodic Levels of Metals in PM10 Aerosols and Their Source Apportionment in Central Delhi, India. J Hazardous, Toxic,

Radioact Waste. 2016;20(4):1–8.

228. Gupta I, Salunkhe A, Kumar R. Source apportionment of PM10 by positive matrix factorization in urban area of Mumbai, India. Sci World J. 2012;2012.

229. Naidja L, Ali-khodja H, Khardi S, Bencharif-madani F, Terrouche A, Lokorai K, et al. Source apportionment of PM2 . 5 and their associated metallic elements by positive matrix factorization at a traffic site in Constantine , Algeria To cite this version : HAL Id : hal-04045347 Source apportionment of PM 2 . 5 and their associated metallic . 2023;

230. Gugamsetty B, Wei H, Liu CN, Awasthi A, Tsai CJ, Roam GD, et al. Source Characterization and Apportionment of PM10, PM2.5 and PM0.1 by Using Positive Matrix Factorization. Aerosol Air Qual Res. 2012;12(4):476–91.

231. Jumaah HJ, Ameen MH, Kalantar B, Rizeei HM, Jumaah SJ. Air quality index prediction using IDW geostatistical technique and OLS-based GIS technique in Kuala Lumpur, Malaysia. Geomatics, Nat Hazards Risk. 2019;10(1):2185–99.

232. Wang N, Ling Z, Deng X, Deng T, Lyu X, Li T, et al. Source Contributions to PM2.5 under Unfavorable Weather Conditions in Guangzhou City, China. Adv Atmos Sci. 2018;35(9):1145–59.

233. Approaches P, Watson JG, Chow JC. The Role of Receptor Models in Creating a Weight-of-Evidence Emission Reduction Strategy: Analytical and Procedural Approaches. 2014;

234. Jandric A, Part F, Fink N, Cocco V, Mouillard F, Huber-Humer M, et al. Investigation of the heterogeneity of bromine in plastic components as an indicator for brominated flame retardants in waste electrical and electronic equipment with regard to recyclability. J Hazard Mater. 2020;390(May).

235. Kiddee P, Naidu R, Wong MH. Electronic waste management approaches: An overview. Waste Manag. 2013;33(5):1237–50.

236. Arku RE. Poverty, Energy Use, Air Pollution and Health in Ghana: A Spatial Analysis. 2015;

237. Joseph AE, Unnikrishnan S, Kumar R. Chemical characterization and mass closure of fine

aerosol for different land use patterns in Mumbai city. Aerosol Air Qual Res. 2012;12(1):61–72.

238. Rodriguez MG, Heredia Rivera B, Rodriguez Heredia M, Rodriguez Heredia B, Gonzalez Segovia R. A study of dust airborne particles collected by vehicular traffic from the atmosphere of southern megalopolis Mexico City. Environ Syst Res. 2019;8(1).

239. Hama S, Kumar P, Alam MS, Rooney DJ, Bloss WJ, Shi Z, et al. Chemical source profiles of fine particles for five different sources in Delhi. Chemosphere. 2021;274.

240. Samiksha S, Sunder Raman R, Nirmalkar J, Kumar S, Sirvaiya R. PM10 and PM2.5 chemical source profiles with optical attenuation and health risk indicators of paved and unpaved road dust in Bhopal, India. Environ Pollut. 2017;222:477–85.

241. Fayad MA, Chaichan MT, Dhahad HA, Al-Amiery AA, Wan Isahak WNR. Reducing the Effect of High Sulfur Content in Diesel Fuel on NOxEmissions and PM Characteristics Using a PPCI Mode Engine and Gasoline-Diesel Blends. ACS Omega. 2022;7(42):37328–39.

242. Rai P, Furger M, El Haddad I, Kumar V, Wang L, Singh A, et al. Real-time measurement and source apportionment of elements in Delhi's atmosphere. Sci Total Environ. 2020;742:140332.

243. Sharma SK, Mandal TK. Elemental Composition and Sources of Fine Particulate Matter (PM2.5) in Delhi, India. Bull Environ Contam Toxicol. 2023;110(3):1–8.

244. Morishita M, Keeler GJ, Kamal AS, Wagner JG, Harkema JR, Rohr AC. Source identification of ambient PM2.5 for inhalation exposure studies in Steubenville, Ohio using highly time-resolved measurements. Atmos Environ. 2011;45(40):7688–97.

APPENDIX

Table 2.1 Overview of vehicles recorded by the DVLA in Accra (2010-2019)

Year	Recorded vehicles	Year	Recorded vehicles
2010	70,570	2015	59,097
2011	77,420	2016	62,011
2012	84,127	2017	70,876
2013	95,303	2018	94,390
2014	64,895	2019	86,020